

**Implementation of a Total Power Radiometer in Software Defined Radios**

by

Matthew Erik Nelson

A thesis submitted to the graduate faculty  
in partial fulfillment of the requirements for the degree of  
**MASTER OF SCIENCE**

Major: Computer Engineering (Embedded Systems)

Program of Study Committee:

Phillip H Jones, Major Professor

John Basart

Mani Mina

Iowa State University

Ames, Iowa

2015

Copyright © Matthew Erik Nelson, 2015. All rights reserved.

## **DEDICATION**

I would like to dedicate this thesis to my wife Jennifer who has stood by me through this long journey towards my Masters. I would also like to thank my parents without whose support I would not have been able to complete this work.

I would also like to thank my friends and family for their continued support and constant encouragement.

**TABLE OF CONTENTS**

<b>LIST OF TABLES . . . . .</b>	<b>vii</b>
<b>LIST OF FIGURES . . . . .</b>	<b>viii</b>
<b>ACKNOWLEDGEMENTS . . . . .</b>	<b>xi</b>
<b>ABSTRACT . . . . .</b>	<b>xii</b>
<b>CHAPTER 1. INTRODUCTION . . . . .</b>	<b>1</b>
<b>CHAPTER 2. RELATED WORKS . . . . .</b>	<b>4</b>
2.1 Digital Radiometers . . . . .	4
2.1.1 Direct Digital Sampled Radiometer . . . . .	5
2.2 Software Defined Radio Based Radiometers . . . . .	6
2.3 Radio Frequency Interference (RFI) Mitigation . . . . .	7
<b>CHAPTER 3. BACKGROUND . . . . .</b>	<b>8</b>
3.1 Radiometer Basics . . . . .	8
3.1.1 Measuring RF power . . . . .	11
3.1.2 Integration and filtering . . . . .	13
3.1.3 Radiometer Performance Metrics . . . . .	14
3.2 Software Defined Radios Basics . . . . .	16
3.2.1 Software Defined Radio Normal Operation . . . . .	17
3.3 Software Defined Radio Development Platform . . . . .	18
3.3.1 Hardware Platform . . . . .	18
3.3.2 Software Platform . . . . .	21

<b>CHAPTER 4. SOFTWARE DEFINED RADIOMETER IMPLEMENTATION . . . . .</b>	<b>24</b>
4.1 Introduction . . . . .	24
4.2 Requirements . . . . .	24
4.3 Theory of Operation of a Software Defined Radio Radiometer . . . . .	25
4.4 Mapping Traditional Radiometer Functions to a Software Defined Radio Radiometer . . . . .	25
4.5 System overview . . . . .	25
4.5.1 Control of the SDR Hardware through GNURadio . . . . .	25
4.5.2 Impact of the Controls Related to Radiometry . . . . .	27
4.6 GNURadio Data Handling . . . . .	27
4.6.1 GNURadio Data Display . . . . .	28
4.7 Square-law Detector Performance . . . . .	28
4.8 Software Defined Radio Performance . . . . .	29
4.8.1 Hardware Requirements . . . . .	30
4.8.2 Software Requirements . . . . .	31
4.9 Software Defined Radiometer Theory of Operation . . . . .	32
4.10 Mapping analog radiometer functions to a software defined radiometer . . . . .	32
4.10.1 Power detection . . . . .	32
4.11 Integrator through a IIR Filter . . . . .	33
4.11.1 Software Defined Radio Radiometer . . . . .	33
4.11.2 RF Front End . . . . .	36
4.11.3 Software Defined Power Detection . . . . .	37
4.11.4 Software Defined Integrator . . . . .	38
4.11.5 SDR Radiometer Summary . . . . .	41
4.11.6 RF Front End . . . . .	41
4.12 General Specifications . . . . .	42
4.13 Comparison of a Software Defined Radio Radiometer vs Traditional Radiometer	42

<b>CHAPTER 5. EVALUATION AND EXPERIMENTAL DESIGN . . . . .</b>	<b>44</b>
5.1 Square-law Detector . . . . .	44
5.1.1 Analog Devices ADL5902 . . . . .	45
5.1.2 Data acquisition and storage . . . . .	46
5.1.3 Tests on the ADL5902 . . . . .	49
5.2 Software Defined Radio Experiments . . . . .	50
5.3 Experiment 1 - Calibration and Normal Radiometer Operation . . . . .	51
5.3.1 Laboratory Setup . . . . .	52
5.3.2 Test Results . . . . .	53
5.3.3 Application with Soil Moisture Readings . . . . .	56
5.4 Experiment 2 - Interfering Signal Mitigation . . . . .	58
5.4.1 Laboratory Setup . . . . .	61
5.4.2 Software Defined Radio Configuration . . . . .	62
5.4.3 Impact of filter on radiometer performance . . . . .	64
5.4.4 Test Results . . . . .	66
<b>CHAPTER 6. RESULTS AND ANALYSIS . . . . .</b>	<b>70</b>
6.1 Introduction . . . . .	70
6.2 Benefits to Software Defined Radio Radiometer . . . . .	72
6.2.1 Cost Benefits . . . . .	73
6.2.2 Weight and component size benefits . . . . .	74
6.2.3 Value added benefits . . . . .	75
6.3 Disadvantages of a SDR Radiometer . . . . .	75
6.3.1 Power Consumption . . . . .	76
6.3.2 Bandwidth constraints . . . . .	76
6.4 Results Summary . . . . .	76
<b>CHAPTER 7. CONCLUSION AND FUTURE WORK . . . . .</b>	<b>77</b>
7.1 Conclusion . . . . .	77
7.2 Future work . . . . .	77

7.2.1	Further testing . . . . .	78
7.2.2	Improving on the FPGA firmware . . . . .	78
7.2.3	Correlation . . . . .	78
7.2.4	Improving stability . . . . .	80
<b>APPENDIX A.</b>	<b>Source code . . . . .</b>	<b>81</b>
<b>APPENDIX B.</b>	<b>EE 518 Test Results . . . . .</b>	<b>108</b>
B.0.5	Test setup . . . . .	109
B.0.6	Lab Experiment . . . . .	110
B.0.7	Lab Results . . . . .	110
B.0.8	Conclusion . . . . .	111
<b>APPENDIX C.</b>	<b>Direct-Sampling Digital Correlation Radiometer . . . . .</b>	<b>112</b>
C.0.9	Implantation in the ISU Radiometer . . . . .	112
<b>BIBLIOGRAPHY</b>	<b>. . . . .</b>	<b>113</b>

**LIST OF TABLES**

Table 4.1	Required Radiometer performance . . . . .	25
Table 4.2	ISU Radiometer requirements . . . . .	30
Table 5.1	ADL5902 Specifications . . . . .	45
Table 6.1	Cost Analysis . . . . .	73
Table 6.2	Weight Analysis . . . . .	75

## LIST OF FIGURES

Figure 3.1	A total power radiometer block diagram . . . . .	9
Figure 3.2	A block diagram of a Dicke radiometer . . . . .	10
Figure 3.3	A block diagram of a Noise Injection radiometer . . . . .	11
Figure 3.4	The ideal radiometer block diagram . . . . .	12
Figure 3.5	A more realistic radiometer model . . . . .	12
Figure 3.6	A simple RC circuit . . . . .	14
Figure 3.7	The USRP N200 from Ettus Research (Image from Ettus Research Website - <a href="http://www.ettus.com">www.ettus.com</a> ) . . . . .	19
Figure 3.8	A block diagram of the Ettus N200 SDR. (Image from Ettus Research Website - <a href="http://www.ettus.com">www.ettus.com</a> ) . . . . .	20
Figure 3.9	The DBSRX2 daughter board from Ettus Research (Image from Ettus Research Website - <a href="http://www.ettus.com">www.ettus.com</a> ) . . . . .	21
Figure 3.10	Screenshot of the GNURadio Companion editor and the N200 Radiometer block diagram used in the author's experiments . . . . .	23
Figure 4.1	A screenshot of the interface made for communication with and controlling the software defined radio . . . . .	26
Figure 4.2	A screenshot showing the ticker tape display for the total power readings. In addition, raw and calibrated noise temperature is shown below.	29
Figure 4.3	A block diagram showing how the radiometer performs the equivalent square law detector in software. . . . .	33
Figure 4.4	A block diagram of the Ettus N200 SDR . . . . .	35
Figure 4.5	The ADISIMRF program used to verify the design of the RF Front End	37

Figure 4.6	A simple RC circuit . . . . .	38
Figure 5.1	An image of the ADL5902 square-law detector used in these experiments	46
Figure 5.2	A screenshot of the Labview GUI interface . . . . .	47
Figure 5.3	A screenshot of the Labview block diagram . . . . .	48
Figure 5.4	Graph showing the linearity of the ADL5902 . . . . .	50
Figure 5.5	A screenshot of the GNURadio program using a noise generator block.	51
Figure 5.6	An image of the typical lab setup used to test the software defined radiometer . . . . .	52
Figure 5.7	Graph of the un-calibrated rQ values of Experiment 1 . . . . .	53
Figure 5.8	Graph of the calibrated noise temperature of Experiment 1 . . . . .	54
Figure 5.9	Raw and noisy graph from the square-law detector used in Experiment 1	55
Figure 5.10	Filtered data from the square-law detector used in Experiment 1 . . .	56
Figure 5.11	Calibrated data from the square-law detector used in Experiment 1 . .	57
Figure 5.12	Figure showing both the SDR and square-law noise temperature data in Experiment 1 . . . . .	58
Figure 5.13	Screenshot of the waterfall display used in Experiment 1 . . . . .	59
Figure 5.14	Side by side comparison of the waterfall display for Experiment 1 . .	59
Figure 5.15	Plot of the noise temperature of Experiment 1 with soil moisture percentage . . . . .	60
Figure 5.16	Image of the HackRF used to generate the offending signal . . . . .	62
Figure 5.17	Image of the GNU Radio Filter Design tool . . . . .	63
Figure 5.18	Graph showing the impact of the filter to the $NE\Delta T$ performance of the radiometer . . . . .	64
Figure 5.19	Graph showing both theoretical and experimental data on the impact to the total power as a function of the bandwidth of the filter . . . . .	65
Figure 5.20	Graph showing the unfiltered total power measurements on the software defined radio . . . . .	66

Figure 5.21	Graph showing the raw total power read from the square-law detector with an interfering signal. . . . .	67
Figure 5.22	Image showing the spectrum view from the software defined radio . . .	67
Figure 5.23	Image showing the software defined radio with the filter on and filtering the offending signal . . . . .	68
Figure 5.24	Graph showing the calibrated total power readings with the filter removing the offending signal . . . . .	69
Figure 5.25	Image of the offending signal being filtered out by the SDR. It can be seen that the signal is no longer visible. . . . .	69
Figure 6.1	Graph of the calibrated total power over a period of fifteen minutes. .	70
Figure 6.2	Graph of the calibrated total power with the standard deviation plotted.	71
Figure 6.3	A screenshot showing the iPython notebook code and related graphs generated for parsing GNURadio data . . . . .	72
Figure 7.1	The key blocks used for creating a correlating radiometer in software. The key blocks is the USRP source, which allows us to address both daughter-boards and the ADD block which sums the signals. . . . .	79
Figure A.1	Blocks used for creating a total power radiometer in software . . . . .	82
Figure B.1	Students rotating the radiometer for an experiment on Agronomy Hall	109

## ACKNOWLEDGEMENTS

I would like to take this opportunity to express my thanks to those who helped me with various aspects of conducting research and the writing of this thesis. First and foremost, Dr. Phillip Jones for his guidance, patience and support throughout this research and the writing of this thesis. I would also like to thank Dr. John Basart who patiently spent many hours with me going over both the fundamentals and details with radiometers. I would like to thank Dr. Brian Hornbuckle for his continued support and for allowing me to utilize his radiometer, lab and students towards my research. Finally I would like to thank Dr. Mani Mina who not only was instrumental in my undergraduate career but continued his support into my graduate path as well. If it was not for Dr. Mina hiring me as the Chief Engineer of the Spacecraft Systems and Operations Lab, I would not be here today.

## ABSTRACT

A software defined radio is defined as a communication system where components of a communication system that are typically done in hardware are now done in software. The result is a highly flexible communication system that can adapt to changes to the system based on requests by the user or due to conditions in the radio frequency channel. Software Defined Radios (SDRs) have been used for a variety of applications, mostly in the area of communications. However, they have not been widely applied to remote sensing applications such as a radiometer. A SDR based radiometer offers a very flexible and robust system more so than a more traditional radiometer which has fixed hardware and usually little room for flexibility and adaptability based on the needs of the radiometer application or due to changes in the radiometers environment. The price of SDRs have also been steadily dropping making implementing them into radiometers a more attractive option compared to using traditional RF hardware. In this thesis we will look into the feasibility and theory of using an off the shelf SDR hardware platform for a radiometer application. In addition, we will look into how we can use the GNURadio software to create a total power radiometer within software and how this software can be used to make easy changes to the functionality of the radiometer. Finally we will look at the preliminary results obtained from laboratory tests of the SDR radiometer system.

## CHAPTER 1. INTRODUCTION

This thesis explores using software defined radio (SDR) technology to develop a radiometer that is on par with a traditional radiometer. In addition to demonstrating a SDR-based radiometer can achieve similar performance, in terms of sensitivity and stability, to a traditional radiometer, it is shown that the inherent flexibility of SDR technology allows implementing functionality beyond what a traditional radiometer typically provides. Furthermore, by reducing cost and increasing flexibility, SDR technology may become an attractive path for broadening the accessibility of radiometry to the general research community.

*Motivation.* Remote sensing refers to activities of recording, observing and perceiving objects or events that are far away (i.e. remote)[Weng (2012)]. Since the object of interest is remote, we cannot physically interact with it using local measurement methods such as placing sensors or probes on the object. Remote sensing can be accomplished in a variety of ways and the list below is the basic types of radiometry that is used today.

1. Visible light: Photography and Photogrammetry,
2. Thermal: Far infrared,
3. Laser distance measurement; Lidar,
4. Radio Frequency (RF): Radiometry.

Each of these methods above has an associated set of pros and cons, thus remote sensing often uses a combination of methods to paint a complete picture of an object. This thesis focuses on the apparatus used in radiometry to capture RF signals, called a radiometer.

Radiometry can be broken in to two methods; active or passive. An active system is one in which a radio frequency signal or pulse is generated and transmitted to the object of interest.

The reflection of this RF signal, or in some cases lack of reflection, gives us information about the object. A passive system is one in which no RF signal or pulse is generated. Instead, this type of radiometer simply listens to the RF energy that is naturally generated by the object or that may be reflected from another source, such as the Sun. Additional applications include: assessing vegetation health and observing celestial objects[Ulaby and Long (2014)]. Radiometers have been focused on Earth for such purposes as helping scientists better understand its water cycle by monitoring ocean salinity [Hardy et al. (1974)] and soil moisture [Liu et al. (2013)]. Radiometers such as these are already in service on satellites such as the Soil Moisture and Ocean Salinity (SMOS) satellite [McMullan et al. (2008)] launched by the European Space Agency (ESA).

The amount of noise that is generated by the object of interest is due to the thermal agitation of the charge carriers, usually the electrons, which is directly correlated to the physical temperature of the source [Nyquist (1928)]. It is because of this correlation that we often refer to the amount of noise received as the noise temperature and it is measured in Kelvins.

*Problem Statement.* While radiometers have proved to be an excellent tool for remote sensing and have been used in research applications for over fifty years, they have not made it into wide spread use. This is due to the fact that many traditional radiometers have the following hurdles:

1. They are expensive,
2. They require advanced knowledge to implement and use,
3. They are typically built and designed for a custom application.

This thesis aims to help address each of these hurdles as follows. The use of commercial off the shelf (COTS) parts and solutions will help reduce cost and the need for a custom design. The use of a software to define key components of the radiometer eliminates the need for a custom build and allows for a flexible system for multiple applications. The use of a user friendly graphical user interface (GUI) reduces the need of advanced knowledge to implement and use the radiometer.

*Contributions.* The primary contributions of this thesis work are:

1. Development of a software defined radio-based radiometer
2. Python based scripts for analyzing data generated by the radiometer
3. A Radio Frequency Interference (RFI)mitigation technique implemented using software defined radio technology

*Organization.* The remainder of this thesis is organized as follows. Chapter 2 gives a discussion of related works. Chapter 3 gives background on traditional radiometers and on software defined radios. Chapter 4 presents details on how software defined radio technology was used to implement a radiometer. Chapter 5 describes the experimentation setup used to verify and evaluate the operation of the implemented radiometer. Chapter 6 examines the results obtained from our performance evaluation experiments. Chapter 7 concludes the thesis and outlines avenues of future work.

## CHAPTER 2. RELATED WORKS

Three areas closely related to the work in this thesis are:

1. Digital radiometers,
2. Software defined radio based radiometers,
3. Radio frequency interference mitigation.

Digital radiometers digitize some part of the signal or the output from the power detection stage of the radiometer. This is similar to a software defined radio radiometer except a software defined radio radiometer digitizes the complete radio frequency (RF) signal. The software defined radio based radiometers discussed is close to the work in this thesis, but do not use commercial off the shelf components or readily available software such as GNURadio to develop the radiometer in software. The radio frequency interference mitigation discussed uses radiometers or digital radiometers that do not collect the entire signal information and therefore use different methods to detect and mitigate the offending signal. The work in this thesis will cover a different method for RFI due to both frequency and amplitude information being preserved when the signal is digitized.

### 2.1 Digital Radiometers

A digital radiometer replaces a portion or all of the radiometer components with digital components[Ruf and Gross (2010)]. The key component in a digital radiometer is the analog to digital converters that convert the analog information to a digital signal that can be processed. There are two types of digital radiometers:

1. Hybrid radiometer,

## 2. Direct digital sampled radiometer.

A hybrid radiometer is a radiometer that uses some traditional analog components but digitizes a certain portion of the radiometer information [Skou and Vine (2006)]. This is often the analog voltage output from the diode of a square law detector. However, it can be other stages such as a digital correlator [Villarino et al. (2002)][Wang et al. (2012)] or a different method for calibration such as digital reference averaging [Bremer (1979)].

Both types of digital radiometers are designed to retain only a portion of the information contained in the RF signal. This information is the total power contained within the signal which is the primary purpose of a radiometer. As it will be discussed later though, retaining the full signal allows for more in-depth digital signal analysis.

### 2.1.1 Direct Digital Sampled Radiometer

A direct digital sampled radiometer samples the incoming RF signal directly and then uses digital signal techniques to extract the total power from the signal.

Iowa State University owns a 1.4 GHz, dual polarization, correlating radiometer. This radiometer was built at the University of Michigan and put into service at ISU in 2006. The ISU radiometer is unique in that it is one of the few direct sampling radiometers in useErbas et al. (2006). This radiometer takes the RF signal and using analog components amplifies and filters the signal, and then sends it directly to an analog to digital converter. At the time the ISU radiometer was built an analog to digital converter (ADC) that is able to sample accurately at 1.4 GHz was expensive and hard to come. However, the ISU radiometer does not sample at 2.8 GHz or above, instead it samples at 1.4 GHz. The ISU radiometer is able to do this because it is only interested in power information which we can extract with an under-sampled signal. The I/Q information from the (ADC) is then sent to a Field Programmable Gate Array (FPGA) which then processes the data. The ISU radiometer is also a correlating radiometer that looks at both the vertical polarization (V-Pol) and the horizontal polarization (H-Pol) and then correlates this information[Fischman (2001)].

## 2.2 Software Defined Radio Based Radiometers

With the advent of software defined radios becoming widely available, there has been other works with using software defined radios for radiometry. The related works presented here outline work that has contributed to using software defined radios in developing radiometers.

*Shirleys Bay Radio Astronomy Consortium.* Radiometers used in radio astronomy [Tiuri (1964)] is nothing new and has been postulated for some time [Ohm and Snell (1963)]. The Shirleys Bay Radio Astronomy Consortium (SBRAC) located in Smiths Falls, Ontario is an organization that is restoring a radio telescope used for radiometry in astronomy. Recently the SBRAC is using software defined radios attached to their eighteen meter radius dish to obtain information by looking at the hydrogen line at 1420.4058 MHz[Leech and Ocame (2007)]. The person in charge of this facility, Marcus Leech, contributed software to the GNURadio specifically for radio astronomy applications. It was this software branch that was used as the base for the GNURadio program that was used in this thesis. Marcus Leech continue to contribute to the GNURadio community and continues to provide support for these functions as well[Leech (2006)].

While parts of the GNURadio program was derived from the work from Marcus Leech, additional features were added such as filtering an offending signal, offending signal detection and built in noise generator. Additional work was done on refining some elements of the GUI interface including adding a waterfall display which is covered in more detail in this thesis.

*Grand Valley State University.* Another example of a software defined radio used as a radiometer is from the University of Illinois and Grand Valley State University built to listen to emissions from Jupiter[Behnke et al. (2013)]. This software defined radio was built using an Analog Devices AD9460 and a Xilinx Spartan-3E-500 FPGA to build the SDR itself. A RF front end was also built to filter and amplify the signal coming into the SDR. Finally, this group also used GNURadio to interface to and talk to the SDR and used both Python and wxGUI to build a working interface. The students reported that the SDR radiometer worked well and was able to do so at a low price point.

The Grand Valley State University radiometer used GNURadio to talk and interface to

the SDR which is the same as the radiometer used in this thesis. However in this case the radiometer was built by the students using the Spartan-3E-500 FPGA and an Analog Devices analog to digital converter. The goal of this thesis however, is to use off the shelf components to make it more accessible to users.

### **2.3 Radio Frequency Interference (RFI) Mitigation**

Radio Frequency Interference (RFI) is a RF signal that is unwanted or undesirable and causes either reduced performance or masks the information that we want. Radio Frequency Interference (RFI) is a common problem with nearly all radiometers because they are highly sensitive receivers so even small signals can cause large problems for the radiometer. It is for this reason why certain frequency bands have been designated for radiometer use by the international community. However, not all entities abide by this and continue to transmit on these protected frequencies. This problem is often exasperated with satellite radiometers since those radiometers are exposed to more potential transmitters from the ground. Current missions such as the Soil Moisture Ocean Salinity (SMOS) satellite has had numerous issues with RFI [Kerr (2012)] that skews the data that they collect and in some cases made the data unusable for soil moisture measurements [Richaume (2012)].

Therefore there is ongoing work in detecting and mitigating this problem to help reduce the problem caused by RFI. Most radiometers do not retain any frequency information of the signal and so different methods have been developed to detect RFI [Forte et al. (2013)] by use of the kurtosis statistic method[De Roo et al. (2007)] or polarization signature method. To mitigate the offending signal, mechanical filters are used to selectively filter out the offending signals [Misra et al. (2012)].

Using mechanical filters is effective in removing the offending signal but does add both weight and complexity to the radiometer. It also adds cost as it requires multiple filters in order to select the narrow band that contains the offending signal.

## CHAPTER 3. BACKGROUND

This chapter will examine background information on the basic operation of a radiometer, a software defined radio and background on the development platform used to build a software defined radiometer. We begin with an overview of a traditional radiometer and how this type of radiometer works. This is followed by high level examination on how a software defined radio operates. Finally we will discuss both the hardware and software selected and used for our development platform to create this software defined radiometer.

### 3.1 Radiometer Basics

The primary task of a radiometer is to measure power. While that statement sounds easy, there are many factors that go in to how well a radiometer can measure the power it observes. A better statement is that a radiometer's primary goal is to accurately measure the correct power within a certain degree of accuracy. In order to accurately and within a high degree of precision measure power a radiometer must take into account factors such as the system noise, the bandwidth of the signal and the stability of the system as a whole[Evans and McLeish (1977)].

In all radiometers there are six stages that is common in all radiometers. They are:

1. Source (antenna or  $T_A$ )
2. Amplification (Gain or  $G$ ),
3. Bandwidth restriction (filtering or  $\beta$ ),
4. Power detection ( $X^2$ ),
5. Integration ( $\tau$ ),

## 6. Output.

Figure 3.1 shows each stage as they relate to each other. We begin with our source which is often an antenna. Amplification or gain in the system then amplifies this signal so that it is easier to measure changes in our noise. Filtering can occur before or after the amplification stage and in some cases filtering is done before and after the filtering stage. Power detection extracts the power information from the signal. Because the signal is often noisy, we use integration to smooth our signal and improve our sensitivity. Finally our output is the total power information. This information may be as simple as a voltage output or may be a calibrated noise temperature.

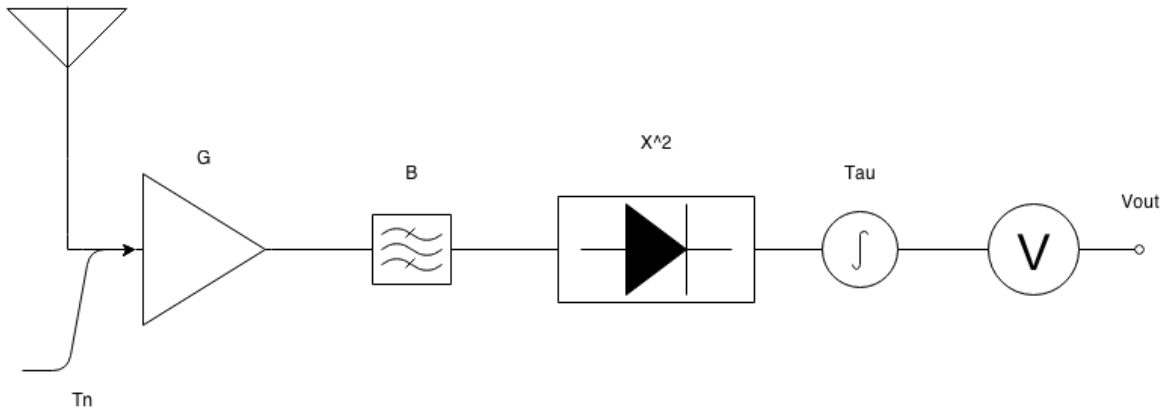


Figure 3.1 A total power radiometer block diagram

In figure 3.1 we have one more component that is common in all radiometers but is not a physical component or stage in the radiometer. That item is additional noise that gets added to the system from within the system itself is called system noise or  $T_N$ .

In addition to the system noise, another very common problem with radiometers is stability. Most instabilities in a radiometer are due to fluctuations that occur in the amplification stage or the Low Noise Amplifiers (LNAs) used. These gain fluctuations can be controlled to a point by closely monitoring and controlling both the voltage and the temperature of the LNAs. However, this is not an easy task and in some cases is not practical. Therefore, other methods have been developed to compensate for these fluctuations. There are three common types of

radiometers designed to adjust for gain fluctuations. They are:

1. Dicke radiometer,
2. Noise injection radiometer,
3. Polarimetric or correlating radiometer.

One of the first methods used is the Dicke radiometer which switches between the measurement of the antenna and a known source[Dicke (1946)]. By referencing this known source very quickly the Dicke radiometer can account for and greatly reduce gain fluctuations.

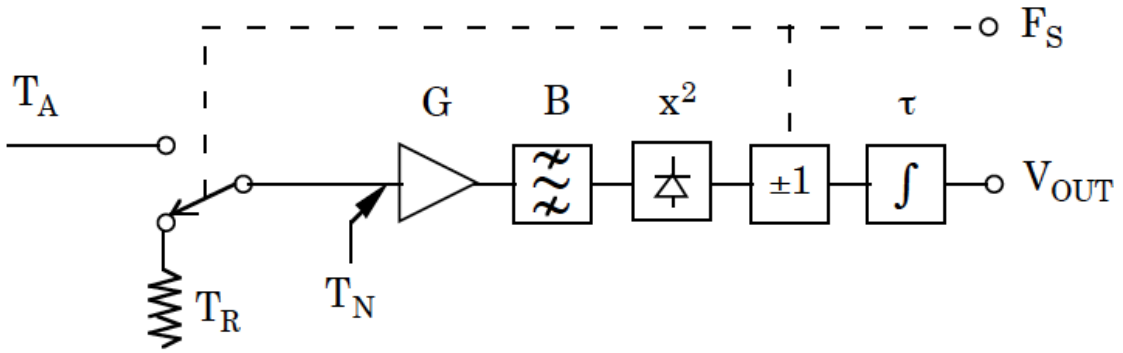


Figure 3.2 A block diagram of a Dicke radiometer

While a Dicke radiometer greatly reduces the fluctuation in the gain of the radiometer and improves stability, it does so at the cost of not seeing the object of interest while it is referencing the known source. This decreases the sensitivity of the radiometer.

A noise injection radiometer is a variation of the Dicke radiometer where a variable noise source is used and injected into the RF chain as seen in Figure 3.3. The output of this noise source is then adjusted so that the noise input plus the signal from our source is equal to the reference noise. This completely eliminates fluctuations however increases the system noise which also reduces our sensitivity of the radiometer.

Our source signal is often times assumed to be not polarized. However, this is not the case and an incoming signal often has some polarization. A correlating radiometer [Fujimoto (1964)]

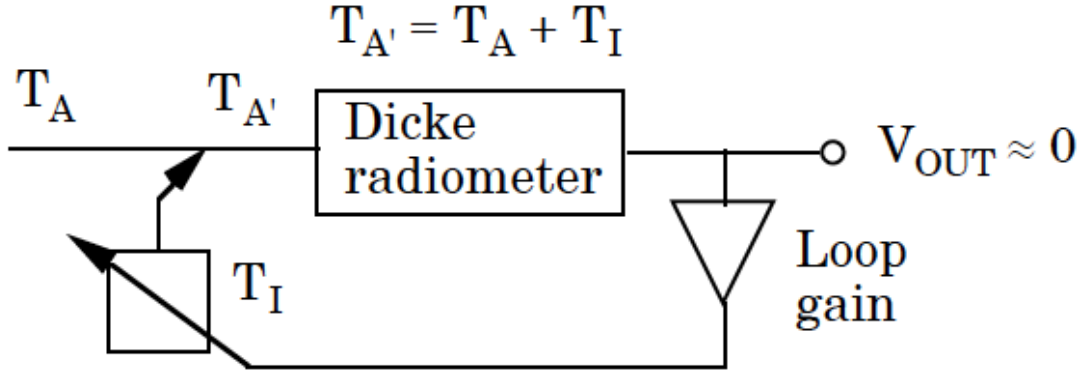


Figure 3.3 A block diagram of a Noise Injection radiometer

uses a dual polarization antenna to split the vertical and horizontal polarization of the signal. Each of these signals is then fed into a radiometer and our correlated. Since gain fluctuations or uncorrelated, they are reduced in the system. This reduces gain fluctuations and also helps maintain the sensitivity of the radiometer. However it adds a much greater complexity to the radiometer and requires two identical receivers.

### 3.1.1 Measuring RF power

To measure power in a radiometer, several factors are taken into consideration. To begin with we have the noise signal coming from the antenna. Our antenna is assumed to be looking at our target of interest and it is assumed that we can relate the antenna noise to the noise from the source. It is often easier to refer to this noise as the brightness temperature. Therefore, the brightness temperature of the source can be related to the brightness temperature at the antenna. We will refer to this brightness temperature as  $T_A$ .

Figure 3.4 shows us an ideal radiometer. That is a radiometer that has an input from the antenna,  $T_A$ , a known bandwidth denoted as  $B$  or  $\beta$  and a known gain denoted as  $G$ . At the end of the block is the detector, which measures the power from the radiometer.

The power coming from the antenna is the combination of the following items:

1. Gain or  $G$  of the system,



Figure 3.4 The ideal radiometer block diagram

2. Bandwidth or  $\beta$  of the system,
3. Signal source or  $T_A$ .

To calculate our power from the radiometer, we multiply each item with the Boltzmann constant referred to as  $k$ . Equation 3.1 gives us the total power, in watts, of an ideal radiometer.

$$P = k * \beta * G * (T_A) (\text{watts}) \quad (3.1)$$

As discussed in the above section, the system noise is another component of the radiometer that needs to be addressed. Figure 3.5 shows the additional noise that is injected into the system.

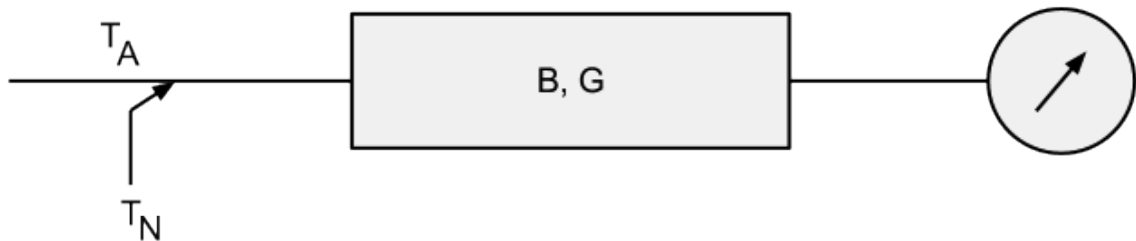


Figure 3.5 A more realistic radiometer model

As it can be seen, this additional noise is added to the noise coming from the antenna source. Therefore,  $T_N$  is added to  $T_A$  and our final equation for the power measured is shown in equation 3.2.

$$P = k * \beta * G * (T_A + T_N) (\text{watts}) \quad (3.2)$$

Figure 3.1 showed us a more typical radiometer and was discussed in the previous section. However, power detection and the associated voltage output has not been discussed. Power detection is accomplished typically with a square-law detector and this output is often run through an integrator to smooth the output[Leinweber (2001)]. Finally we have the output which is a voltage represented as  $V_{out}$ . This results in equation 3.3.

$$V_{OUT} = c * (T_A + T_N) * G \quad (3.3)$$

Here  $V_{OUT}$  is shown by the addition of both the noise from the system  $T_N$  and the noise from the antenna,  $T_A$  and multiplied by the gain in the system,  $G$  [Skou and Vine (2006)]. A constant factor  $c$  is useful for when we are looking at a radiometer like a Dicke radiometer in which the value of  $c$  is  $\frac{1}{2}$ . In most applications outside of a Dicke radiometer,  $c$  is 1 and can be ignored.

The voltage output from this radiometer is then either measured or may also be sampled by an analog to digital converter. This voltage then represents the total power measured by the radiometer, however this measurement is not calibrated.

### 3.1.2 Integration and filtering

Filtering with a traditional radiometer is usually accomplished by using mechanical filters. Often these are band-pass filters that limit the bandwidth that the radiometer sees. Other filters, such as a low pass filter are also used, but usually to smooth out the output from the square law detector. Another item used to help smooth out the signal from the square law detector is an integrator.

A RC filter is analogous to an integrator where the R and C values determine our time constant and our integration time for the filter[Aitken (1968)]. We know a RC filter is analogous to an integrator by looking at equation 4.3.

$$\frac{1}{RC} \int V_i dt \quad (3.4)$$

To begin with, we look at what an analog RC filter looks like.

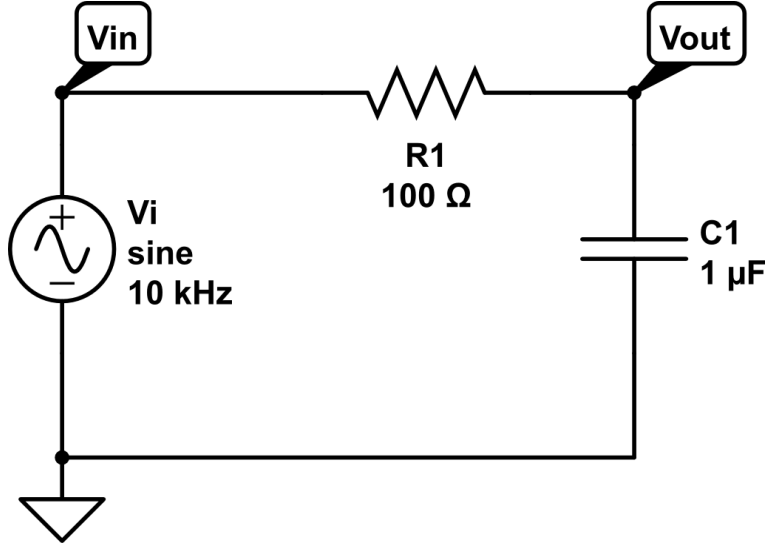


Figure 3.6 A simple RC circuit

This circuit can be represented by equation 4.4.

$$\frac{V_{in} - V_{out}}{R} = C \frac{dV_{out}}{dt} \quad (3.5)$$

This integration smooths out the signal from the square law detector and also improves our sensitivity of the radiometer. This will be further explained the next section.

### 3.1.3 Radiometer Performance Metrics

There are two criteria that determines how well a radiometer performs. The first criteria is with the sensitivity of the radiometer. This tells us how well the radiometer can differentiate between the information we want and the noise we do not want. The second criteria is stability. A radiometer needs to be calibrated to give us useful information. Stability refers to how much change or drift a radiometer is experiencing which in turn can affect the accuracy of our data.

*Sensitivity.* Sensitivity of the radiometer relates to the amount of power that the radio selects from the antenna. This selection is then dependent on the bandwidth that the radiometer is able to listen to. The radiometer however detects not only the signal of interest but also receives a noise signal as well. This noise is added to the signal and can not be separated from the signal. Because this noise is added to the signal, we must be able to determine a change in

the signal while the noise signal is also present.

To understand this, let us look at the example of  $T_A$  has a value of 200 K and  $T_N$  has a value of 800 K. Since  $T_N$  is added to our antenna signal, we have a total noise temperature of 1,000 K. This means that if we want to detect a change as small as 1 K, we must be able to measure the difference between 1,000 K and 1,001 K[Skou and Vine (2006)].

The ability of a radiometer to detect these small changes is the radiometer's sensitivity, or the standard deviation of the output signal from the radiometer. This sensitivity is also referred to as the Noise Equivalent Delta ( $\Delta$ ) Temperature or  $NE\Delta T$  and is shown in equation 3.6.

$$NE\Delta T = \frac{T_A + T_N}{\sqrt{\beta * \tau}} \quad (3.6)$$

The sensitivity of the radiometer is based on both the bandwidth,  $\beta$ , of the incoming signal and the integration time,  $\tau$ . As it can be seen in the equation, we want to have as much bandwidth as possible. In a traditional radiometer, this bandwidth is often fixed and is dependent on the band-pass filters used in the radiometer. We can however control  $\tau$  and a longer integration time will help improve the sensitivity of the radiometer to a certain degree.[Ulaby et al. (1981)]

*Stability.* Stability and accuracy are additional problems that need to be considered when looking at the radiometer system. To begin we can once again look at the power received equation 3.2.

As we look at this equation, we can see that if  $k$ ,  $\beta$ ,  $G$ , and  $T_N$  are constant, then stability can be assured. The Boltzman constant  $k$  is a known constant and we can also assume that our bandwidth,  $\beta$ , will also remain constant. Gain and the noise temperature however will vary.

Fluctuations in gain is the largest factor that affects stability in the system and this can be seen in equation 3.7. As discussed earlier, it is this factor that has been a driving force for changes to the design of a radiometer as demonstrated by the Dicke and Correlating radiometer designs.

Gain fluctuations are caused by two factors: the physical temperature of the amplifier and the voltage that feeds the amplifier. High accuracy voltage regulators can help control

fluctuations in voltages that can in turn affect the gain. A factor however that is harder to control is temperature. Various methods have been used to control the temperature when the radiometer is used in fluctuating temperature environments such as the outdoors or in space.

$$\Delta T_G = T_{sys} \left( \frac{\Delta G}{G} \right) \quad (3.7)$$

With stability we need to either attempt to stabilize the radiometer as best as we can or compensate for the gain fluctuations. Compensation has been discussed and three types of radiometers have been identified that attempt to compensate for these fluctuations. To control the stability many radiometers will use highly accurate voltage regulators and will control the temperature of the LNA through methods such as thermal electric coolers.

### 3.2 Software Defined Radios Basics

The basic concept behind a SDR is that it will digitize the RF signal as soon as possible. Once digitized, it is now evaluated by a computer, FPGA, or a dedicated System on Chip (SoC). A canonical software defined radio architecture is one that consists of a power supply, antenna, multi-band RF converter, and a single chip that contains the needed processing and memory to carry out the radio functions in software [Mitola (1995)]. This allows us to extract certain hardware functions, such as filtering, into the digital domain which can then be manipulated by software. Since software is now manipulating the signal, we can rapidly change what functions we execute on the signal by changing the software. This gives SDRs a high amount of flexibility as components that are normally done in hardware can now be done in software and can be changed by simply uploading new software or firmware to the system. This also gives us a benefit in cost as certain components are no longer needed and changes done in software do not require additional hardware to be added or to be swapped out.

An ideal software defined receiver simply has an antenna connected to an analog to digital converter which sends information to a processing unit such as a Field Programmable Gate Array (FPGA) or computer. For a transmitter, we reverse it and use a digital to analog converter to produce the correct waveform which is then transmitted by the antenna. In reality,

SDRs require some additional hardware to make a viable working transceiver. Amplification is still required to amplify the incoming signal and to amplify the signal going to the antenna. Some SDRs also use a mixing stage to move a high frequency signal to a lower frequency signal. This allows for less expensive analog to digital and digital to analog converters to be used.

### **3.2.1 Software Defined Radio Normal Operation**

Software Defined Radios (SDRs) are used for a variety of applications but their primary application has been in the area of communications. They appeal to applications where being able to change a modulation scheme or filter on the fly is desirable. In these areas, SDRs often outperform a traditional hardware only radio with their ability to rapidly change their operations by simply changing their software. Early SDRs were expensive due to the high costs in the analog to digital converters (ADCs) needed and in the high speed Field Programmable Gate Arrays (FPGA) used. In recent years however, the cost of SDRs have decreased due to the cost of these key components decreasing in cost as well. Even though the cost has gone down the performance of SDRs have increased and this has lead to new developments in applications for using SDRs in new and different ways.

Software defined radios have been used in a number of applications. Some applications they have been used in are:

1. Cellular communications,
2. Wireless local area networks,
3. Personal area networks,
4. Digital broadcast.

There are of course other applications than those listed and more applications added as new communication methods continue to evolve [Jondral (2005)]. But this is the strength of a software defined radio, it is capable of performing all of these operations and can be adapted to new ones by simply updating the software that defines it.

### 3.3 Software Defined Radio Development Platform

The work of this thesis is to use an off the shelf software defined radio (SDR) to perform the same operation or better of a traditional analog radiometer. Using a SDR radio also means that we are able to be more flexible in how the radiometer performs, is capable of frequency agility and adapting to changing conditions such as interference. Using a software defined radio also allows for implantation of different radiometer types such as a correlation radiometer or a polarimetric radiometer that uses Stokes parameters [Wang et al. (2012)]. Normally, these require changes to hardware, but all of these types of radiometers can be implemented in software increasing the flexibility of the system.

#### 3.3.1 Hardware Platform

The key component for a software defined radio radiometer is the hardware that will do most of the work of sampling and processing the signal. The equipment selected for this work is the Ettus Research Group N200 SDR and can be seen in figure 3.7. The N200 has the following features that made it well suited for our specific application:

- Dual 14-bit ADC,
- 50 MS/s Gigabit Ethernet streaming,
- Modular daughter-board system for RF front end

This SDR utilizes daughter boards as the RF front end to the SDR and up to two daughter boards may be installed into a N200. Another important reason the N200 is selected was due to its ability to handle up to 50 MHz of bandwidth to the computer and up to 25 MHz of RF bandwidth per daughter-board plugged in to the SDR. This means that it is possible to have two receive cards that can stream up to 25 MHz bandwidth each.

The N200 utilizes a flexible architecture through the use of daughter-boards for a variety of RF interface systems based on the frequency range desired and if receive and/or transmission is needed. Figure 4.4 shows the overall architecture of the N200 SDR. These daughter boards directly receive the RF signal and then outputs the analog I and Q signals that are then sampled



Figure 3.7 The USRP N200 from Ettus Research (Image from Ettus Research Website - [www.ettus.com](http://www.ettus.com))

by the N200 A/D converter for reception or receives the I and Q values from the N200 D/A converter for transmission.

The flexible architecture of the N200 and the ability for it to handle large amounts of bandwidth made this hardware ideal for the software defined radio radiometer work done in this thesis.

*The DBSRX2 Receiver.* The daughter board selected is the DBSRX2 card as this card is receive only and operates between 800 MHz and 2.4 GHz. An image of the daughter-board can be seen in figure 3.9. The DBSRX2 also has built in amplification that is adjustable through software. These daughter boards have the required RF hardware for the signal to be processed. In this application it was required that the signal was detected at 1.4 GHz with a bandwidth of 20 MHz. The DBSRX2 receiver met this requirement and was selected to be used with the N200. In this radiometer application transmission is not needed and is illegal in the 1.4 GHz band, which is reserved for passive radiometer applications.

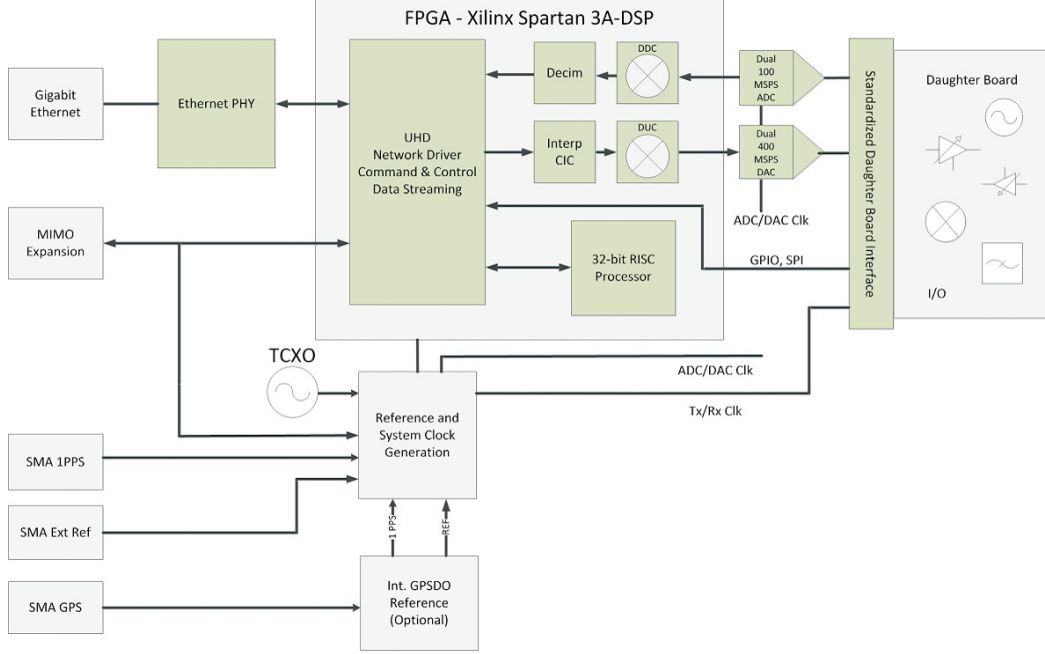


Figure 3.8 A block diagram of the Ettus N200 SDR. (Image from Ettus Research Website - [www.ettus.com](http://www.ettus.com))

The DBSRX2 has several key components on it that is used to take the analog RF signal and prepare it for digitization by the analog to digital converter. First the signal is amplified through a Programmable Gain Amplifier (PGA). This PGA is accessible from the software and can be configured by the software. Next the signal goes into a direct-conversion integrated circuit that directly converts the RF signal to analog I and Q values. The integrated circuit, a Maxim MAX2112 device, also includes a Low Noise Amplifier (LNA), mixer and Low Pass Filter (LPF). This essentially amplifies the signal, mixes into baseband and then applies a low pass filter.

These analog I and Q values are then passed to the N200 to be sampled by the analog to digital converter. The IQ values are differential signals to minimize noise possible interference.

Since we are using the DBSRX2 after the LNAs that are already in use, the noise temperature added by the DBSRX2 will be small. The DBSRX2 adds approximately 5 dB to the noise factor of the system. Again though, since this is at the end of the RF chain, the total contribution of the DBSRX2 to the overall system noise temperature is small, and has been calculated to be 1.05 dB to the overall noise factor of the system.

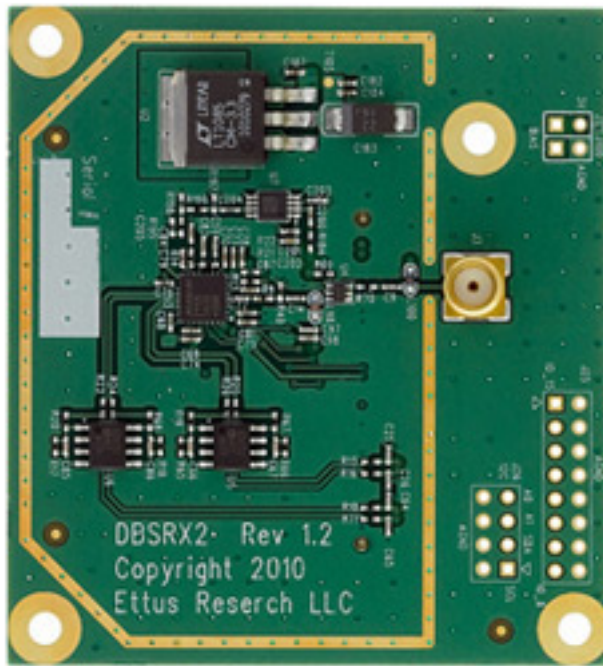


Figure 3.9 The DBSRX2 daughter board from Ettus Research (Image from Ettus Research Website - [www.ettus.com](http://www.ettus.com))

### 3.3.2 Software Platform

Software of course plays a critical role in a software defined radio and also in our software defined radio radiometer. There are two pieces of software that are in play with the software defined radio we are using. The first is the firmware that is used in the FPGA of the N200. This firmware provides low level processing of the signal so it can be sent to the software located on the computer. It also provides a link for controlling key aspects of the software defined radio such as additional gain, bandwidth and the center frequency. This firmware is already pre-loaded into the FPGA by Ettus Research and can be upgraded through tools provided by Ettus Research.

The second is the software that is running on the host computer. It is this software that provides the calculations on the I/Q data to give us the information we need and also creates a GUI for the user to interface with the radio. For this software, we will be using GNURadio, an open source software program that is used in software defined radios including the N200 SDR

that we have.

GNURadio will be used to do all signal processing that is needed. GNURadio is an open source software define radio framework that runs on multiple OSes and offers a rich set of features. In addition, GNURadio is well supported by the Ettus Research group and is the preferred software for interfacing with their hardware.

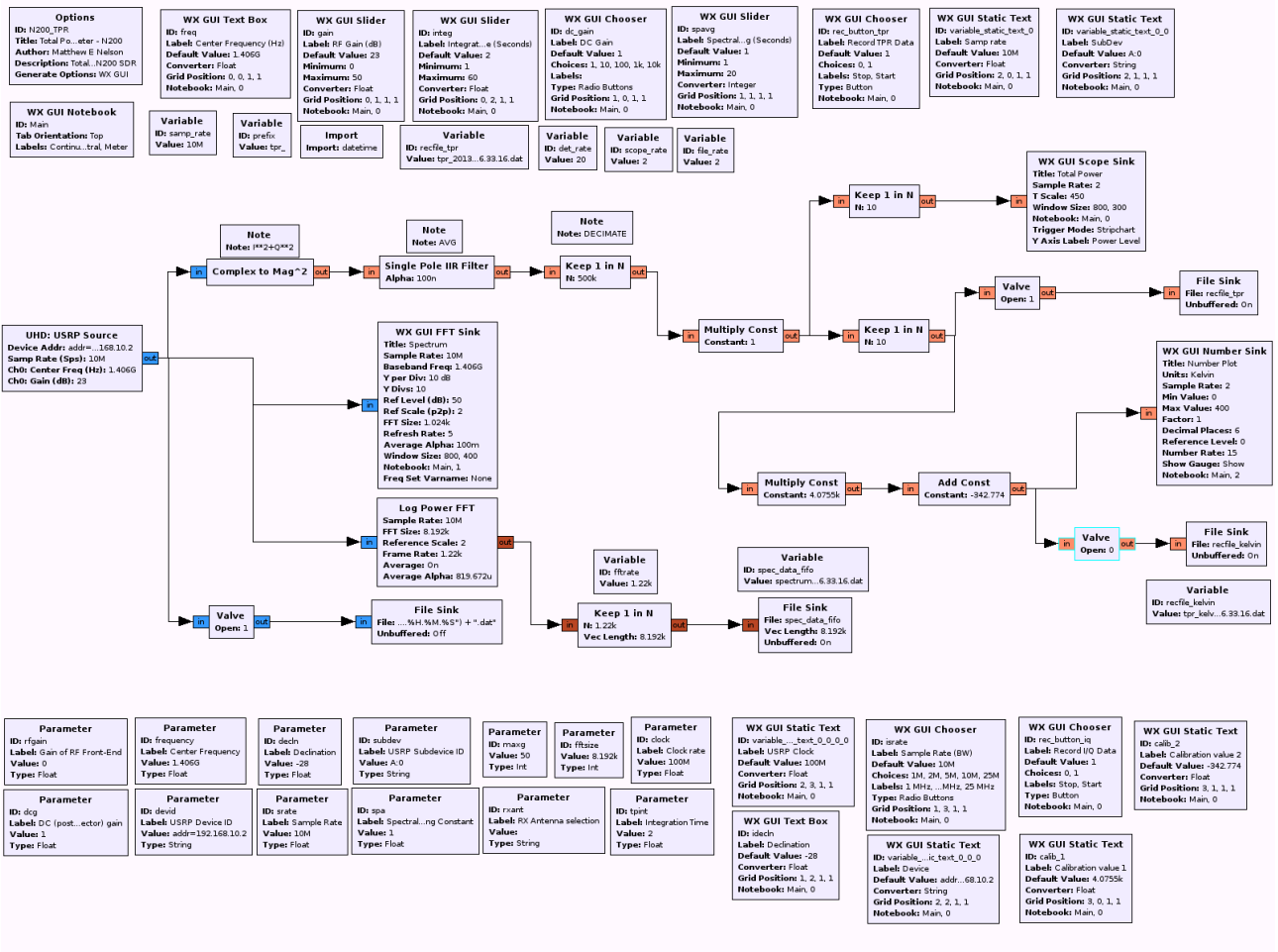
An easy to use interface was another driving requirement for our implementation of a radiometer in a SDR. GNURadio helps us with this through the use of the GNU Radio Companion or GRC. This was important as it was anticipated that operators of the radiometer have a limited knowledge about programming. GRC uses a simple to use graphical system to design and build radio components in software.

GNURadio Companion works by having the common functions as blocks that can be picked and placed on the screen. Once placed, the blocks can be wired up, much like LabView, and the flow of data can be controlled in this fashion. While GNURadio Companion provides most of the essential blocks used in most applications additional blocks can be added if needed. This is because GNURadio is built using Python and the blocks in GNURadio Companion are simply blocks of Python code. To compile a GNURadio Companion flow diagram, you simply run the sheet, which then generates the Python code that is then executed.

GNURadio uses a combination of Python and C++, where Python handles most of the interface and the C++ is most of the drivers and low level interface to the hardware. This allows for an easy to use system but still meets the demanding performance needed for handling large amounts of data.

GNURadio Companion also includes blocks that allow it to create a GUI type of interface. The typical method it uses for this is using wxGUI although GNURadio Companion does also include blocks that can use QT for generating widgets as well. However, the wxGUI tends to work better and has better support in GNURadio than QT.

Through these blocks we are able to only manipulate the data we need to perform a total power radiometer in software but to also create a user interface that allows us to control the radiometer as well. We are also able to display the information in real time so the user can see changes in power and even monitor spectral information during the operation of the radiometer.



## CHAPTER 4. SOFTWARE DEFINED RADIOMETER IMPLEMENTATION

### 4.1 Introduction

One of the principal goals with this research was to implement a fully functioning total power radiometer within software. The N200 provides us the link between the RF signal captured by the antenna and converts that to a format that can now be used by the to manipulate the signal. Once the signal has been passed to the computer, GNURadio will implement the correct algorithms to detect the power within the signal, filter and output the information. One of the advantages of course with a SDR is that filtering can also be done within the software. In addition, thanks to the WxGUI that GNURadio uses, we can also build a user interface that can control several key variables that are useful for us. This includes controlling the gain on the programmable gain amplifier on the DBSRX2 card, the sampling or bandwidth of the signal, the center frequency, and also the integration time. All of these can now be controlled in real time as well. GNURadio will also store the power data so that we are able to do further analysis of the data using a software program like Matlab or Python. Because GNURadio is a very flexible system we are able to do more with the signal such as filtering, polarimetric radiometer, and frequency analysis. We are also able to add additional features and improvements through updates to the software.

### 4.2 Requirements

To help us quantify the required performance of the radiometer, we referred to information provided to us by Dr. Brian Hornbuckle but also derived from existing radiometers. As stated earlier, although a radiometer measures power, we often convert this to an equivalent brightness

temperature. Specifically, we are looking at the brightness temperature of the antenna added to the brightness temperature of the object of interest. We also have to be able to detect a minimum amount of power. Since changes in noise can be small, the better the sensitivity of the radiometer, the better we can detect these small changes.

The requirements given are outlined in the table below.

Table 4.1 Required Radiometer performance

Parameter	Value	Units
Minimum bandwidth	20	MHz
Operational frequency	1400 - 1420	MHz
$NE\Delta T$	1	Kelvin

### 4.3 Theory of Operation of a Software Defined Radio Radiometer

### 4.4 Mapping Traditional Radiometer Functions to a Software Defined Radio Radiometer

### 4.5 System overview

#### 4.5.1 Control of the SDR Hardware through GNURadio

The N200 sends all data across the 1 Gbps connection to be read in by a host computer running GNURadio. This data is the raw I/Q values that is read by the on board A/D and processed by the on board FPGA. An example of a very simple GNURadio software implementation would simply take this data and store the data to a hard drive in a file. This can be very handy if we want to simply record the data and then process it later. However, depending on the sample rate, it can consume a large amount of storage. A short recording can easily consume 1-2 GB with a sample rate of 10 Msps. It also does not give us any immediate feedback on the radiometer and it does not give us controls of the radiometer such as frequency, integration time or other key variables. Fortunately GNURadio has tools that allows us to build up a very rich application that is able to give us the data we need and control the software defined radio as well.

The GNURadio Companion allows us to create python code that is used to not only receive the data from the SDR but also perform signal processing on the incoming information. Additional controls are added that allow for tuning of the signal processing parameters and control of the radio functions. This allows us to build up an application that can be run on any computer that is capable of running GNURadio.

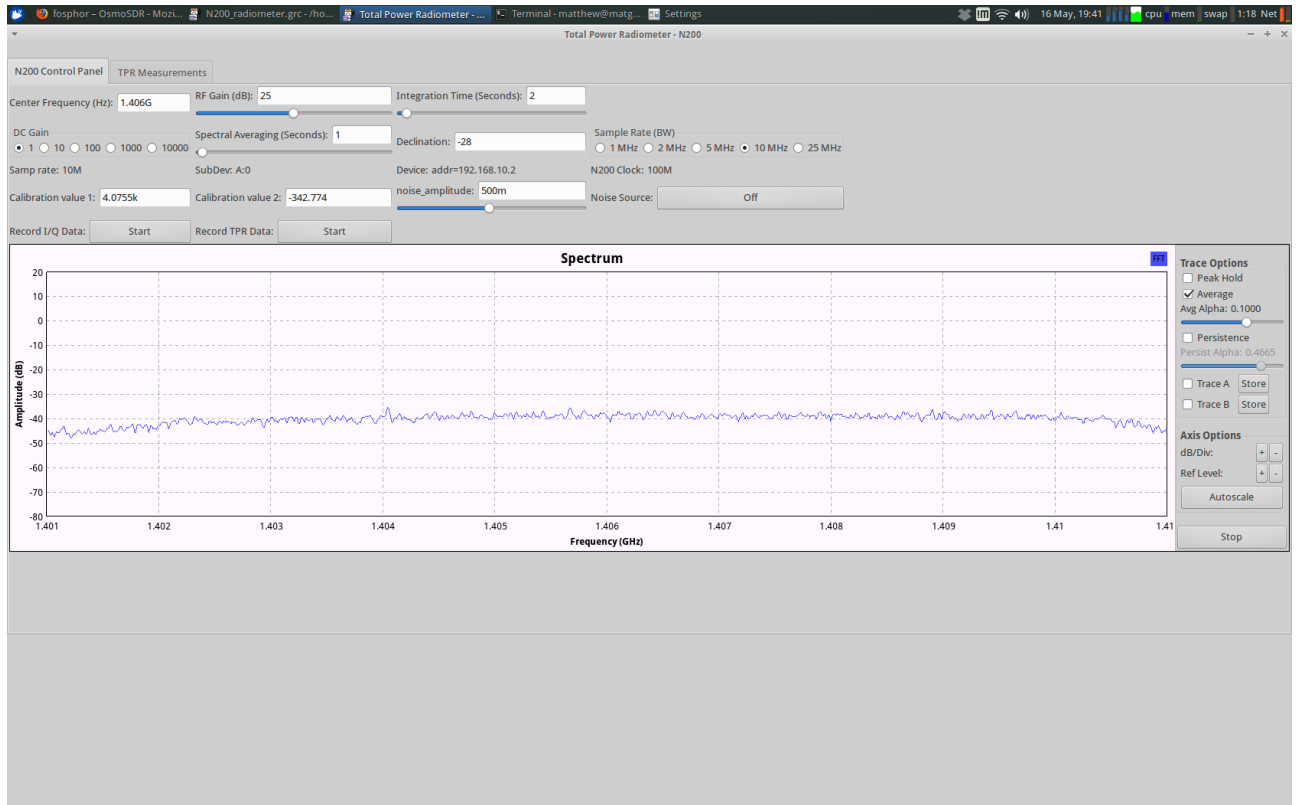


Figure 4.1 A screenshot of the interface made for communication with and controlling the software defined radio

Through this interface we are able to control several key aspects of not only the radio hardware within the SDR but also with the behavior of the radiometer as well. Hardware control of the SDR hardware allows us to change frequency and also adjust gain values within the N200. Bandwidth is another parameter that can be altered from here as well. Bandwidth affects the bandwidth for the RF signal, but also has an impact on the radiometer sensitivity as well. Additional controls allows for alterations to the radiometer and includes being able to adjust the integration time of the radiometer.

#### 4.5.2 Impact of the Controls Related to Radiometry

The controls that have been added for controlling the radiometer can have a large impact on the performance of the radiometer. There is a reason why these controls were added to the GUI for the radiometer and that is they play key roles in how the radiometer performs.

For any radiometer noise temperature is a large consideration and is critical to the design of the radiometer. One method to determine how well a radiometer is to look at the sensitivity of the radiometer. We can do this by looking at the smallest change in temperature the radiometer can see. We will call this the Noise Equivalent  $\Delta T$  or  $NE\Delta T$  of the radiometer. The equation for this is shown below.

$$NE\Delta T = \frac{T_A + T_{sys}}{\sqrt{\beta * \tau}} \quad (4.1)$$

$\beta$  can be changed by changing the sample rate of the SDR. The sample rate effectively controls the bandwidth in which the SDR is operating at. This also gives us a band-pass filter as well, since the SDR will not respond to frequencies outside of this bandwidth.

$\tau$  is the integration time for the radiometer. This parameter is set by the user through the GUI and allows us to change the integration time in seconds.

## 4.6 GNURadio Data Handling

Once we have the data that has been processed by the software defined radio we will want to display this information and be able to store the data so we can analyze it later if needed. Data display can be handled GNURadio where we can plot the total power over time. This allows the user to be able to visualize the total power and be able to determine if the total power has increased or decreased over the time window shown.

Although not usually needed for a total power radiometer we also have the ability to look at the signal in terms of a frequency versus amplitude. This allows looking for any unusual signals that may be interfering with the system or causing erroneous data with our radiometer.

Finally, we will want to store the data so we can do additional analyses on it at a later time. The GNURadio program allows us to store the data in two formats. The first format

is storing the raw I/Q data from the radiometer. This format allows us to playback the data through GNURadio at a later time. This can be useful for if we wish to change parameters in GNURadio such as bandwidth or integration time. It is also a good diagnostic tool as we can check that the signal coming in is clean or if we need to apply additional filters to remove an unwanted signal. This file may be quite large, consuming several gigabytes of data for a 20 MHz wide signal in a matter of minutes of record time.

The second format is the total power that has been calculated by the radiometer. This file is much smaller since much of the signal information has now been reduced to simple power versus time information. This allows for easy manipulation through any math program such as Matlab for analysis.

#### **4.6.1 GNURadio Data Display**

The information from the software defined radio can be displayed through GNURadio to show a number of things. Since we have both frequency and magnitude information we can display this information. We are able to also display the information that shows the total power that is being seen by the radiometer as well.

We are not limited to just total power from the radiometer. If the radiometer has been calibrated, those calibration points can be entered and GNURadio can calculate the calibrated noise temperature. Additional information may also be added as needed. For example, we are able to view the full spectrum that the radiometer sees. This can be a useful tool for looking at potential RFI issues.

### **4.7 Square-law Detector Performance**

The Square-law detector was added to our system in order to give us another reference point and to help verify the power output that the software defined radio. Performance of our square-law detector is based on two items; the sensitivity of the diode used in the square-law detector and the analog to digital converter used to convert the analog voltage to a digital value. The sensitivity of this device accounts for most of the performance factor of the system. In our system the output of this square-law detector is then feed directly into an analog to

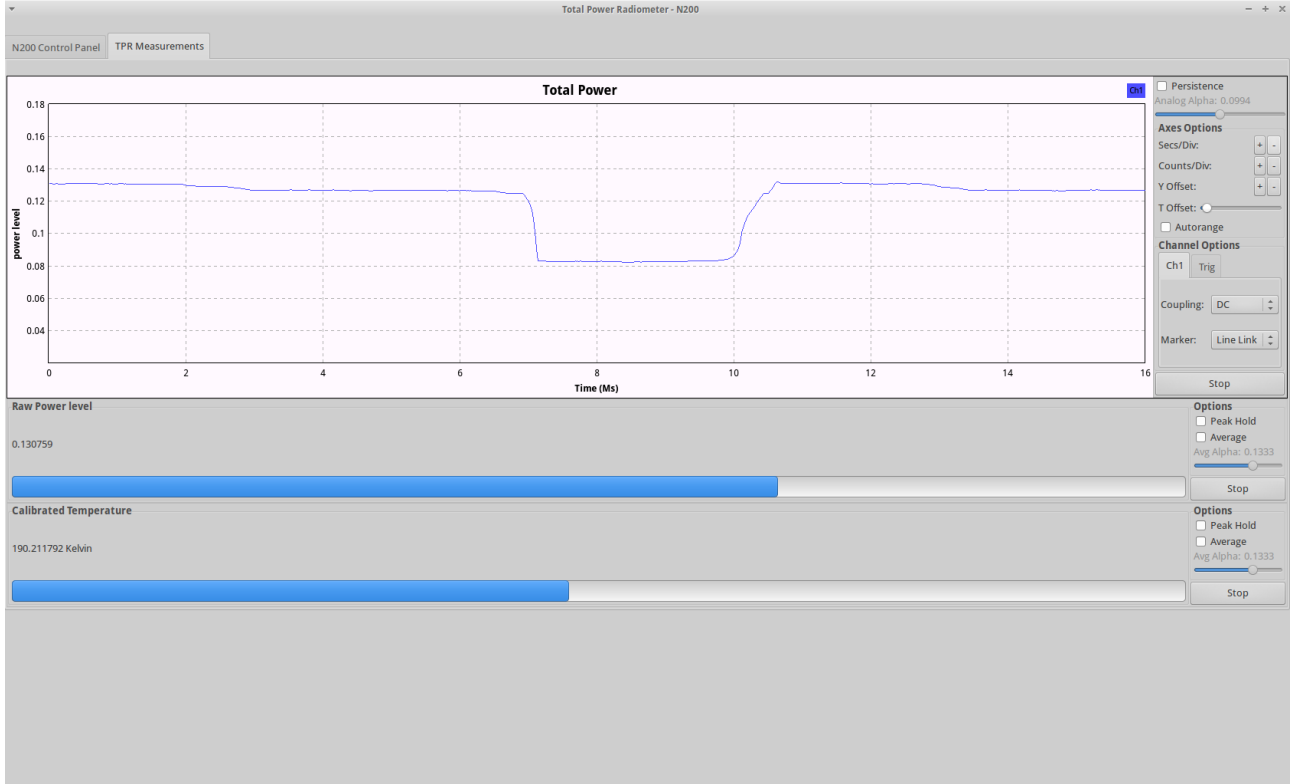


Figure 4.2 A screenshot showing the ticker tape display for the total power readings. In addition, raw and calibrated noise temperature is shown below.

digital converter. Therefore, the performance of this A/D converter needs to be accounted for as well [Terlep (2002)].

For our square-law detector, it has a noise output of  $25nV/\sqrt{Hz}$  at 100 kHz and will detect a signal as low as  $-60$  dBm. This works will with our needs since the RF front end brings the noise floor to approximately  $-30$  dBm.

## 4.8 Software Defined Radio Performance

Performance of the software defined radio is governed by the system that takes in the RF signal and then digitizes the signal. Once the signal is in digital form, we no longer are concerned about loss of performance due to additional noise that may get added to the system. For this reason, we attempt to digitize the signal as soon as possible.

For the N200 this is done by the DBSRX2 daughter-board that plugs into the N200 base

system. While this board does play a part in the overall system performance, because this sits later in the chain however the impact to the performance is low as shown in equation 4.14. However, this module does need to be in the frequency range of the radiometer, or in our case 1.4 GHz. This board meets that criteria. Ideally, we still want the noise figure on this board as low as possible, even though the impact is low. The DBSRX2 does meet this having a noise figure of approximately 5 dBm.

Requirements for this system was based on information provided by Dr. Brian Hornbuckle and was also based on requirements of a typical radiometer. This list is outlined in table 4.2 shown below.

Table 4.2 ISU Radiometer requirements

<b>Requirement</b>	<b>Value</b>	<b>Units</b>
Frequency Range	1400 - 1420	MHz
Bandwidth	20	MHz
Polarization	Dual	
Sensitivity	-30	dBm
Accuracy	1	Kelvin

#### 4.8.1 Hardware Requirements

The selection of the N200 SDR from Ettus Research was based on many of the requirements outlined in table 4.2. In addition, we wanted the hardware to be flexible but also affordable. There are many kinds of software defined radios on the market. However, we choose the N200 based on the availability of the device, the large community support, especially with regards to support by GNURadio, and because it meets and often exceeded the requirements stated above.

Flexibility was another key aspect of the N200 that made it an excellent selection for this research. The N200 uses a daughter board setup for bridging the RF interface to the rest of the electronics. Several daughter boards are available that have different frequency ranges and offer both receive, transmit and transceiver designs. For the radiometer we need to operate around 1.4 GHz and receive only. Based on those requirements we choose the DBSRX2 daughter board. This board is designed from 800 MHz to 2.3 GHz and has a fairly low noise figure.

The current RF front end to the radiometer is designed for a 20 MHz wide signal. This requirement was one of the main driving points for selecting the N200 SDR as it can support up to 50 MHz in bandwidth between the N200 and the host computer. This is accomplished by using a 1 Gbps Ethernet connection between the N200 and the host computer.

#### 4.8.2 Software Requirements

The driving force for the software requirement was to have a system that was easy to use yet powerful enough to handle the amount of data that is required. One reason for the development of this platform is to make radiometers more accessible to other researchers and other programs such as education and even amateur radiometer work. Therefore, ease of use was taken into consideration when selecting the hardware and the associated software used with it.

The data flow model for the hardware selected uses the FPGA to perform low level signal processing on the signal and moves high level processing to the host computer. This allows for less processing requirements on the physical hardware but requires a host computer that is able to process the incoming information. It also requires a software package that is able to process this information efficiently.

Because a requirement is an easy to use system GNURadio was selected as it includes GNU-Radio Companion (GRC). GRC is a supplemental program which uses a graphical interface for creating the radio environment. It also includes options to create a user interface during the operation of the N200 as well. This allowed us to rapidly create both the critical radio components needed for the radiometer and also a control interface.

This software meet the criteria of allowing a simple to use interface to be built and used in the control and data recording of the information required. It also uses a simple interface for making changes to the program. These changes can be both in the GUI and also to how the program processes the information.

## 4.9 Software Defined Radiometer Theory of Operation

### 4.10 Mapping analog radiometer functions to a software defined radiometer

In order to recreate a radiometer in software we need to identify the key components of a radiometer and then recreate those components in software. As discussed in chapter three, the three components identified that are key to a radiometer is listed below.

1. Power detection
2. Integration
3. Bandwidth limitation or filtering

The following sections will now examine how these items are mapped from their analog component to the software or digital component.

#### 4.10.1 Power detection

Power detection is a key ability that allows a radiometer to function. At its core a radiometer is a power detector. Therefore, the implementation of power detection is a crucial function of a software defined radio radiometer.

To implement a total power radiometer in software we first need to look at how we implement a total power radiometer traditionally. Traditionally, a square law detector is used to detect the average power that is seen by the radiometer. This simple device uses a diode that gives a small voltage output based on the RF power present. This small voltage is then amplified and can now be calibrated with a known source to give us a noise temperature.

To implement this in software we need to build a square law detector mathematically. We can then give this to the software defined radio to process the information accordingly. A square law detector mathematically is the sum of the squares. Once the signal has been digitized, it is expressed in data bits of I and Q, which represent in-phase and quadrature-phase of the signal. By squaring each term, we get the desired result of the power of the signal [Sarijari et al. (2009)][Rashid et al. (2011)] can be shown in equation 4.2.



Figure 4.3 A block diagram showing how the radiometer performs the equivalent square law detector in software.

### 4.11 Integrator through a IIR Filter

Another step that we typically do in a traditional radiometer is to integrate the signal over time. This gives us an average of the signal and smooths out the output. In addition, we will show later that the integration time can be adjusted to help improve our sensitivity of the radiometer.

In a traditional radiometer, we can integrate by using a simple integrator circuit, which consists of an op-amp, resistor and capacitor. This circuit configuration is also equivalent to a low pass filter circuit as well, and the two are interchangeable. We can then look at how we filter in the digital domain, and this is done with an infinite impulse response filter or IIR. We can use this digital filter to then integrate the signal for our total power radiometer. Again, this relationship between the IIR filter and the integrator is explained in chapter 2 and is mathematically shown in equation 4.12.

#### 4.11.1 Software Defined Radio Radiometer

A Software defined radio consist of both hardware and software that allow it to perform the operations of a radio or communication channel. A software defined radio used for radiometer applications is identical to a software defined radio used for, as an example, a 802.11b radio with one major difference. Since we need to amplify the signal more than what most communication applications require; we do require more powerful or additional LNAs to boost this signal. In addition, since the first LNA plays a major role in the overall system noise and this system noise does affect performance of the radiometer, the selection of this LNA is important. However, all other components are the same components used in other applications.

A software defined radio radiometer behaves analogous to a more traditional radiometer and thus the application is the same as a traditional radiometer. This includes applications such as radio astronomy that includes applications in Earth Science such as soil moisture and ocean salinity[Ruf and Gross (2010)]. A software defined radio radiometer can also allow for new application development that can expand the remote sensing field. Since we have moved the majority of the hardware to software this allows us to further shrink the size and weight of the radiometer. This allows for other radiometer applications such as Unmanned Aerial Vehicles (UAVs) for scanning soil moisture and ocean salinity remotely[McIntyre and Gasiewski (2007)].

We will now introduce the three major components that make up a software defined radio radiometer.

#### **4.11.1.1 N200 Software Defined Radio**

The key component for a software defined radio radiometer is the software defined radio or SDR that will do most of the work as a radiometer through software. The equipment selected for researching into this topic was the Ettus Research Group N200 SDR. The SDR selected utilizes daughter boards as the RF front end to the SDR and up to two daughter boards may be installed into a N200. This is an important consideration as one of the requirements is to be able to look at both the V-Pol and the H-Pol signal coming from the antenna. By having a dual receiver SDR it is possible to correlate the signal and other signal analysis can also be done. Another important reason the N200 is selected was due to its ability to handle up to 50 MHz of bandwidth to the computer and up to 25 MHz of RF bandwidth per daughter-board plugged in to the SDR. This means that it is possible to have two receive cards that can stream up to 25 MHz bandwidth each.

The N200 utilizes a flexible architecture for a variety of RF interface systems based on the frequency range desired and if receive and/or transmission is needed. These daughter boards directly receive the RF signal and then outputs the analog I and Q signals that are then sampled by the N200 A/D converter for reception or receives the I and Q values from the N200 D/A converter for transmission.

The daughter board selected is the DBSRX2 card as this card is receive only and operates

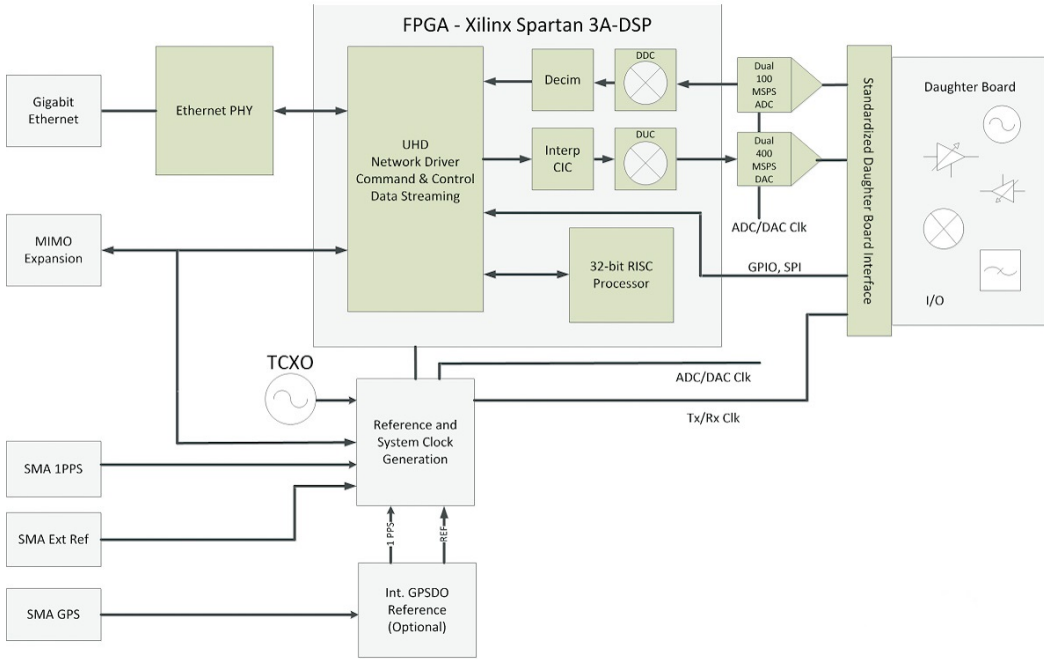


Figure 4.4 A block diagram of the Ettus N200 SDR

between 800 MHz and 2.4 GHz. The DBSRX2 also has built in amplification that is adjustable through software.

#### 4.11.1.2 GNURadio Software

For the software portion of the radio, we settled to use GNURadio, an open source software package that is well supported by the community and by the Ettus Research Group and the N200 SDR. GNURadio also comes with what is known as GNURadio Companion or GRC. This program provides us with a GUI interface and allows for the drag and drop of blocks that represent certain functions that can be used with the SDR. GNURadio and GRC use Python as its main scripting language and GNURadio uses C++ code for directly accessing the hardware. The hardware interface for the N200 is provided by Ettus through drivers that allow GNURadio to talk to the hardware. Like GNURadio, these drivers are also available to all platforms. Ettus has released these drivers to the open source community and continues to support the hardware drivers and GNURadio integration.

GNURadio operates on multiple platforms including Windows, Mac OS X, and Linux.

Linux is by far the most popular platform to work on and most of this thesis research was completed within the Linux environment. Testing is also done though with a MacBook Pro running OS X 10.9. The OS X implementation is well supported and is installed through MacPorts. While windows is technically supported, it is often difficult to install and many of the libraries required are not 64-bit. For these reasons windows was not used for executing GNURadio, but was used for some of the data analysis using Python.

Through GNURadio, we can now write code that will take the data given to us from the SDR and manipulate the signal as we need to mimic a radiometer. The power detection, filtering and recording of this data is all done through GNURadio. This also means that we are shifting more of the computational power done on the signal from the FPGA to a computer running GNURadio. There are ways to change this behavior and upload code directly to the FPGA. However, for this thesis it was easier to debug and work with GNURadio by keeping the processing on the desktop computer. It does however mean that the host computer must be powerful enough to handle the signal and specifically the large bandwidth that we wish to send to it.

#### **4.11.2 RF Front End**

The RF front end plays a critical role in the radiometer as the LNAs used in the front end has a large impact on the system noise generated by the radiometer itself. A traditional radiometer utilizes both amplification through the LNAs and also includes filtering to the desired bandwidth. A SDR radiometer does not require the filters as we are able to create these in software, however the amplification stages need to remain.

A typical RF front end uses a 3 stage Low Noise Amplifier (LNA) to amplifier the noise while keeping the noise contributed to the system as low as possible. As with any radiometer, the first LNA is the most critical as it contributes the most to the overall system noise temperature. For this reason a LNA that did not have a large gain but had a low noise figure is chosen. The second and third LNA has higher gain values at the cost of a higher noise figure, although not by much. However, since they are further down the chain, they do not contribute as much to the total system noise. The reason for this is further explained in chapter 3.

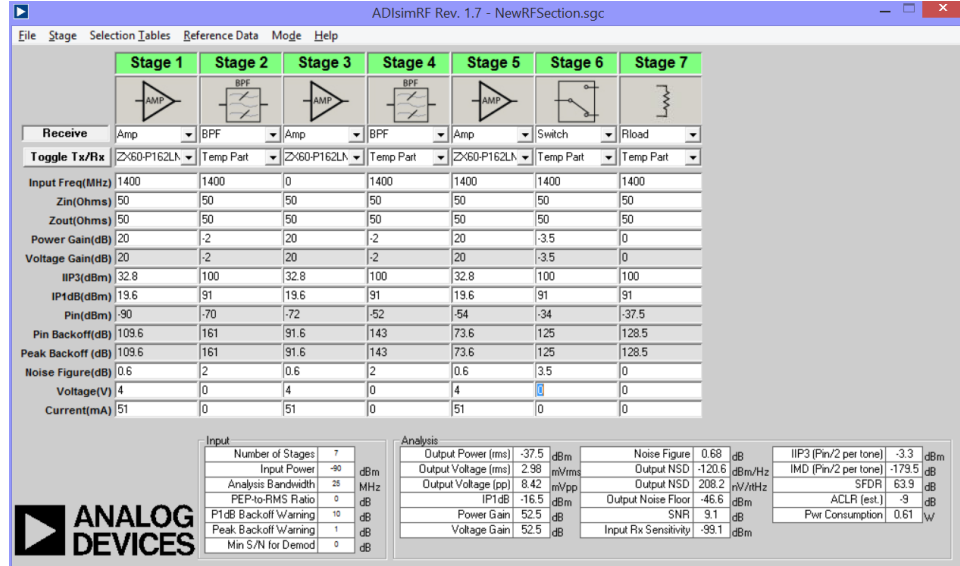


Figure 4.5 The ADISIMRF program used to verify the design of the RF Front End

#### 4.11.3 Software Defined Power Detection

A traditional radiometer uses a square-law detector which takes the input signal and produces a voltage that is proportional to the square of the voltage. This allows us to take an analog RF signal and convert the noise voltage that for all intents and purposes has a mean value of zero, and produce a noise power.

For a SDR, the incoming signal is sampled and converted to I/Q values by the hardware within the SDR. The I/Q values together can be used to reconstruct both the phase, frequency and amplitude information of the signal and can do so much more accurately than if we just recorded the frequency and amplitude information. In GNURadio we are then able to square these values within software which give us our peak voltage of the signal. This block in GNURadio mathematically performs what is shown in equation 4.2.

$$I^2 + Q^2 = P_{out} \quad (4.2)$$

Therefore, like the analog square-law detector we are taking peak voltage values, which has an equivalent noise voltage and a mean value of zero, and square them to produce a noise power that is proportional to the square of this amplitude.

Like the analog square-law detector, this signal will fluctuate rapidly and to improve the sensitivity of the radiometer we wish to integrate this signal. We now want to look at how we can replicate a RC filter or integrator in the software defined radio.

#### 4.11.4 Software Defined Integrator

A RC filter is analogous to an integrator where the R and C values determine our time constant and our integration time for the filter[Aitken (1968)]. We know a RC filter is analogous to an integrator by looking at equation 4.3. A SDR however operates in the digital domain at discrete intervals. One type of filter that can be used is the Infinite Impulse Response (IIR) filter.

$$\frac{1}{RC} \int V_i dt \quad (4.3)$$

To begin with, we look at what an analog RC filter looks like.

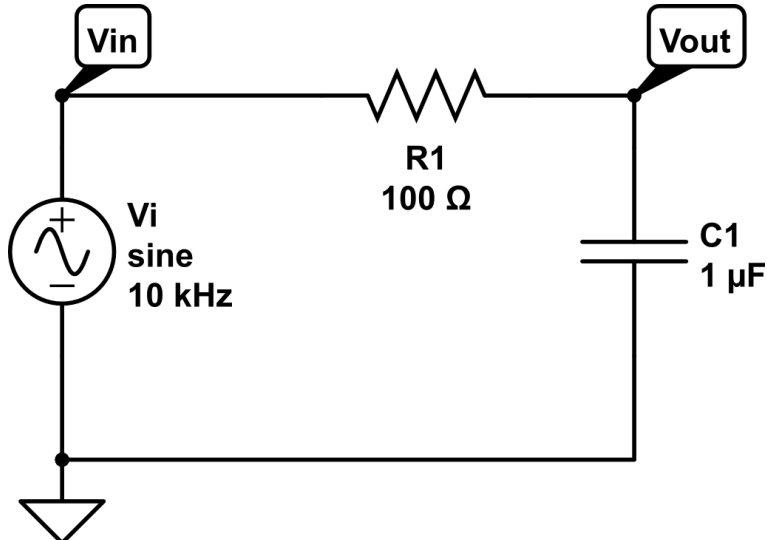


Figure 4.6 A simple RC circuit

This circuit can be represented by equation 4.4.

$$\frac{V_{in} - V_{out}}{R} = C \frac{dV_{out}}{dt} \quad (4.4)$$

A Finite Impulse Response (FIR) filter is a digital filter that can take an impulse signal and decays to zero after a finite number of iterations. This type of digital filter can be represented by equation 4.5 which mathematically expresses the FIR Filter.

$$y_n = \sum_{i=0}^{P-1} c_i x_{n-i} \quad (4.5)$$

This simply says that the nth output is a weighted average of the most recent P inputs.

An Infinite Impulse Response (IIR) filter is the same as the FIR filter, except that we add a summation term which feeds back the previous output.

$$y_n = \sum_{i=0}^{P-1} c_i x_{n-i} + \sum_{j=1}^Q d_j y_{n-j} \quad (4.6)$$

Equation 4.6 shows that a FIR filter is a IIR filter, except that  $Q = 0$ [Cross (1998)].

To get a better understanding on how the digital IIR filter relates to the RC filter analog, we can look at the Fourier Transform and the relationship of the input to the output in the frequency domain.

$$H(f) = \frac{\sum_{j=0}^{P-1} c_j e^{-2\pi i j f T}}{1 - \sum_{k=1}^Q d_k e^{-2\pi i k f T}} \quad (4.7)$$

In equation 4.7,  $f$  is our frequency in Hz and  $T$  is the time between samples in seconds and is related to our sampling frequency.

We now want to show the link between our analog RC circuit and the IIR filter. Looking at equation 4.4, which represents the differential equation relating the input voltage  $V_{in}$  to the output voltage  $V_{out}$ , we can substitute for input and output of our IIR filter. Since we are now in the time domain, we need to define what  $T$  is and we can do that using equation 4.8.

$$T = \text{time between samples} = \frac{1}{\text{sampling rate}} \quad (4.8)$$

We can now relate our input voltage to the input to our IIR filter and the output voltage to the output of our IIR filter.

$$x_n = v_{in}(nT) \quad (4.9)$$

$$y_n = v_{out}(nT) \quad (4.10)$$

We can now rewrite our difference equation with  $x_n$  and  $y_n$ .

$$\frac{x_n - y_n}{R} = C \frac{y_n - y_{n-1}}{T} \quad (4.11)$$

Finally, we can solve for  $y_n$  which results in our final equation for showing how a IIR filter is related to an RC filter.

$$y_n = \frac{T}{T + RC} x_n + \frac{RC}{T + RC} y_{n-1} \quad (4.12)$$

It can be seen that an IIR filter can have the same frequency response as we expect from an analog RC filter. As our sampling rate approaches infinity, the approximation gets closer to the original response from the analog RC circuit.

For the cutoff frequency of a RC circuit, we know that it has the relationship shown in equation 4.13.

$$f_c = \frac{\sqrt{3}}{2\pi RC} \rightarrow RC = \frac{\sqrt{3}}{2\pi f_c} \quad (4.13)$$

The  $RC$  term gives us our time constant of the circuit and can be used to calculate out our coefficients. We are not concerned about the actual values of  $R$  and  $C$  with our IIR filter, instead we just need the product of  $R$  and  $C$ .

In GNURadio most of the work is done for us. We can simply enter in our desired cutoff frequency and GNURadio will calculate our IIR filter coefficients. However, this shows that an IIR filter works much like an analog RC low pass filter.

Like a traditional radiometer, the SDR will use an antenna to look at the target of interest. SDRs still use a RF stage that takes the power from the source and amplifies it. The difference though begins after that. A SDR will then sample and generate I and Q values that represents the amplitude and phase of the signal. From there, this data is sent to a computer to be

processed. We can then use this information to calculate the power that is being seen. In addition, we can manipulate the signal in other ways such as applying a filter to filter out an unwanted source.

#### 4.11.5 SDR Radiometer Summary

As we have shown the two of the major components of a traditional radiometer, the power detection and integration of the signal can be replicated in software and therefore can be implemented in a software defined radio. The information can now be stored, displayed or both for further analysis.

There is one component of the software defined radio that we are not able to implement in software and that is with the signal amplification. This however does play a major role in the performance of the radiometer and is a key element that should not be overlooked. While this is not implemented in software, it still plays a critical role in our software defined radio radiometer.

#### 4.11.6 RF Front End

Hardware with a software defined radio still plays a critical role. A traditional software defined radio will focus on digitizing the signal as soon as possible and the hardware used will be focused on performing that critical digitizing process. For a software defined radio radiometer, we still want to digitize as soon as possible, but we also need to consider our noise factor. Most software defined radios are designed for communication purposes such as implementing 802.11b or other wireless protocols. In these scenarios a higher noise factor is not as detrimental to the overall system as it is with a radiometer. This is because we have a known signal that is magnitudes greater than the noise floor. In a radiometer however, we do not have this large separation between the information we need and the noise of the system. And so our noise factor is a more critical component.

To counter this, we use Low Noise Amplifiers to amplify the signal but it can also help lower our noise factor. The first LNA in the chain contributes a large amount to our noise factor, so

by selecting a LNA that has a low noise factor, it reduces the noise factor for the system. This can be shown by looking at the equation that calculates our noise factor.

$$F = F_1 + \frac{F_2 - 1}{G_1} + \frac{F_3 - 1}{G_1 G_2} + \frac{F_4 - 1}{G_1 G_2 G_3} + \cdots + \frac{F_n - 1}{G_1 G_2 G_3 \cdots G_{n-1}} \quad (4.14)$$

While additional components do add to the noise figure, their contribution is significantly lower than the first LNA put in the RF chain.

This however is the only major change we need to do for doing radiometer work with an off the shelf radiometer. The rest will be done within software which is the principal reason for using a software defined radio.

## 4.12 General Specifications

In general, since we are digitizing the signal early in the RF signal chain, the noise figure of the RF components in the SDR do not add a significant amount of noise to the system. Additional performance metrics that require examination include how much bandwidth the system can handle. The information below outlines the specification of the devices used and its impact on the performance of the SDR as a digital radiometer.

## 4.13 Comparison of a Software Defined Radio Radiometer vs Traditional Radiometer

As outlined above, a software defined radio implements a traditional radiometer but in the digital domain. For power detection, we simply sum the squares of the I and Q values that have been sampled by the software defined radios analog to digital converters. As with a traditional radiometer, we also want to filter this information to remove much of the jitters that comes from the rapid fluctuations in the power readings. This is done using an IIR low pass filter, which mimics a traditional RC low pass filter. Once completed, we now have the total power reading from the radiometer and we can now store, display or do both with this information.

A traditional radiometer may also use an analog to digital converter in order to digitize the analog voltage from the square-law detector. Because the sample rate of this voltage is low,

almost any analog to digital can be used for this. At this point however, there is no frequency information, only the magnitude information is being retained and recorded.

## CHAPTER 5. EVALUATION AND EXPERIMENTAL DESIGN

Testing and verification ensures that the new components that we have added to the system are working as intended and has not caused a negative impact on the overall system performance. To do this, several tests were conducted and verification was obtained by using a well known method of detecting power in a radiometer, a square-law detector.

Testing began with the square-law detector as this was one of the first components that was obtained. Next, testing was done with the software defined radio as a whole. Finally, a cold bath test was done with both the software defined radio and with the square law detector as a system to verify both functionality and to compare the results from both devices.

Additional testing was also performed to test functions that may be added that are not found on a typical radiometer. This test involved injecting a signal and having the software defined radio remove the offending signal. A comparison was then performed to show the difference between the SDR radiometer which is able to remove the offending signal and the square-law detector which is not able to remove it unless additional hardware filters are placed in front of it.

In addition to these tests, a few real world tests were also done in the Spring of 2012 and the Spring of 2014. These tests were conducted by Dr. Brian Hornbuckle's E E 518 class as part of their lab requirement for the test. These test results can be found in Appendix 2.

### 5.1 Square-law Detector

To verify the results of the information that the software defined radio is obtaining a square-law detector is used to measure the power of the incoming signal in parallel to the software defined radio. This signal is split using a power divider so that the information will be the same

to both devices with the exception for the 3 dB plus insertion loss the power divider adds. This allows us to verify the software defined radio with a proven system. Square-law detectors have traditionally been used in radiometers and have been proven to work in radiometer applications. They are also a very simple device which means there is little that can go wrong with using them.

### 5.1.1 Analog Devices ADL5902

The square-law detector that we obtained is the Analog Devices ADL5902. The ADL5902 is a true rms responding power detector that has a square law detector, a variable gain amplifier, and an output driver. It also has a temperature sensor and will compensate for temperature variations. The output driver allows for the small signal from the square law detector to be amplified to a level that most analog to digital devices can detect. It should be noted that this is not an amplifier for the incoming RF signal, just to amplify the small signal from the diode. This driver however does have low noise and has a noise output of approximately  $25nV/\sqrt{Hz}$  at 100 kHz. The ADL5902 operates from 50 MHz to 9 GHz and in most cases can detect down to  $-60$  dBm. This works well in our application since the radiometer operates at 1.4 GHz and after the amplification stage we usually see between  $-40$  to  $-30$  dBm of power.

The specifications of the ADL5902 can be seen in Table 5.1 shown below.

Table 5.1 ADL5902 Specifications

Parameter @ 900 MHz	Value	Units
Frequency Range	50 to 9000	MHz
Dynamic Range	61	dB
Minimum Input Level, $\pm 1.0$ dB	60	dB
Maximum Input Level, $\pm 1.0$ dB	1	db
Logarithmic Slope	53.7	mV/dB
Output Voltage Range	0.03 to 4.8	V

The ADL5902 outputs an analog signal that falls between 0.03 volts and 4.8 volts. It outputs a change of 53.7 millivolt per dB detected by the ADL5902.

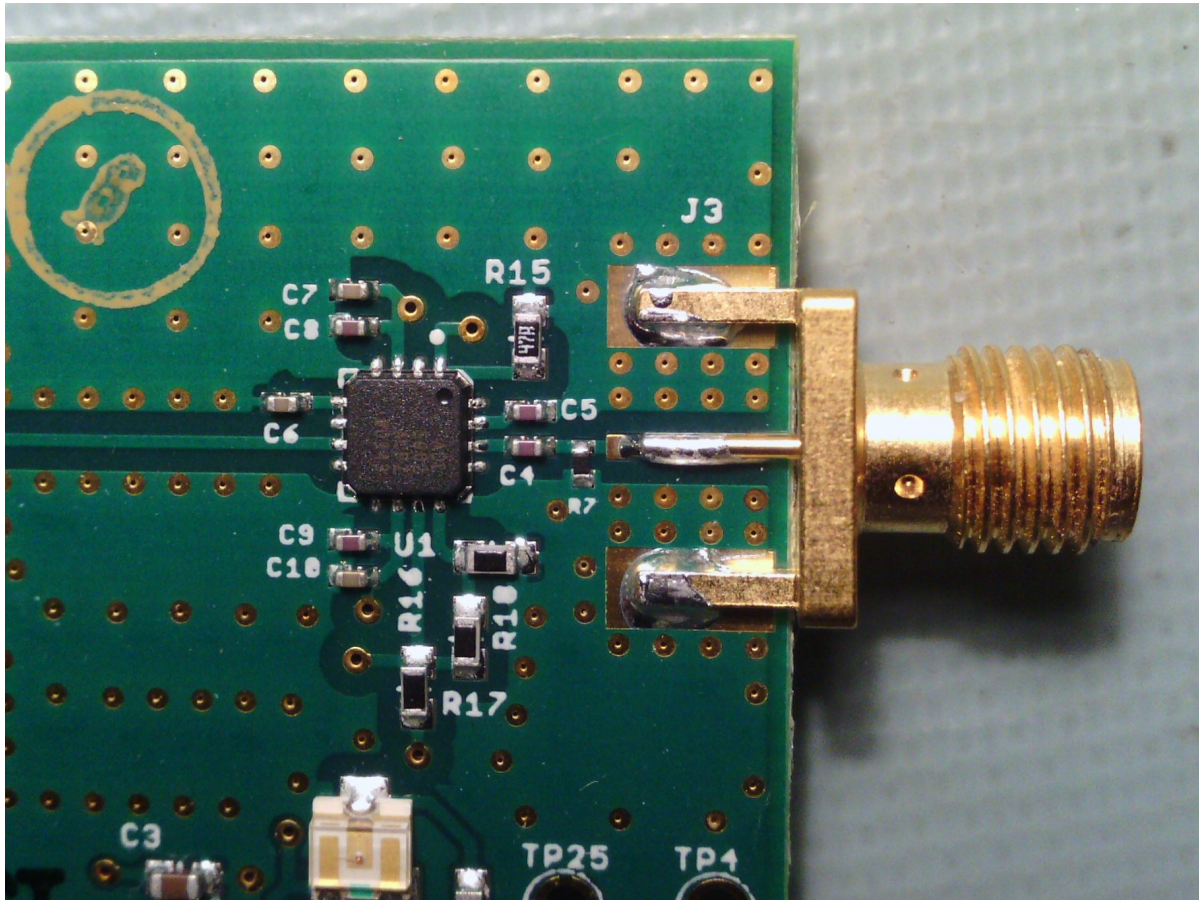


Figure 5.1 An image of the ADL5902 square-law detector used in these experiments

### 5.1.2 Data acquisition and storage

In order to analyze the data, a method was developed to acquire the data and store it for later use. For the N200 software defined radio, this is done automatically by the GNURadio program. Both the complete signal and the power information is stored to a file for later analysis. The square-law detector however outputs information as an analog voltage that is linearly proportional to the RF power measured. This required a system that can capture the analog signal from the ADL5902 and then send the data to be stored. The National Instruments USB-6009 data acquisition unit was selected as met the requirements for a easy to use yet had enough resolution to obtain accurate information. The USB-6009 unit has 8 analog inputs that can sample up to 48 ksps with a resolution of 14-bits which is more than adequate for the

experiments. To use the USB-6009 a fairly simple Lab View program was created to obtain, display and store the data from the ADL5902. This program retrieved the information from the USB-6009 and stored the data in both Labview's binary format and in a more human friendly ASCII format. The USB-6009 then connects to a host computer through the USB interface. This made obtaining the data and using device straightforward to use.

### 5.1.2.1 Labview Acquisition program

The Labview program was created to talk to the USB-6009 and then store the data. In addition, it is able to display in real time the current readings coming from the USB-6009. This was beneficial during testing of the program but is also good information to have while running an experiment.

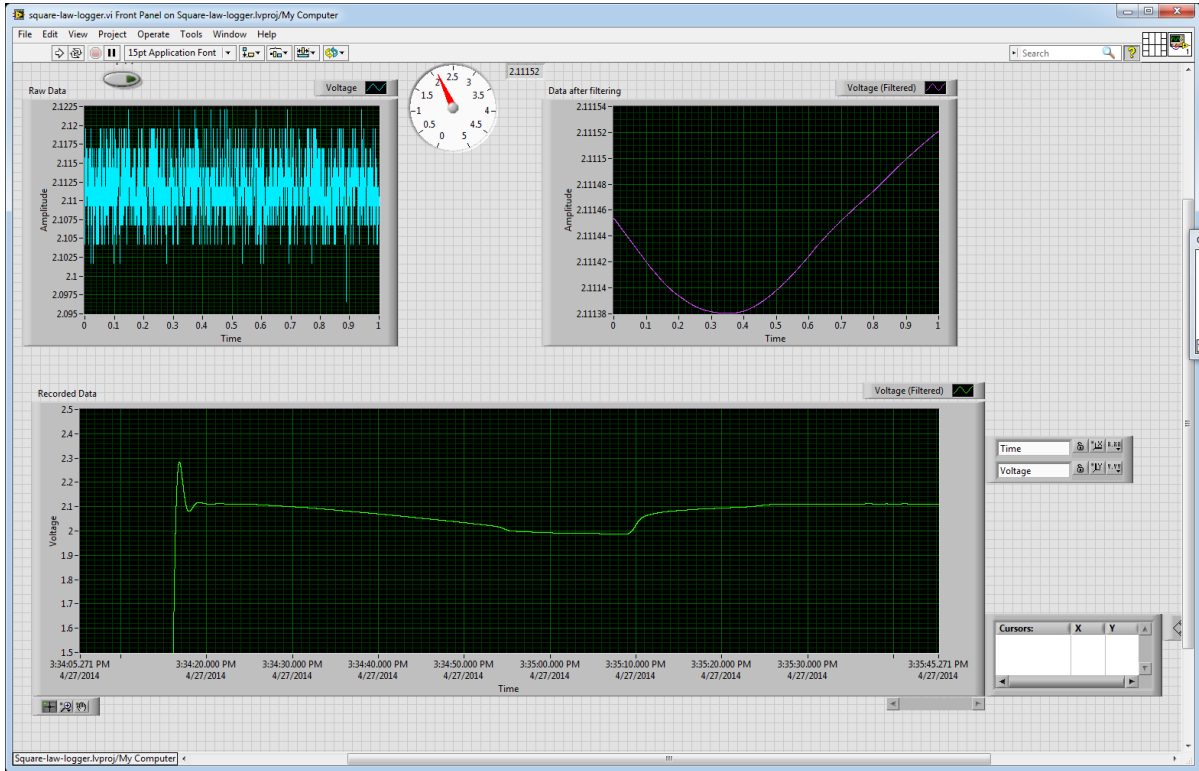


Figure 5.2 A screenshot of the Labview GUI interface

The Labview program uses National Instruments DAQ assistant which allows for quick configuration and setup for the computer to talk to a number of NI devices. Labview also

includes blocks that allows us to easily record the data to a file. These blocks made up most of the program and resulted in a program that was quickly made.

While the USB-6009 allows up to 48,000 samples per second, we don't need such a high rate. A rate of 1,000 samples per second was determined to provide more than enough data. With such a high rate of samples however, the resulting output will be noisy due to the natural noise found in the RF signal. Like the software defined radio, we want to filter this noise as well to produce a smoother output. This was accomplished using a filter block in Labview to help reduce the noise.

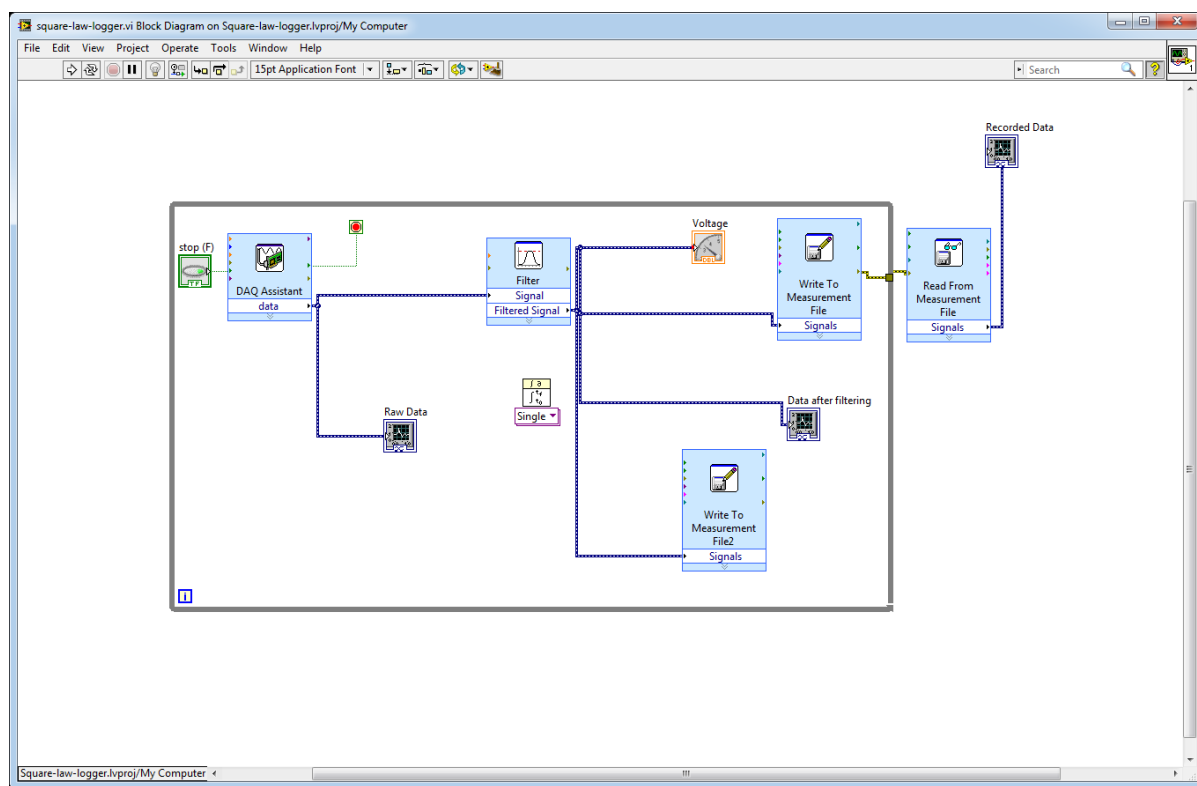


Figure 5.3 A screenshot of the Labview block diagram

This program allowed for the data from the square law detector to be easily recorded. Using Labview also allows us to customize the interface more to our liking and other features such as adding calibration information can also be added as well.

### 5.1.3 Tests on the ADL5902

To test the ADL5902 a signal generator was used that had a controlled output. The specific signal generator that was used was an older model that allowed us to change the output in 10 dBm increments. The signal generator was also configured for 1.4 GHz as that is the frequency the ISU RF front end is configured to listen at. Ideally a noise generator would have been desirable, however a noise generator with adjustable power output could not be located on campus.

The ADL5902 is available from Analog Devices in an evaluation board. This board pairs the ADL5902 with a AD7466 12-bit analog to an analog to digital converter. This board can then be mated with Analog Devices BlackFin processor which acts as a USB gateway for the AD7466 data. A test program written in LabView is also provided as well.

The test program provided by Analog Devices allows us to query the ADL5902 and record the raw ADC value. This program also allows us to enter in the frequency used during testing, the temperature during the test, and allowed for calibration of the ADL5902. All of the data is then stored into an Excel spreadsheet which can be accessed later.

For this test we used the signal generator set to 1.4 GHz and started at  $-60$  dBm for the output signal. This was selected as this is the lowest the square law detector can detect. The output power was then incremented on the signal generator in 10 dBm steps. There was no change to any other parameter. This was done up to 0 dBm. Any higher and there was risk of damage to the ADL5902. This test was then repeated several times and was done with the signal generator stepping up from  $-60$  dBm to 0 dBm and from 0 dBm to  $-60$  dBm.

The data collected was then graphed using Excel. The graph shown in [5.4](#) Shows that the ADL5902 has a linear output and matches the expected value based on the input.

Once it was confirmed the ADL5902 does in fact have a linear response, we then looked at ways to work with the ADL5902. The graph above was generated using Analog Devices program that talked to the Blackfin processor on the daughter-board. However, the information for talking to the Blackfin is proprietary. Therefore, the daughter-board was removed for future tests and instead we used the USB-6009 data acquisition board to read the raw analog voltages

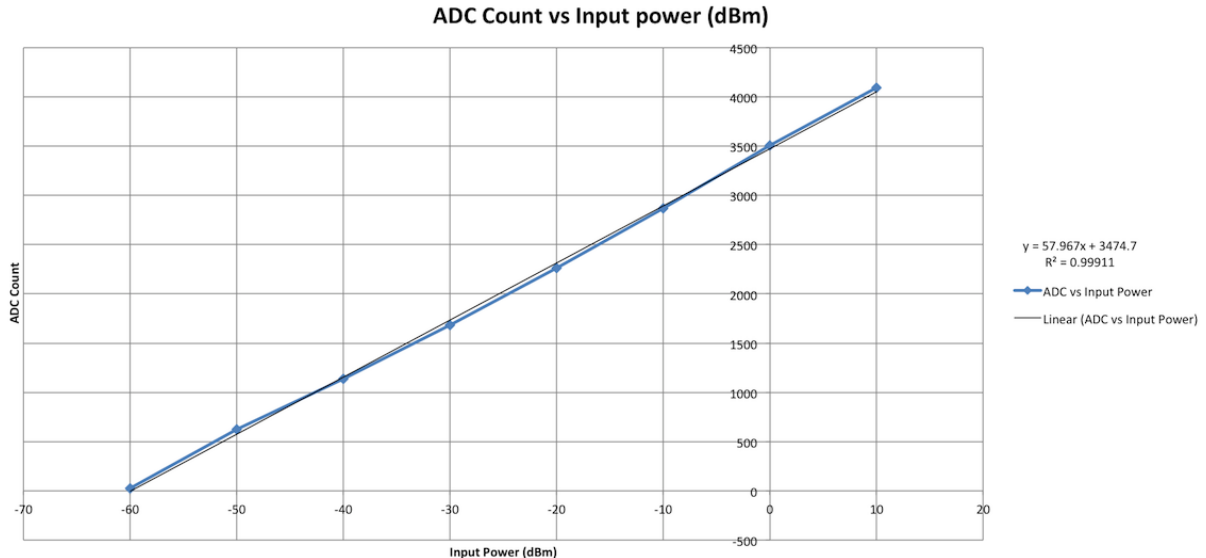


Figure 5.4 Graph showing the linearity of the ADL5902

from the ADL5902. This information was then stored later for additional analysis.

## 5.2 Software Defined Radio Experiments

Once it was confirmed that the square-law detector was working within the specifications that were given, testing then moved to the software defined radio. Once the Python program was established for replicating a total power radiometer in software, this was then loaded into GNURadio and used to control the N200 SDR.

Before testing the program with the N200, testing was done with the built in noise generator in GNURadio. This was used to test its ability to measure small changes in noise. This simulated noise verified that the program written was able to detect changes in noise power using a simulated Gaussian source. It was also desired to also use a hardware based noise generator, however a suitable noise generator could not be located on campus.

After this was done additional tweaks were made to both the GUI interface and to the program that performs the calculations for the total power radiometer. The essential components were moved to a custom block which helped to clean up the block diagram. Details on how this works was discussed in chapter three.

Three experiments were conducted to verify the operation of the software defined radio.

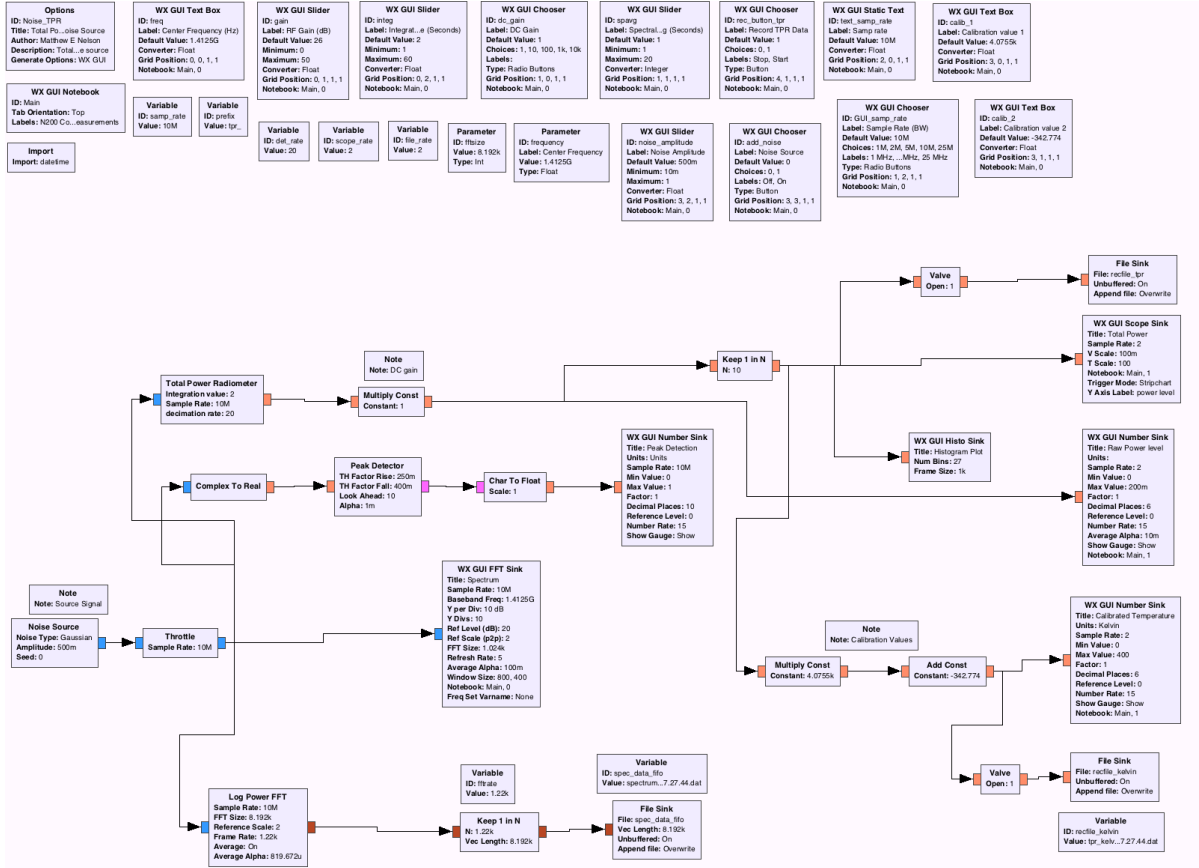


Figure 5.5 A screenshot of the GNURadio program using a noise generator block.

One experiment that tested stability will be discussed in chapter 5. The other two experiments will be discussed in detail here. These two experiments verified that the software defined radio behaved in similarly to the square-law detector and also demonstrated an additional function that the square-law detector was not able to do.

### 5.3 Experiment 1 - Calibration and Normal Radiometer Operation

To fully test both the total power radiometer in the software defined radio and the square-law detector, a cold water bath experiment was established to verify that both the square-law detector and SDR was able to measure real world changes in the noise. In addition, this would also give us a calibration line to calibrate the radiometer.

### 5.3.1 Laboratory Setup

For this experiment the ISU radiometer was setup in the Make to Innovate lab located in Howe Hall at Iowa State University. This lab was picked as it has an electronics area and has test equipment needed for certain experiments as well as the needed power supplies to power the equipment. To measure the change in noise, a 50 ohm matched load was attached to the input of the LNAs and this output was then feed to a power divider which divides the signal between the software defined radio and the square-law detector. This does add a 3.1 dB loss to both devices, however this was acceptable for these experiments.

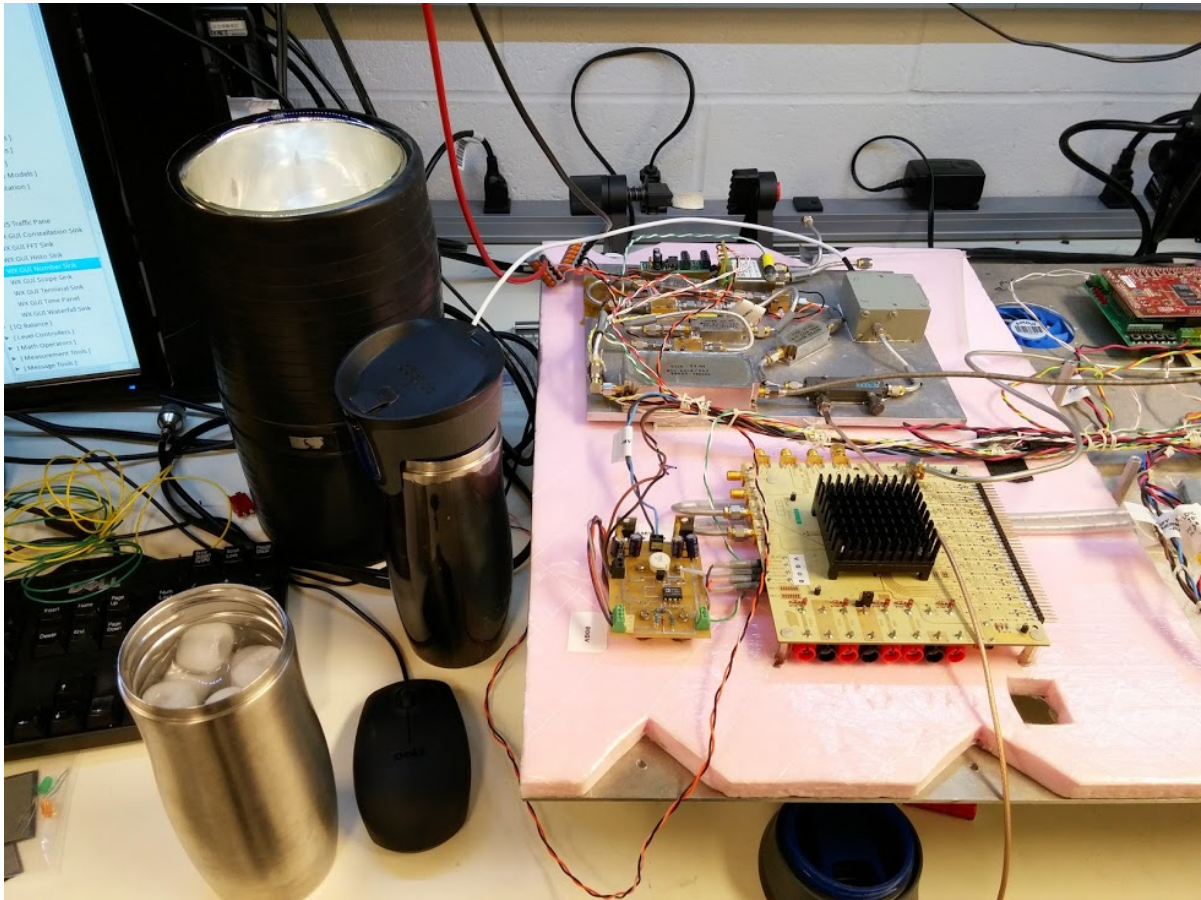


Figure 5.6 An image of the typical lab setup used to test the software defined radiometer

The 50 ohm load was then submersed into a hot or cold bath. These baths were temperature controlled first by using Liquid Nitrogen (LN2) which is known to boil at 77 Kelvin and an ice water bath which is known to be at 273.15 Kelvin. The temperature of these could easily be

monitored and maintained. The load was submersed in each bath for a minimum of 2 minutes to allow for it to reach the same temperature as the bath. The noise measured was then recorded using GNURadio with the N200 SDR and with the USB-6009 to record the square-law data. In addition to the total power measurements, the raw I-Q data was also recorded. This allowed us to replay the experiment through GNURadio for further study.

### 5.3.2 Test Results

The first data we will look at will be with the software defined radio. The SDR records the total power measurements to a binary file that either Matlab or Python can read. In our results, we used iPython Notebook to read and generate the graphs used in this thesis. We will begin by looking at the raw total power readings which we will call raw Q values or rQ values. These are the uncalibrated total power readings from the software defined radio.

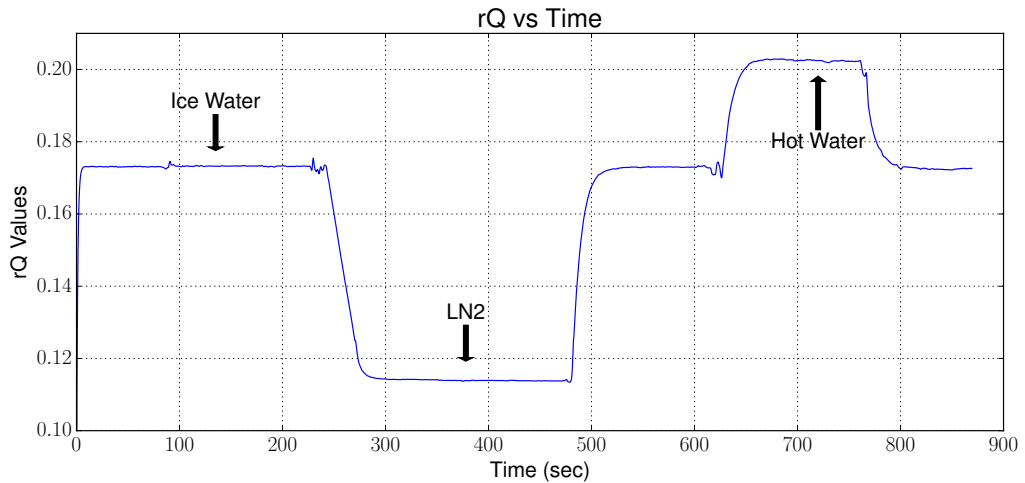


Figure 5.7 Graph of the un-calibrated rQ values of Experiment 1

Figure 5.7 shows the total power reading versus time and is also marked when the matched load was submerged in Ice Water, LN2, or a hot water bath. Since we know what the temperatures are for the ice water and LN2, we can now calibrate these readings to a noise temperature reading. This is done by reading in a calibration file we have stored in csv format and performing linear algebra to solve the slope of the line. This was done in our iPython Notebook using the following code.

```
a = numpy.array ([[ rQ_values [0] ,1.0] ,[ rQ_values [1] ,1.0]] ,numpy.float32)
b = numpy.array ([ temp_values [0] ,temp_values [1]])
z = numpy.linalg.solve(a,b)
```

Now that we have our calibration points, we can now re-graph this data but now calibrated as a reference noise temperature. Figure 5.8 shows a calibrated graph of the data in relation to noise temperature. In addition, we have colorized this graph to show warmer to cooler temps. This is helpful as we often refer to these as noise temperatures.

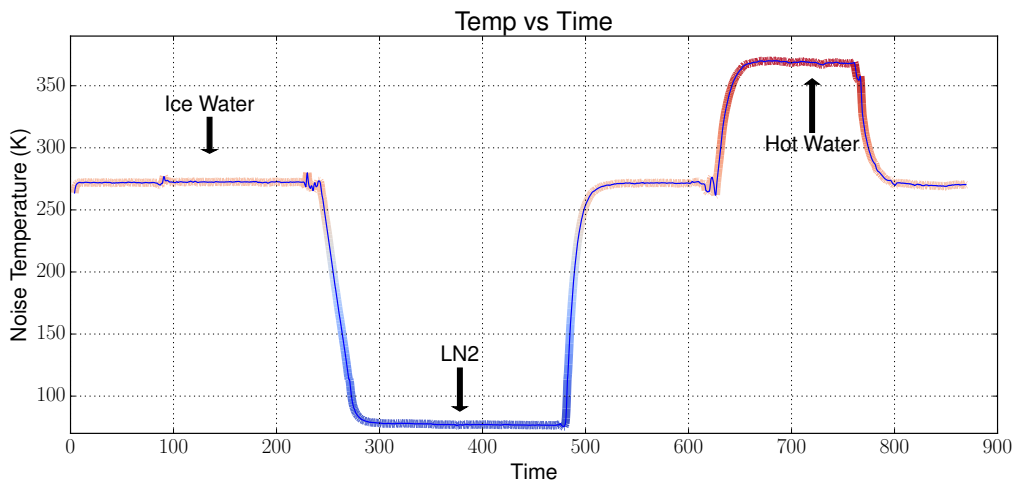


Figure 5.8 Graph of the calibrated noise temperature of Experiment 1

Now that we have looked at the software defined radio data, we want to look at the square-law detector with the end result of comparing the two. The square-law detector gives us power information as a voltage, so once again we will need to calibrate this to the known temperature references. However, before that we need to do one other step with the data. Unlike the software defined radio, there is no filter or integrator to help smooth out the data, so the square-law data is very noisy. Our first step will be to filter the data. Figure 5.9 shows our raw data that we get from the square-law detector.

Once again we can use Python to process this information and specifically we can use SciPy which includes several useful signal processing modules. For our use, we will use a low pass filter to clean up the signal. The following code allows us to do just that.

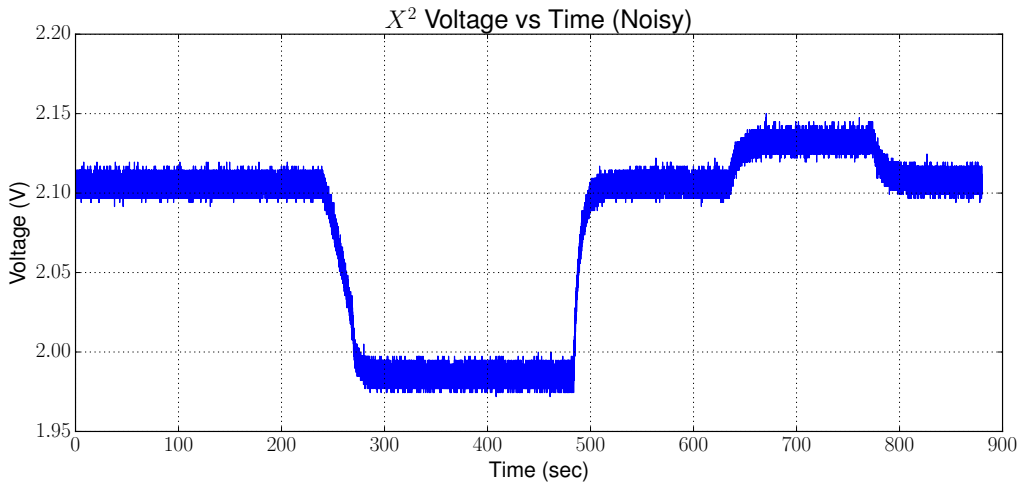


Figure 5.9 Raw and noisy graph from the square-law detector used in Experiment 1

```

from scipy import signal
N=100
Fc=2000
Fs=1600
h=scipy.signal.firwin(numtaps=N, cutoff=40, nyq=Fs/2)
x2_filt=scipy.signal.lfilter(h,1.0,x2_voltage)

```

Figure 5.10 now shows our data that has been filtered by the low pass filter. This is similar to the low pass filter that is also used by the software defined radio.

Using the same technique as earlier, we can now calibrate the raw voltages from the square-law detector to the noise temperature. Like the software defined radio data, we can calibrate the voltages from the square-law detector to the physical temperature that our matched load is placed in. Figure 5.11 shows the data from the square-law detector calibrated to our known temperature points. This now allows us to directly compare the square-law detector to the software defined radio data since we have a common reference point in which to compare the data.

We now want to compare both the Software Defined Radio and the square-law to make sure that they match up. Since both the SDR and the square-law are now calibrated to a noise

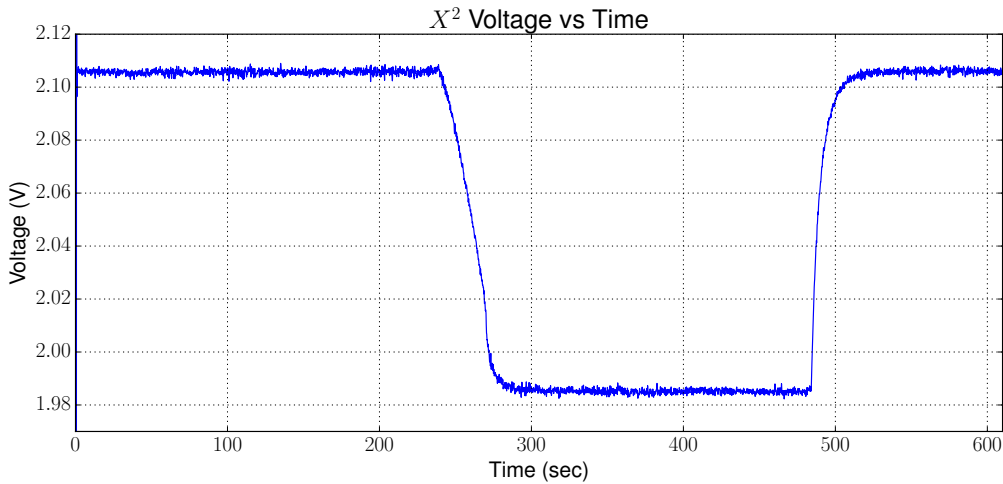


Figure 5.10 Filtered data from the square-law detector used in Experiment 1

temperature, we can easily graph both of the data and compare to see how well they match up.

We can see in Figure 5.12 that both the software defined radio and the square-law detector match up very nicely. This shows that both the square-law detector and the software defined radio agree when properly calibrated. This verifies that the software defined radio can indeed operate as a total power radiometer and the data we obtain from this setup agrees with an analog and more traditional radiometer.

### 5.3.3 Application with Soil Moisture Readings

A common application of radiometers is in the measurement of soil moisture. All items naturally emit RF energy due to the random excitation by the electrons in the object. The amount of noise that gets generated varies by temperature, but the amount that reaches the antenna varies by the amount of moisture in the soil. If we can calibrate the radiometer to two known soil conditions, then we can measure the various levels of soil moisture in the soil. At this time, we will simply look at the percentage of moisture in the soil, which will vary from zero percent or dry soil to one hundred percent or very wet soil. The drier the soil, the more thermal noise we receive and the "warmer" the noise temperature. Wet soil on the other hand attenuates the thermal noise and shows up as a "cooler" noise temperature.

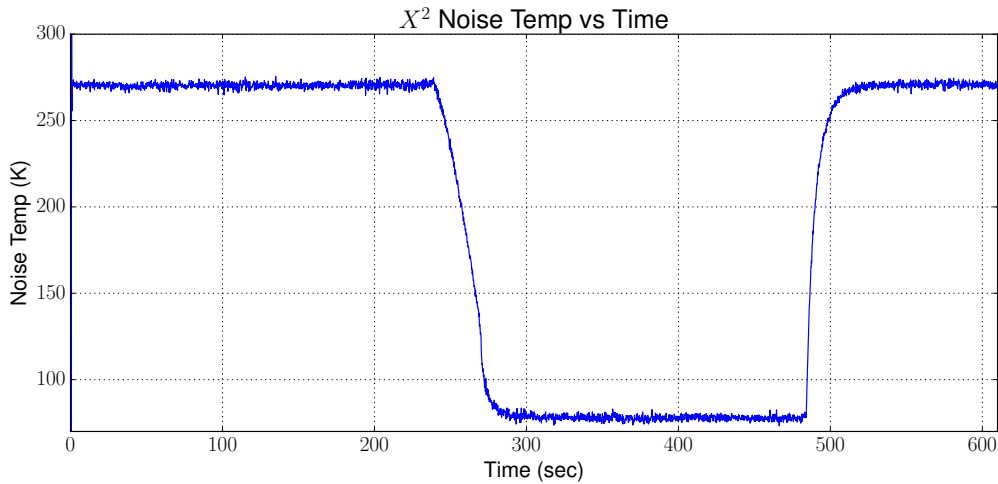


Figure 5.11 Calibrated data from the square-law detector used in Experiment 1

Using the Software Defined Radio, we can set up two methods to visually look at the noise temperature and thus the soil moisture percentage. Since we do not have an antenna hooked up, we will simulate this by using two reference temperatures. In this case the ice water bath and the LN2 that we just used and was shown earlier.

A unique visual aid we can use with GNURadio is a waterfall display. This display gives us information that includes frequency, amplitude and time. It is referred to as a waterfall display due to the fact the display continually moves from top to bottom and looks like a waterfall. Amplitude information is given by mapping the range of amplitudes to a color bar. Frequency is given on the x-axis and time is on the y-axis. Figure 5.13 shows a screen shot of the waterfall display in the GUI created in GNURadio Companion for this experiment. This is the same program we have used but with the waterfall display now added. The data for the waterfall is pulled directly from our source block or in our case the N200 software defined radio.

Let's take a look at two screen shots of the waterfall. We will put them side by side so we can better compare the display when the thermal load is in the ice water bath and when the load is in LN2.

In figure 5.14 we can see that the ice water screen shot appears warmer than the right side screen shot which appears cooler. There is a limitation in GNURadio and the waterfall display that limits what the range for the power readings are. The overall power that we see

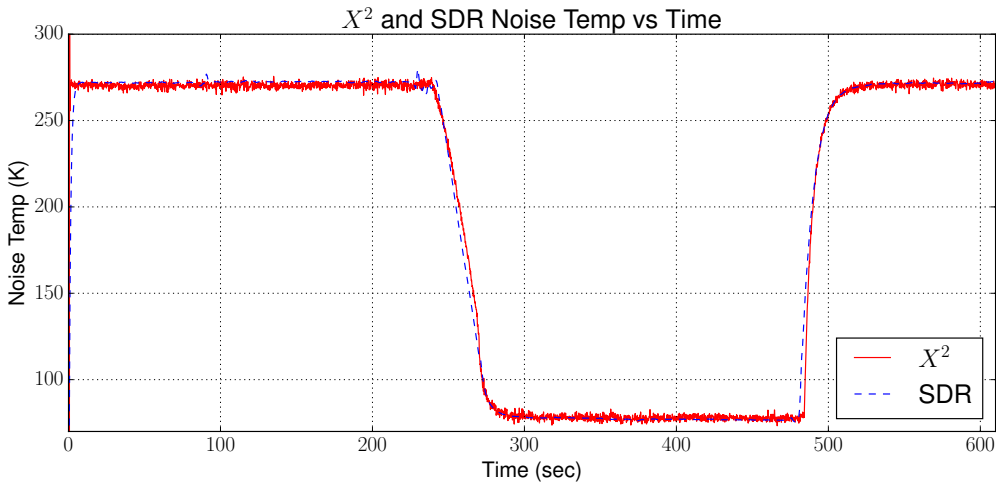


Figure 5.12 Figure showing both the SDR and square-law noise temperature data in Experiment 1

only changes by about 3 dB and our current range in the waterfall display is set to 10 dB. If we could reduce the range, the color change would be even greater and more pronounced. However, this does show that a change can be seen visually with color to indicate the noise temperature.

If we assume that our LN2 is dry soil and that our ice water bath is wet soil, we can now interpolate the data to this scale and show the information we obtained in Experiment one as both a noise temperature and soil moisture. Figure 5.15 shows the same data we looked at earlier but we have now added a scale to show soil moisture as a percentage.

While this demonstrates that we can collate our total power readings with a soil moisture percentage, we would use actual field tests to calibrate the radiometer. In addition, we could also calibrate to soil moisture content instead of a percentage if desired. Both methods have been done with traditional radiometers[Jonard et al. (2011)][Shi et al. (2003)].

#### 5.4 Experiment 2 - Interfering Signal Mitigation

The addition of an unwanted signal can be a determinant to the radiometer and has an adverse effect on how the radiometer operates. In today's world though, it is getting more difficult to control intentional radiators as the RF spectrum becomes crowded with more devices.

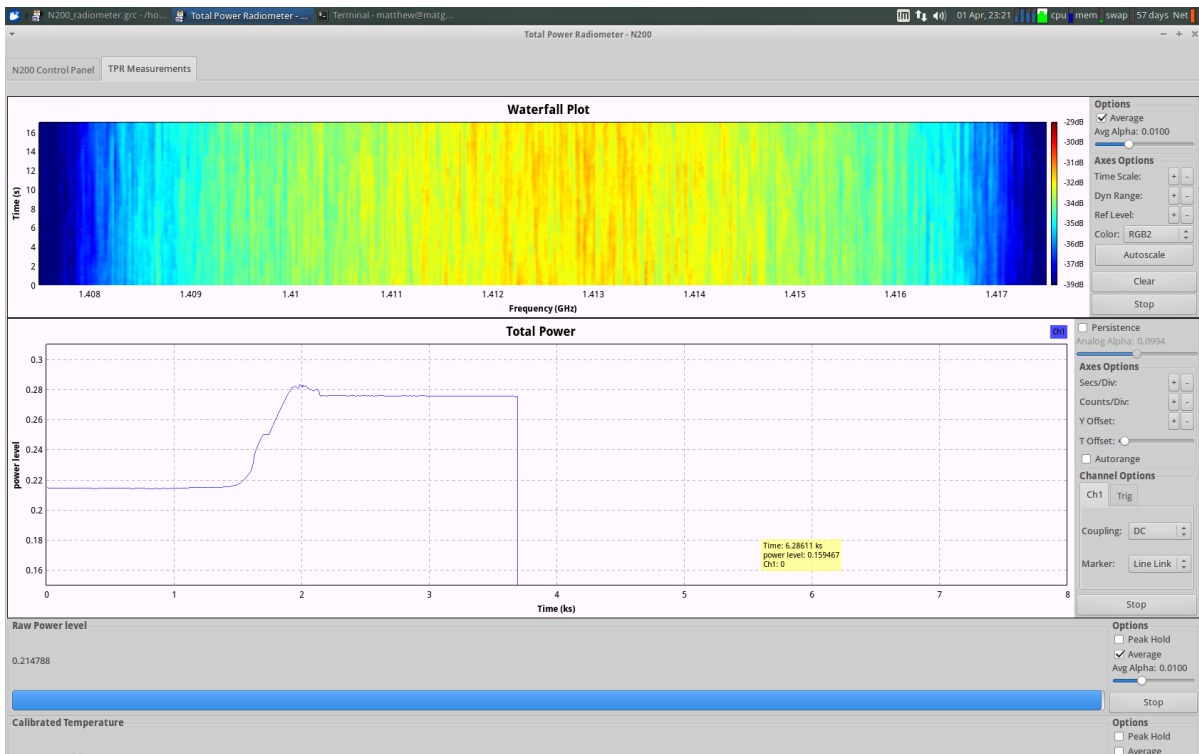


Figure 5.13 Screenshot of the waterfall display used in Experiment 1

This problem becomes even a greater issue with radiometers used in orbiting spacecrafts as they are able to see large areas[Misra et al. (2012)]. Even though the band we are working in of 1.4 GHz is an internationally protected frequency, there can still be both intentional and unintentional radiators that cause interference.

RFI detection and mitigation is not a new topic in radiometry and there have been other methods in both the detection and mitigation of these signals[Forte et al. (2013)][McIntyre and

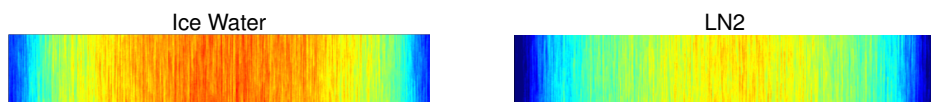


Figure 5.14 Side by side comparison of the waterfall display for Experiment 1

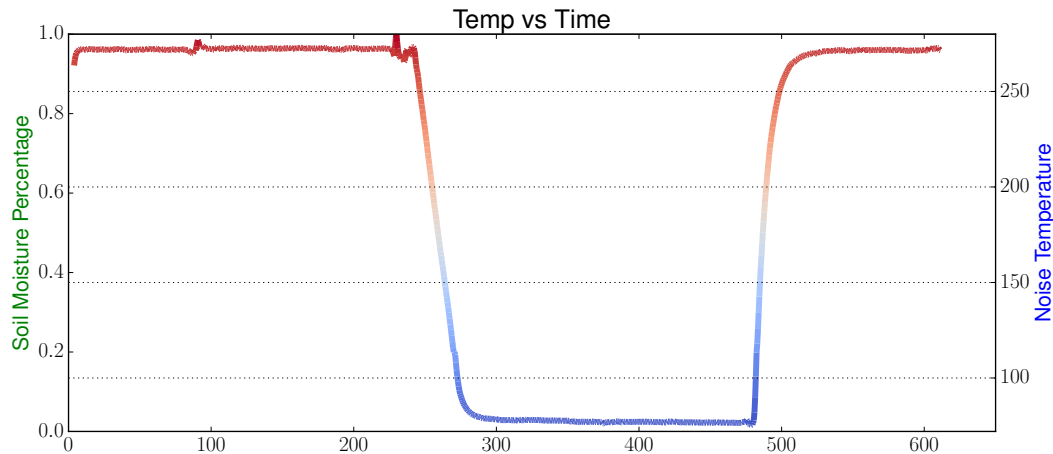


Figure 5.15 Plot of the noise temperature of Experiment 1 with soil moisture percentage

Gasiewski (2012)][De Roo et al. (2007)][Ellingson et al. (2003)].

Experiment 2 is used to show additional benefits of using a software defined radio compared to a more traditional radiometer by being able to filter out these unwanted signals. One benefit of using a SDR is that key components such as filters are created in software instead of using hardware. This means that filters can be created on the fly and can be adjusted simply by updating the software.

For this experiment we will use both the Software Defined Radio running GNURadio with the radiometer firmware and a square-law detector that is connected to a data acquisition unit. The experiment uses a 50 ohm matched load that is attached to the radiometer. This matched load is then submerged into two different baths, a Liquid Nitrogen at 77 K and an Ice bath at 273.15 K which is identical to experiment one. The difference with this experiment is that an offending signal is generated and then inserted into the RF signal chain. It is amplified by the LNAs and then split to both the SDR and the square-law detector. Another SDR, the HackRF One is used to act as a signal generator and generates the offending signal. This allows for flexibility in both the amplitude and frequency of the generated signal.

### 5.4.1 Laboratory Setup

We will use a similar setup to experiment one with the addition of a signal source that we will inject into the RF chain. Our signal source will be another software defined radio, the HackRF One shown in figure 5.16. This SDR is a cheaper SDR and thus has lower specifications than the Ettus Research N200. However, for the task of a signal source, it will suit our needs. Except for this additional SDR as our interfering signal source, the setup is exactly as experiment one using the same LNAs and other hardware.

The ISU RF front end was once again used to amplify the signal. One difference however is that a power combiner, which is the same as a power divider, was used to hook up to a signal generator. The signal generator then provided the offending signal. By using the signal generator we can control how much power and what frequency the offending signal is at. In this case we are performing this in a controlled setup and would know ahead of time where the offending signal is. In the future the SDR defined could identify the offending signal and then filter it out.

Like the other tests, a power divider is used to split the signal after the ISU RF front end which was then feed to a square-law detector and then the N200 SDR. The square-law detector was then hooked up to a National Instruments USB-6009 DAQ which is then feed into the LabView program to be processed and recorded. The N200 continued to use the GNURadio program that was created to record the total power coming out. However, it has been modified with a band reject filter to filter the offending signal.

For this experiment, the HackRF will generate a sinusoidal wave at a fixed frequency. We will then change the amplitude of this signal a few times during the experiment. This allows us to verify that the signal is still present in the total power measurements in both the software defined radio and the square-law detector. Since the square-law detector does retain any frequency information, this was the only method to verify the operation of the signal generator with the square-law detector.

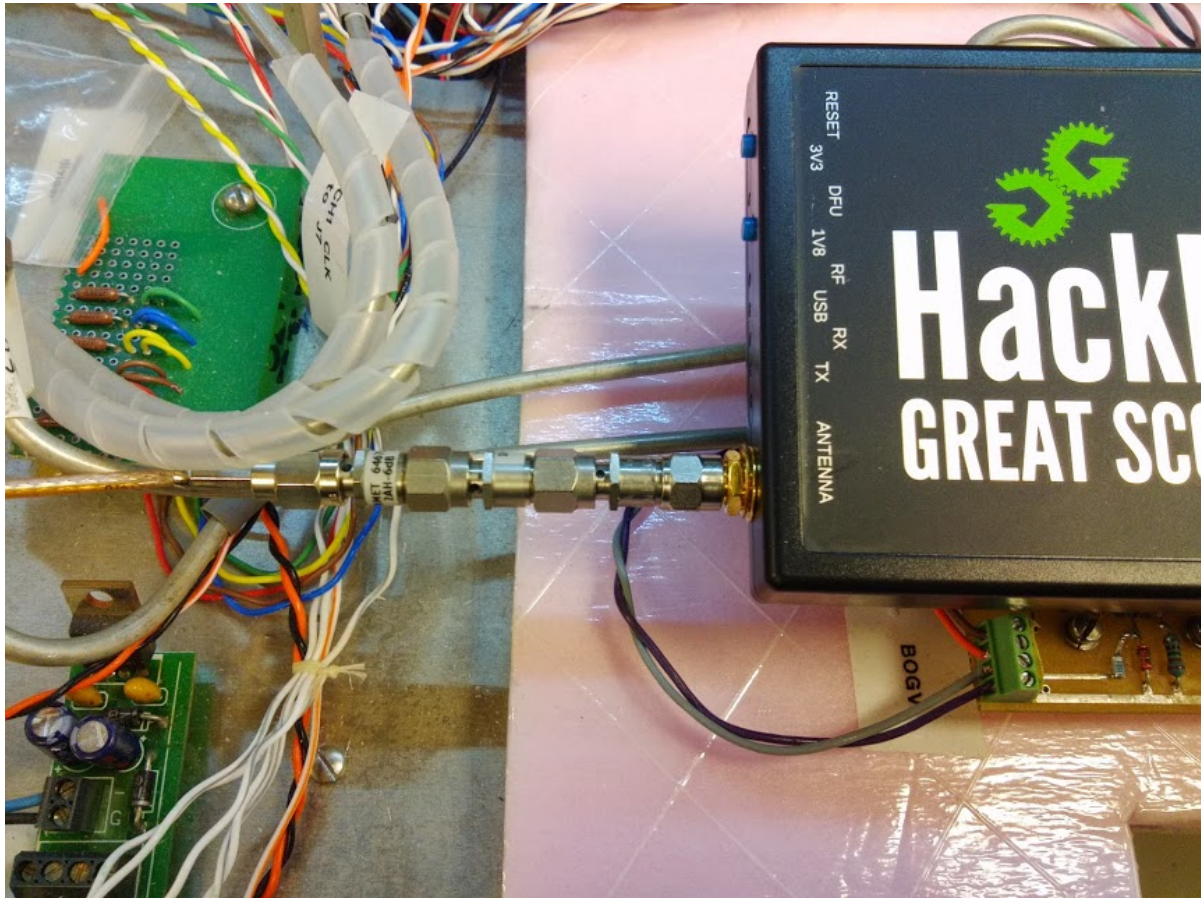


Figure 5.16 Image of the HackRF used to generate the offending signal

#### 5.4.2 Software Defined Radio Configuration

This test was designed to test a problem that a software defined radio would be to cope with while a square law detector would not be able to cope with it. This test injected a known signal at 1.406 GHz to interfere with the normal operation of the radiometer. In this test, the square law detector, since it is a wide band device, would not be able to accurately measure the change in the total power of the signal. However, the SDR is able to create a digital filter to filter out the offending signal. Since this is done in software, the SDR is able to adapt to change much faster than an analog radiometer.

Our Software Defined Radio software is now altered to include a band-reject filter that will filter out the offending signal. The filter was first designed using the included GNU Radio

Filter Design tool that is part of the suite of software with GNURadio. Figure 5.17 shows a screen shot of the tool when designing the band-reject filter for this application. This tool generates filter values also called taps that GNURadio will use for defining the filter. The GUI program shown in figure 5.17 allows us to interactively create a filter. However, in our GNURadio program, we can call this program directly from our program to generate the taps needed. This is quite easy to do since both GNURadio and the program that generates the taps are both Python programs.

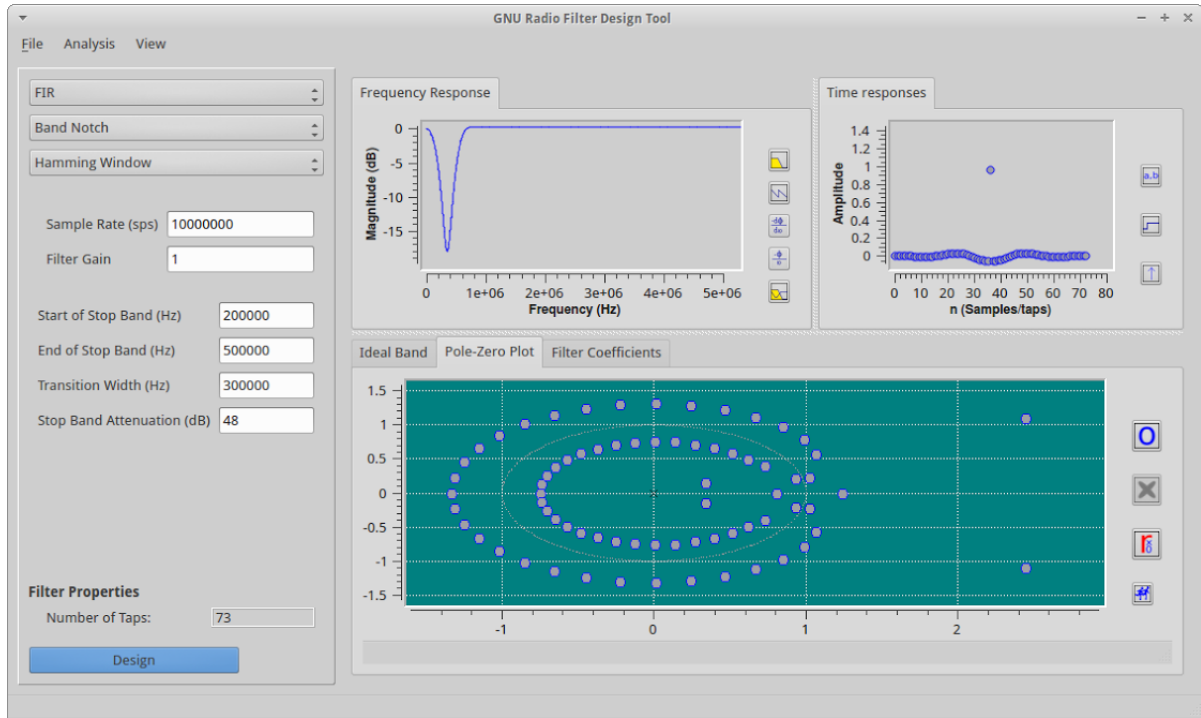


Figure 5.17 Image of the GNU Radio Filter Design tool

Now that the taps have been calculated it is now applied to the filter in the system. The band-reject filter will of course affect our performance as we will lose some bandwidth to the filter. However, as shown it is still possible to function as a total power radiometer while filtering this signal.

### 5.4.3 Impact of filter on radiometer performance

There is a trade-off when using filters to remove the offending signal. The larger the filter is that is used, the more information that is lost in the signal. Equation 5.1 shows how the filter impacts the  $NE\Delta T$  for the system. Figure 5.1 shows that as the bandwidth of the filter goes up, the  $NE\Delta T$  also increases which results in the radiometer to be not as sensitive and may not be able to detect a fine enough change in the noise temperature. Figure 5.1 also shows that if we put a limit on what we expect our sensitivity to be, then that limits how much we can filter out. In the case shown in 5.1, we placed a limit of .2 Kelvin as the maximum  $NE\Delta T$  we wished to have. This meant that we can only filter up to 5 MHz before we exceed this value.

$$NE\Delta T = \frac{T_A + T_N}{\sqrt{(\beta - \beta_{filter}) * \tau}} \quad (5.1)$$

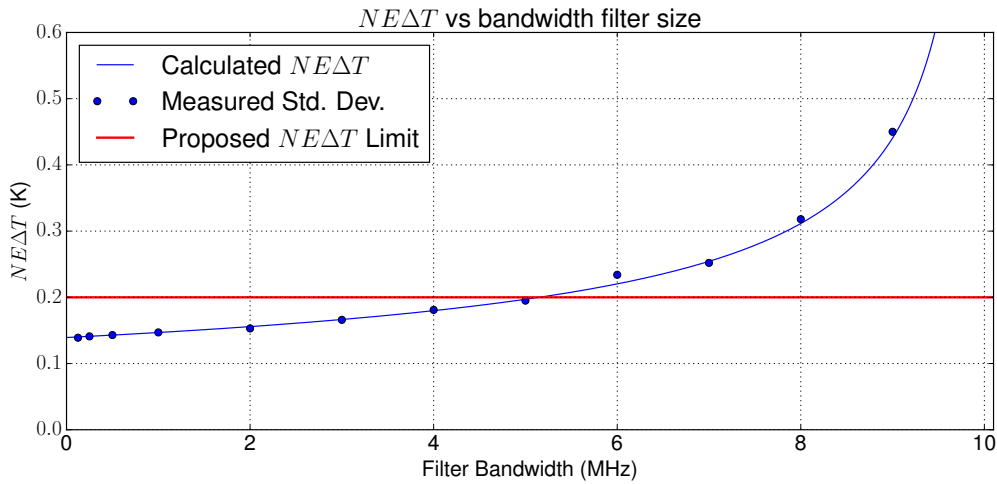


Figure 5.18 Graph showing the impact of the filter to the  $NE\Delta T$  performance of the radiometer

Another impact that the filter has is how much power we expect to see at the radiometer. We will refer to equation ?? that shows the power received as a function of the bandwidth, gain, system noise temperature and measured noise temperature. This equation is now re-written in 5.2 to show that the bandwidth decreases as our filter bandwidth increases.

$$P = k * (\beta - \beta_{filter}) * G * (T_A + T_N) \quad (5.2)$$

A simple test was conducted that looked at what the theoretical power measured based on equation 5.2 and what was measured with our SDR radiometer configuration. Figure 5.19 shows the results of this test.

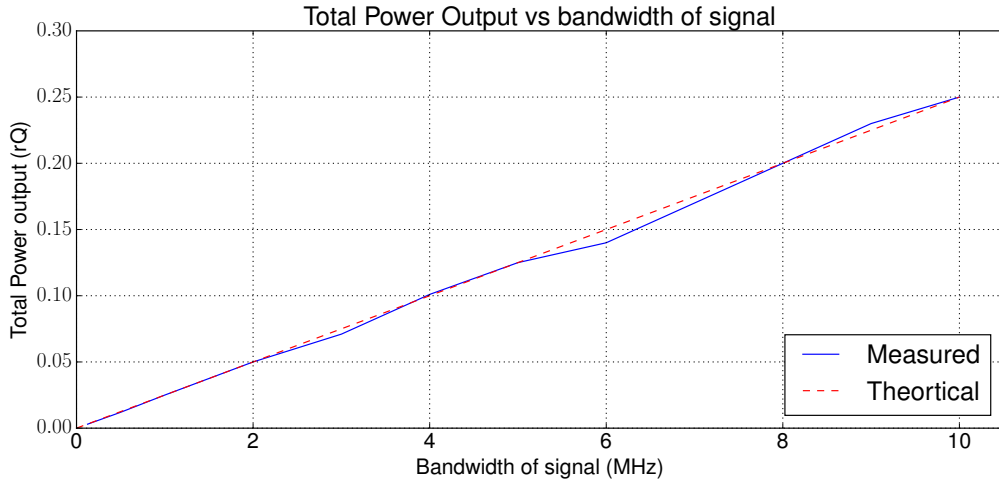


Figure 5.19 Graph showing both theoretical and experimental data on the impact to the total power as a function of the bandwidth of the filter

As expected as the system increases the bandwidth of the filter, the total bandwidth seen is decreased and this results in a decrease in the total power that we might expect at the radiometer. This means that at a certain point we may not be able to obtain the power information we need.

Filtering has other impacts to the signal that needs to be addressed. Filtering a signal does have a cost associated with it in terms of the computational cost. This depends on how tightly we need to have the filter and the sampling rate at which we are running the software defined radio. In an ideal world we would have filters that have very steep frequency response rates. However, this is computationally very expensive and so we often compromise by having less steep frequency response due to computational limits.

Another factor with filters that does not directly impact the system but does need to be discussed is delays. In the experiments in this thesis the graphs were compensated for delays due to the filters used. A FIR filter that is used to filter out the offending signal has a very predictable delay and is computed in equations. Another type of filter that is used is the

IIR filter used in the power detection stage of the total power radiometer software. An IIR filter however does not have a linear delay time and is instead based on the filter and the frequency it is filtering. There are tools however that can be used to calculate this delay and this allows for us to properly compensate any delay with filtered signal. This is important for doing comparison graphs with the square-law detector which does not use as many filters and does so at different frequencies.

#### 5.4.4 Test Results

We begin by looking at the what happens to our total power readings with no filter applied. As we stated in the Lab Setup portion, the frequency of the offending signal will not change, but the amplitude will. This will mean that we should see clear indications of the total power changing as the amplitude of the offending signal changes.

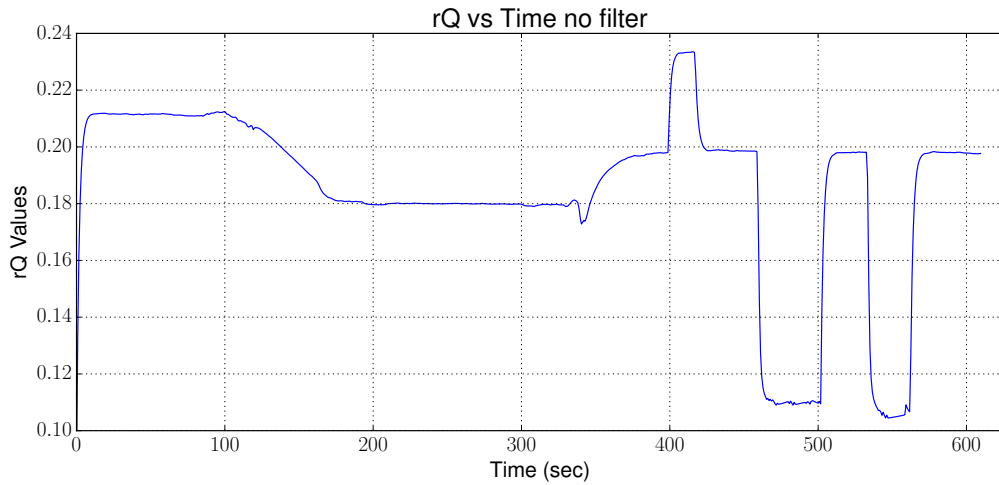


Figure 5.20 Graph showing the unfiltered total power measurements on the software defined radio

We can see that there are pulses that occur in the graph in figure 5.20 and that changes in the amplitude of the offending signal affect our total power readings. These same pulses can also be seen in the square-law detector data as well which can be seen in figure 5.21.

We can clearly see in both the software defined radio and the square-law detector that there is an interfering signal. If we now look at the spectrum view on the software defined radio, we

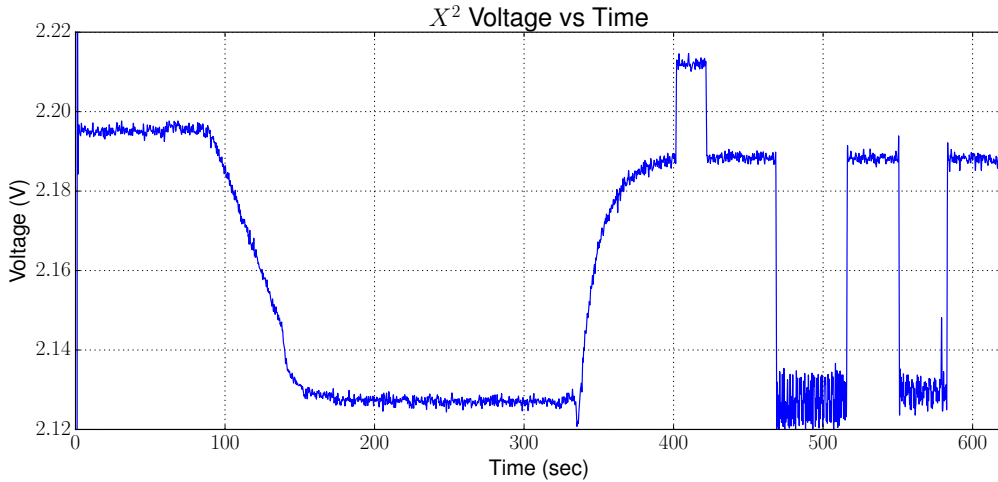


Figure 5.21 Graph showing the raw total power read from the square-law detector with an interfering signal.

can see the signal in question which is at 1.405 GHz. Figure 5.22 shows us what the software defined radio sees which is a spike at 1.405 GHz. The square-law detector of course has no frequency information, so our only method to detect an interfering signal is by looking at the total power readings. In our case there is elevated readings and we can see the spikes in the square-law data. However, we do not know where in the spectrum the signal is at.

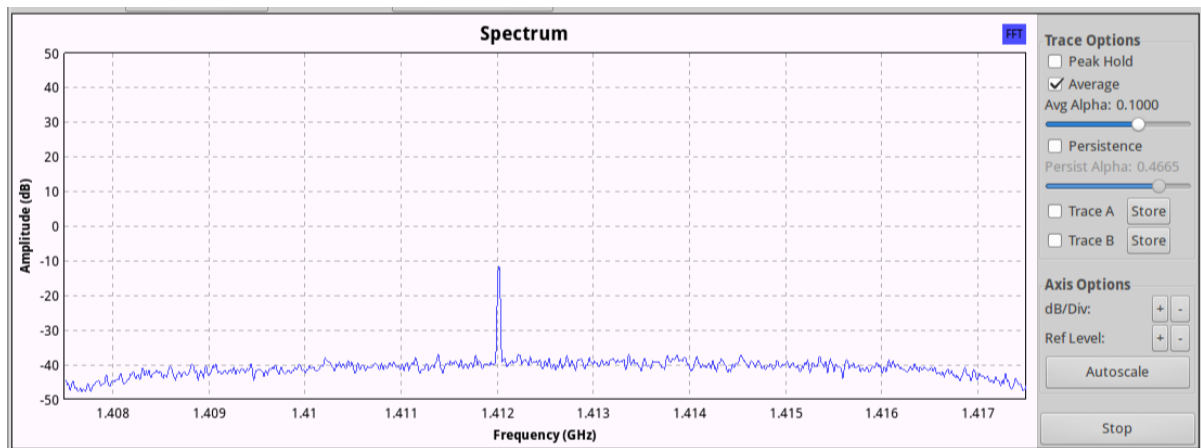


Figure 5.22 Image showing the spectrum view from the software defined radio

Since we know where the offending signal is, we can now design our filter to filter out this signal. In our GNURadio program we can specify both the frequency and the bandwidth our

band-reject filter that we desire. Ideally we want to keep the bandwidth of the filter as tight as possible to the offending signal but we also want to make sure our filter is effective in removing the signal. Figure 5.23 shows the spectrum display from the software defined radio with the filter now turned on and filtering the offending signal.

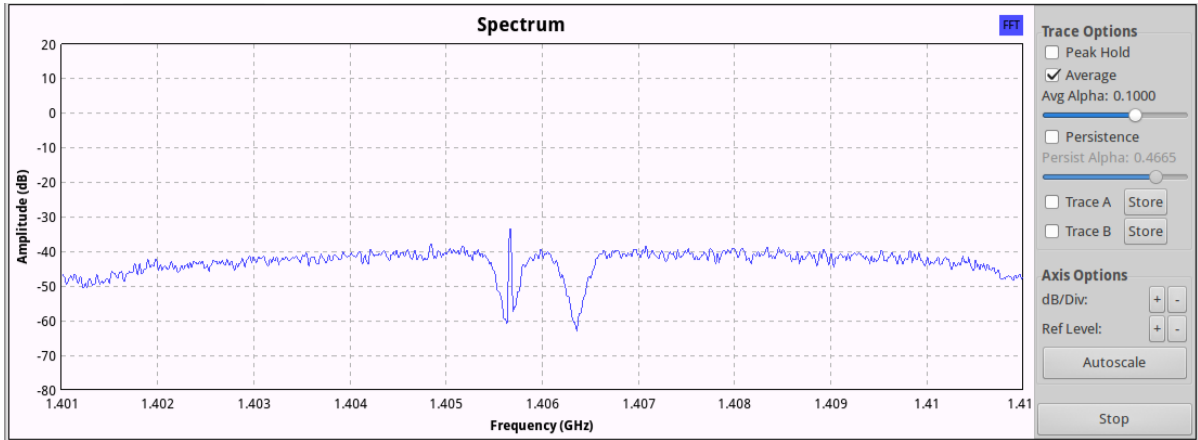


Figure 5.23 Image showing the software defined radio with the filter on and filtering the offending signal

Since we have now removed the offending signal, we will want to re-run our experiment and once again compare the difference between the software defined radio and the square law detector. We can begin by looking at the software defined radio total power readings. In figure 5.24 we can see a calibrated graph of the noise temperature seen by the software defined radio. This graph is very similar to the graphs we expect from our total power radiometer. However, we want to compare this to our square-law detector as well.

Figure 5.25 now shows both the software defined radio and the square-law detector calibrated total power readings. In this graph you can see that the software defined radio is able to make normal readings where the square-law detector still shows the changes in amplitude which would make both calibration and obtaining useful data difficult.

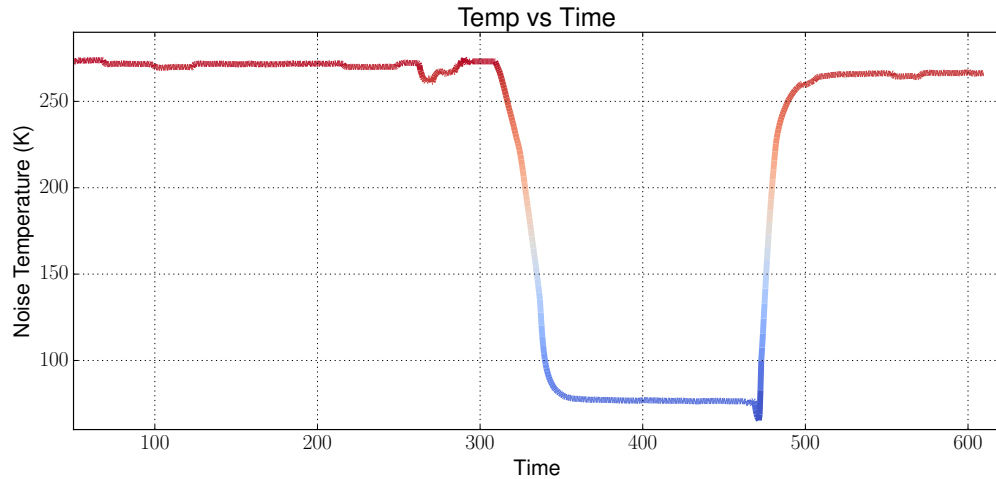


Figure 5.24 Graph showing the calibrated total power readings with the filter removing the offending signal

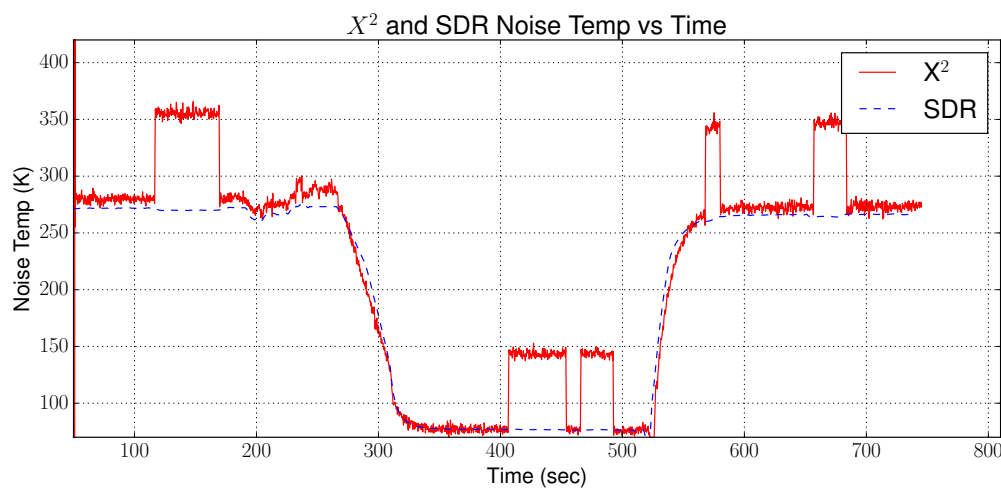


Figure 5.25 Image of the offending signal being filtered out by the SDR. It can be seen that the signal is no longer visible.

## CHAPTER 6. RESULTS AND ANALYSIS

### 6.1 Introduction

To verify stability of the radiometer, we look to see how much change the radiometer records over a relatively long period of time. To test this a matched load was submerged in a liquid nitrogen bath for an extended period of time, in this case for fifteen minutes. The readings were then looked at to study the trend of the data. The data is graphed in figure 6.1.

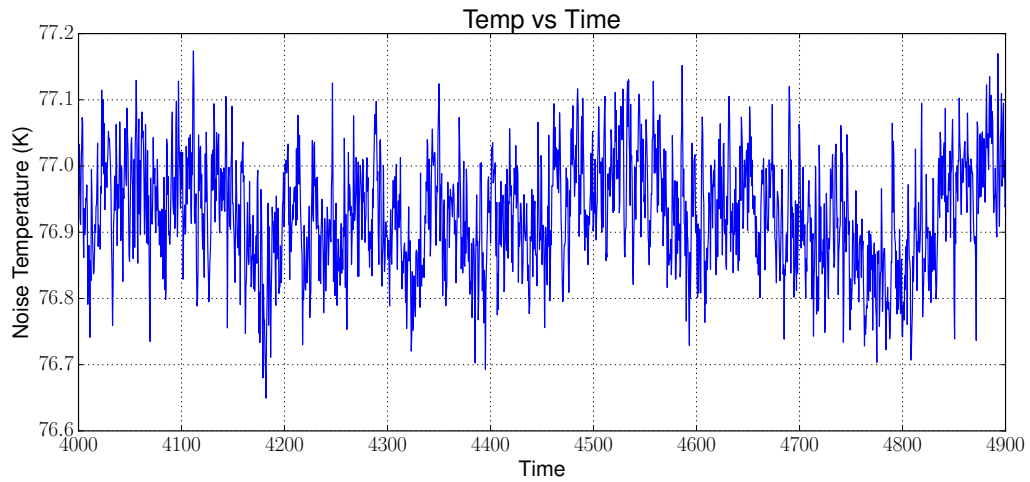


Figure 6.1 Graph of the calibrated total power over a period of fifteen minutes.

As it can be seen in figure 6.1, the amount of change over a period of one hour is quite small. The standard deviation for this sample is 0.09 kelvin. The  $NE\Delta T$  calculated using 10 MHz for the bandwidth, an integration time of 2 seconds and with our sample at 77 Kelvin is calculated to be 0.10 Kelvin with a system temperature of 350 Kelvin. Therefore, our system is behaving as we expect it to for this stability test.

Figure 6.2 shows a graph of the total readings but with the standard deviation now plotted.

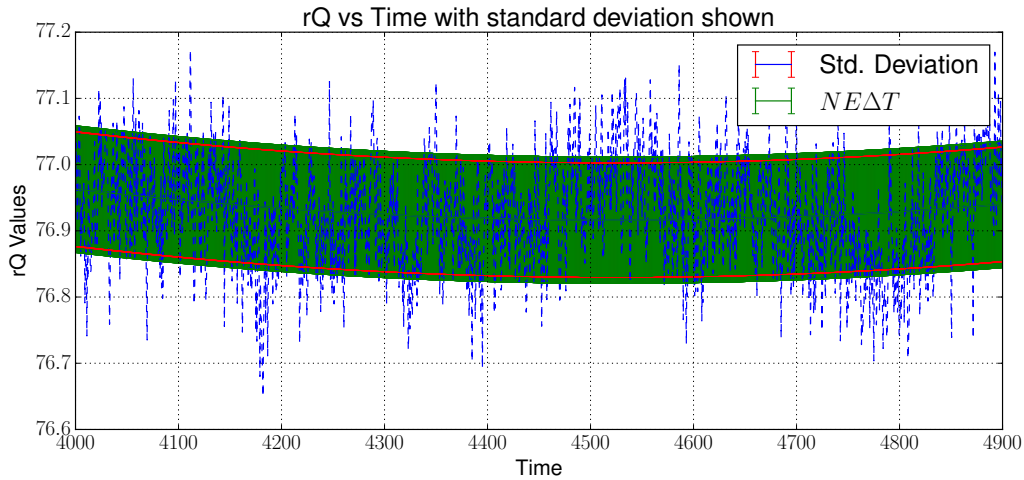


Figure 6.2 Graph of the calibrated total power with the standard deviation plotted.

This shows that the system is stable and is operating as expected within our expected  $NE\Delta T$ .

Once the experimental data was obtained the next step is to analyze the data and format the data so that it is easy to read and comprehend. The total power readings and the raw I/Q data generated from GNURadio is stored as a binary file stored in little-endian format. Total power data is stored as a float values and I/Q data is stored as complex values. Data from the square-law detector is stored as a comma delimited ASCII file.

Matlab is one tool we can use to process the information that is stored by GNURadio. Appendix A contains the Matlab source that will read the total power file generated by GNURadio. It then calculates information such as the  $NE\Delta T$  and the calibration points based on the user input. We can also use Matlab to graph this information as well.

While Matlab is one tool, other tools can be used. Python for example is also capable of reading in these files and when paired with NumPy and SciPy can be used to perform analysis on the data as well [Uengtrakul and Bunnjaweht (2014)]. In addition, the open source mathematical program Octave should also be able to read and work with these files. For this thesis both Matlab and Python was used to provide analysis on the data.

Most of the graphs generated in this thesis was generated using iPython notebooks. IPython notebooks uses Python but allows it to be executed in a web browser either locally or on a server.

Using iPython notebooks however also allows us to add additional information using Markdown and basic HTML. This allowed the author to paint a complete picture of the experimental results illustrating pictures of the setup and the code and steps used to analyze the data. You can find these notebooks on the author's Github site and can use NBViewer to view them. An example link is [.](#)

```
In [3]: tpr = 'tpr_2014.06.12.Lab0.dat'
Uses SciPy to open the binary file from GNURadio

In [4]: f = scipy.fromfile(open(tpr),dtype=scipy.float32)
Because of the valve function in GNURadio, there are zeros that get added to the file. We want to trim out those zeros.

In [5]: f = numpy.trim_zeros(f)
Create an index array for plotting

In [6]: y = numpy.linspace(0,1,numpy.size(f))

Plot the data

In [7]: plot(y,f)
xlabel('time')
ylabel('rQ Values')
title('rQ vs Time')
grid(True)
```

Figure 6.3 A screenshot showing the iPython notebook code and related graphs generated for parsing GNURadio data

## 6.2 Benefits to Software Defined Radio Radiometer

A study was conducted on what benefits a software defined radio radiometer would have over a more traditional radiometer. This was focused on looking at three main areas; cost, weight and size, and the value a SDR radiometer can add over traditional radiometers.

### 6.2.1 Cost Benefits

Software defined radios have become more commonplace in recent years and this has generated a number of Commercial Off The Shelf (COTS) solutions. A COTS solution is often a lower cost solution due to the mass manufacturing that takes place. This has driven the cost of many SDRs to under one thousand dollars while still having excellent performance characteristics. The N200 SDR purchased for this research cost fifteen hundred dollars and the daughter-board cost one hundred and fifty dollars approximately. Other software defined radios however have come out on the market since then. Ettus for example has some that are below one thousand dollars and the author has also obtained the HackRF One SDR that now sells for three hundred dollars. The main difference with the different software defined radios on the market is with both the resolution, or how many bits the ADC is, and the bandwidth they are able to handle.

Table 6.1 Cost Analysis

Device	Quantity	Cost
<b>SDR Solution</b>		
N200 SDR	1	\$1515
LNA at \$60 ea.	3	\$180
DBSRX2 Daughter-board	1	\$152
GNURadio	1	\$0
Total		\$1847
<b>ISU Radiometer</b>		
LNA, FPGA, ADC, Microcontroller and power supplies	1	\$10,000 <sup>1</sup>
<b>Commercial Off the Shelf Unit</b>		
Spectracyber 1420 MHz Hydrogen Line Spectrometer	1	\$2,650

As seen in table 6.1, even the higher cost Ettus research equipment is a lower cost option than the custom built ISU radiometer purchased from University of Michigan and even a comparable off the shelf radiometer. It should be noted that the radiometer from the University of Michigan is also a dual polarization radiometer so there are two RF front ends and two ADCs that feed into a FPGA board. It would be quite easy to add dual polarization to the Ettus N200 SDR as it does support two daughter-boards. This would increase the cost to \$2,179 for the additional

---

<sup>1</sup>Purchase price in 2005

LNA<sup>s</sup> and daughter-board.

The largest cost benefit is that key components that you find in a radiometer, the filters and square-law detector can now be all done in software instead of needed additional equipment. The system is also much more frequency agile, which means it can work on a broader range of frequencies than most traditional radiometers with very little change in hardware and in some cases may require no change in hardware. Some of this does depend on the SDR hardware however. The Ettus N200 for example uses daughter-boards to provide the RF interface. While these boards provide a high quality in the RF signal, it does come at a cost and are usually designed for certain bands of frequencies. Other low cost SDRs however are also very wide range in the frequencies they will work in. The HackRF for example works from 10 MHz to 6 GHz, but does so at the cost of lower resolution, less gain in its front end and a lower bandwidth that it can handle.

### **6.2.2 Weight and component size benefits**

A typical radiometer has many components that are involved in the design of the radiometer. This includes filters, LNAs and the power detection or square-law detector used. These components add both weight, size and costs to the radiometer. A software defined radio however digitizes the signal and we are able to replace the filters and square-law detector with their software equivalent. While a software defined radio does add both the ADC and usually a FPGA to do the processing on the signal, advances in semiconductor technology has continued to shrink these components. These components are also lighter than the filters often used in radiometers.

Size is another benefit as since semiconductor technology has continued to shrink components. Again, since items like the filters and square-law detector are removed and done in software this helps to reduce the overall size.

---

<sup>2</sup>Estimated, no data available

Table 6.2 Weight Analysis

Device	Mass
<b>SDR Solution</b>	
N200 SDR	1.2 kg
LNA at .03 kg ea	.09 kg
DBSRX2 Daughter-board	.1 kg
Total	1.39 kg
<b>ISU Radiometer</b>	
LNA, FPGA, ADC, Microcontroller and power supplies	22.7 kg
<b>Commercial Off the Shelf Unit</b>	
Spectracyber 1420 MHz Hydrogen Line Spectrometer	6 kg <sup>2</sup>

### 6.2.3 Value added benefits

A software defined radio radiometer adds additional value for two reasons. One, it is able to work with both frequency and magnitude where most radiometers do not. This allows for additional analysis on the signal and can help identify issues such as an interfering signal that was demonstrated in this thesis.

Second, we are able to have an agile system that is able to adapt to changing conditions with very little or no change to hardware. Different types of radiometers can be implemented such as a Dicke radiometer, dual polarization radiometer or a radiometer that can perform Stokes parameters. In addition, since we have both frequency and power information we can create a system that is able to adapt to changing conditions such as dealing with an interfering signal.

## 6.3 Disadvantages of a SDR Radiometer

Although we have outlined a number of advantages of using a COTS SDR Radiometer and how a SDR can add additional value to the radiometer system, there are some disadvantages to a SDR Radiometer.

### 6.3.1 Power Consumption

One of the largest drawbacks to a SDR radiometer can be in the power consumption of the SDR. With the move to perform functions such as power detection and filtering we now require additional computational power to perform these tasks. With those computational cycles additional power is now required. The use of FPGAs and SoC however can help to minimize these power concerns as they are more efficient than using a full scale x86 based processor and on board computer system.

Power and CPU requirements also increase as we add additional functionality such as filtering an offending signal. While these additions may not require additional hardware, it can require additional processor or computational requirements. This will cause additional strain on the processor and also in the memory requirements for the SDR as well.

### 6.3.2 Bandwidth constraints

While SDR technology has advanced, bandwidth is still a constraint that affects SDRs and in turn a SDR Radiometer. Bandwidth plays a critical role in the radiometer's sensitivity as explained in this thesis, therefore the fact that many SDRs are limited in bandwidth does create a disadvantage. In many cases this bottleneck takes place in both the transport and processing of large bandwidth systems. This also relates to the power consumption disadvantage since larger bandwidth also means requiring additional computational cycles as well.

In contrast, a square-law detector usually has a very large bandwidth, as much as one gigahertz, and is why we usually need to filter to the frequency band of interest.

## 6.4 Results Summary

## CHAPTER 7. CONCLUSION AND FUTURE WORK

### 7.1 Conclusion

In this thesis we have shown that an off the shelf SDR can be used to perform as a radiometer. Using a SDR has several advantages such as a more flexible system and can result in a less expensive system. Since a SDR offers high flexibility, changes to the system can be done very quickly and helps in future proofing the system. Since off the shelf components were used, it also allowed for a lower cost system that is able to perform variations of power detection in a radiometer without adding more costly RF components. Finally, this type of radiometer is very flexible and allows for it to adapt to possible changing conditions. This again happens with no change to the RF hardware and instead happens within the software of the system.

### 7.2 Future work

The main purpose of this research is to demonstrate and prove that an off the shelf software defined radio is capable of operating like a radiometer and can do so within the same or better specifications that are seen in most radiometers today. To do that, we used a very basic radiometer setup and configured our SDR to behave as a single input radiometer. It was also assumed that the input from the RF front end of the radiometer was stable, which in our case was accomplished by stabilizing the temperature of the active components in the RF Front end.

However, this temperature stabilization requires extra weight and bulk to be added to the radiometer. In the application that the ISU radiometer was designed for, this was not a major drawback to the system. However other applications may require a system that does not have this type of temperature stabilization. For those type of systems, other radiometers use different

methods to account for and adjust for fluctuations in the RF front end.

### **7.2.1 Further testing**

The software defined radiometer can be used in other configurations as well such as a polarimetric radiometer or even possibly as a Dicke radiometer using a digitally created noise source. More testing is needed to compare some of these other modes to a traditional radiometer to verify their operation, but in theory these additional configurations should operate the same in a software defined radio as they do with a traditional radiometer.

### **7.2.2 Improving on the FPGA firmware**

For this thesis we focused on the software that would run on a PC or comparable computer system running a full operating system like Linux. This aids speeding up development by using software tools such as GNURadio to rapidly develop the software used to create a radiometer in software. While this works just fine for testing the theory on an off the shelf SDR acting as a radiometer, it does require hardware that is capable of running a full operating system and the associated software. For some applications of a radiometer, this is not a huge concern. In the case for the ISU radiometer, the concern is not that large since the radiometer is not designed to be portable and requires additional support equipment such as a generator anyway. However, other remote sensing applications, such as space based applications, would require a more efficient method. It is very possible to move the software generated in GNURadio into the firmware of the N200. This will help to offload the work needed by the computer and would allow for the computer or similar system to act as more of a control method and for data storage.

### **7.2.3 Correlation**

One such method is to correlate the information with another input which can be another antenna looking at the same source or can be two polarization from the same antenna[Clapp and Maxwell (1967)][Aitken (1968)]. This results in two receiver systems looking at the same source and you have two signals,  $S_1$  and  $S_2$ . Since we are looking at the same source, both

signals will be correlated in time, and when multiplied they will provide an output proportional to the strength of the source signal. The noise introduced by each receiver will then have a lower correlation due to the random nature of the noise. This results in a radiometer with a greater sensitivity due to the reduction of the noise even though two receivers are used [Fujimoto (1964)].

The N200 software defined radio was chosen as it is capable of having two different daughter-cards plugged in. Therefore, it is possible to have both sources enter the software defined radio and once digitized we can sum the magnitudes of the two incoming sources. This is quite easy to do and is shown in figure 7.1.

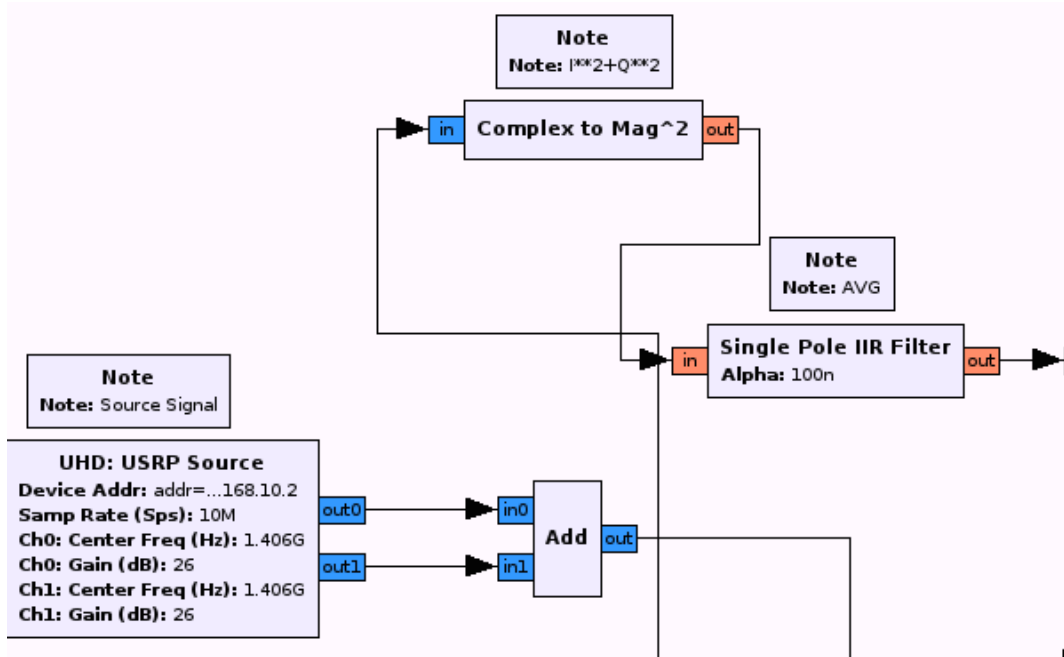


Figure 7.1 The key blocks used for creating a correlating radiometer in software. The key blocks is the USRP source, which allows us to address both daughter-boards and the ADD block which sums the signals.

Although figure 7.1 shows a correlating software defined radio radiometer, it has not been tested. In theory, this should correlate the signal and improve the sensitivity of the radiometer, however further testing is needed.

#### 7.2.4 Improving stability

One of the largest challenges with a radiometer is improving the stability of the radiometer. Drifts in temperature can greatly affect the gains from the LNAs and also change how much noise all components in the radiometer contribute. A software defined radio can help as we are digitizing the signal as soon as possible. This helps in eliminating the analog components for power detection and even for filtering, but does not eliminate all physical hardware, mainly the LNAs. In this thesis, we did not focus on this issue since the RF front end of the ISU radiometer is temperature controlled. All components are mounted to an aluminum block which is attached to a thermal electric cooler. This system then maintains the temperature within 1 degree C.

However, a more compact, lower cost and easier setup would be to just have the LNAs attach directly to the SDR without any temperature compensation. While this can be done, we have now lost stability in the LNAs and we need to compensate for that. One method that is discussed by William Goggins is to use a feedback loop to continuously adjust a variable attenuator [Goggins (1967)]. In Goggins paper, he discusses using a servo that mechanically controls the attenuator. However, since we are in the digital domain, we can control this all in software, and doing a feedback loop is quite easy for a computer to do.

Another method uses multiple temperature points that can be referenced at any time. By using two known temperature references, we can quickly calibrate the radiometer[Hach (1968)].

## APPENDIX A. Source code

The following is the source code to several programs that make the radiometer possible. The first is the Python code used with the Ettus N200 software defined radio. This code is a heir block, which means it can be imported into GNURadio and used as a block. This python code should work on any platform that has the GNURadio libraries installed and also the USRP drivers for communicating with the N200. Other SDRs and other source blocks can be used as well, just replace the USRP source with the source you intend to use. This code can also be easily modified to communicate with any SDR that GNURadio can communicate with. This code was generated using GNURadio Companion.

The second code is the Matlab script that can be used to parse the output from GNURadio. This code will plot the total power output as well as perform some other functions such as a  $NE\delta T$  calculation and also allows for calibration points to be entered as well. This code can be used as a foundation for other programs.

The third code supplied is Python code that can be used to read the data generated and plot it. In many ways it mimics the functions of the Matlab script buy uses Python, NumPy and SciPy to perform the mathematical functions. This may be a better option for those that wish to look at the data but do not have access to Matlab since Python is free to download.

Finally, this code has been included in this thesis as a point of reference. It may be out of date and some other pieces of code was also used for the experimentation used in this thesis. Copies of this thesis source L<sup>A</sup>T<sub>E</sub>Xcode, and any other code used can be found on the author's GitHub repository, <https://github.com/matgyver/Radiometer-SDR-Thesis>.

## Python code for total power radiometer

The main code that acts as the total power radiometer is the TPR.py code. This module adds a custom block to GRC that can then be called and used like any other block in GRC. A screenshot of the blocks used in this is shown below.

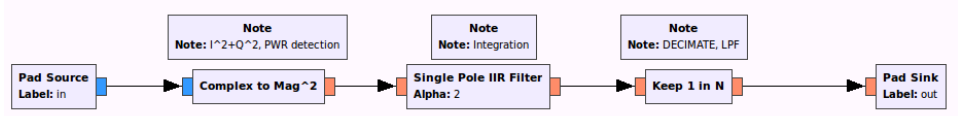


Figure A.1 Blocks used for creating a total power radiometer in software

### Total Power Radiometer Block

```

#!/usr/bin/env python

#####
# Gnuradio Python Flow Graph
# Title: Total Power Radiometer
# Author: Matthew Nelson
# Description: Blocks for power detection, integration and LPF
# for a total power radiometer
# Generated: Sun Apr 12 23:03:59 2015
#####

from gnuradio import blocks
from gnuradio import filter
from gnuradio import gr
from gnuradio.filter import firdes

class TPR(gr.hier_block2):

```

```

def __init__(self, integ=1, samp_rate=1, det_rate=1):
    gr.hier_block2.__init__(
        self, "Total Power Radiometer",
        gr.io_signature(1, 1, gr.sizeof_gr_complex*1),
        gr.io_signature(1, 1, gr.sizeof_float*1),
    )

#####
# Parameters
#####

self.integ = integ
self.samp_rate = samp_rate
self.det_rate = det_rate

#####
# Blocks
#####

self.single_pole_iir_filter_xx_0 = filter.
    single_pole_iir_filter_ff(1.0/((samp_rate*integ)/2.0),
    1)
(self.single_pole_iir_filter_xx_0).set_processor_affinity
([1])
self.blocks_keep_one_in_n_4 = blocks.keep_one_in_n(gr.
    sizeof_float*1, samp_rate/det_rate)
self.blocks_complex_to_mag_squared_1 = blocks.
    complex_to_mag_squared(1)

```

```

#####
# Connections

#####
self.connect((self.blocks_complex_to_mag_squared_1, 0), (
    self.single_pole_iir_filter_xx_0, 0))

self.connect((self.blocks_keep_one_in_n_4, 0), (self, 0))

self.connect((self, 0), (self.

    blocks_complex_to_mag_squared_1, 0))

self.connect((self.single_pole_iir_filter_xx_0, 0), (self

    .blocks_keep_one_in_n_4, 0))

def get_integ(self):
    return self.integ

def set_integ(self, integ):
    self.integ = integ
    self.single_pole_iir_filter_xx_0.set_taps(1.0/((self.

        samp_rate*self.integ)/2.0))

def get_samp_rate(self):
    return self.samp_rate

def set_samp_rate(self, samp_rate):
    self.samp_rate = samp_rate
    self.single_pole_iir_filter_xx_0.set_taps(1.0/((self.

        samp_rate*self.integ)/2.0))

    self.blocks_keep_one_in_n_4.set_n(self.samp_rate/self.

```

```
det_rate)

def get_det_rate(self):
    return self.det_rate

def set_det_rate(self, det_rate):
    self.det_rate = det_rate
    self.blocks_keep_one_in_n_4.set_n(self.samp_rate/self.
        det_rate)
```

## Matlab code for reading and displaying data from GNURadio

---

### GNURadio Parsing Code

```
%Radiometer Parsing script
%Matthew E. Nelson
%Updated 6/8/2014
%Rev. 2.15
%
-----


%Revision History
%1.7 - Added CSV input file format. Gave up on reading LVM
%1.8 - Added User input box
%1.9 - Added Calibration points for square law detector
%1.91 - Cleaned up some code
%1.92 - Futher clean up of unused code
%1.93 - Fixed dialog boxes not showing the entire title
%2.0 - Added filter to clean up noisy x^2 data
%2.1 - Added NEdeltaT (NEAT) calculation, minor change to plot
    labels
%2.11 - Added square law voltage to dBm conversion
%2.12 - Fixed bug on when doing NEAT calc, added a time base
    calculation
%for plots
%2.13 - Added calibration line plots
%2.14 - changed graphs to a time base
```

*%2.15 - Added plotting of both  $x^2$  and N200 on same graph for comparasion*

*%This script uses the read\_float\_binary.m file to read in a file written by*

*%GNURadio. This data can then be manipulated by Matlab and graphed. This*

*%script can also accept calibration coefficients in order to calculate the*

*%calibrated noise temperature. This requires that two data points are*

*%recorded to known sources such as LN2.*

*%Data files using the GNURadio flow diagram written by Matthew Nelson use a*

*%valve block to turn "on and off" recording. However, data is still*

*%written to the file, but they will be all zeros. This script has a simple*

*%routine to remove all zeros. If this is not desired (for example turning*

*%on and off the recording) please comment it out.*

*%In April I switched from a UBW32 board to a NI USB DAQ to obtain the*

*%square law data. This changed the output file from a csv file to NI's*

```
%TDMS binary format. The original CSV code will remain but will
be
%commented out.

%In theory, this script may also run on Octave, but the file I/O
package
%will be needed to use the file dialog box.

%
-----


%Clear the workspace
clear all;
%
-----


%Constants
%set's the window size to filter the square-law data
windowSize = 200;
%Receiver Noise Temperature for NEAT calc
Trec = 400;
%Integration Time for NEAT calc
tau = 2;
%Bandwidth for NEAT calc
beta = 10e6;
%
-----


%User Dialog entry
```

```

%The User input box will accept the calibration points from the
user and

%will output the calibration data.

%Setup dialog options
options.Resize='on';
options.WindowStyle='normal';
options.Interpreter='tex';

%Setup MsgBox options
CreateStruct.Interpreter = 'tex';
CreateStruct.WindowStyle = 'modal';
%
-----


%Ask for user input for calibration
prompt = {                         Enter calibration temp 1 (K),
'Enter calibration temp 2 (K)', 'Enter Calibration value 1:', ,
Enter Clibration value 2:};

dlg_title = 'Calibration for N200';
num_lines = 1;
def = {'371', '77', '.170', '.103'};

N200answer = inputdlg(prompt, dlg_title, num_lines, def, options);

prompt = {                         Enter calibration temp 1 (K):'
,'Enter calibration temp 2 (K):', 'Enter Calibration value 1:', ,
'Enter Clibration value 2:'};

```

```
dlg_title = 'Calibration for X^2';
num_lines = 1;
def = {'371','77','2.1','1.9'};
x2answer = inputdlg(prompt,dlg_title,num_lines,def,options);

%Calibration variables based on two temperature points

N200temp1 = N200answer(1);
N200temp2 = N200answer(2);

%Enter the measured data points for temp1 and temp2
N200data1 = N200answer(3);
N200data2 = N200answer(4);

%Calibration variables based on two temperature points

x2temp1 = x2answer(1);
x2temp2 = x2answer(2);

%Enter the measured data points for temp1 and temp2
x2data1 = x2answer(3);
x2data2 = x2answer(4);

%Store the values into a and b
syms a b;

%Solve our two calibration points for the SDR
y = solve(N200data1*a+b==N200temp1,N200data2*a+b==N200temp2);
```

```
N200calib1 = double(y.a);
N200calib2 = double(y.b);

msgbox(sprintf('The calibrations points for the N200 is: %f and %
f',N200calib1,N200calib2));

N200calibration = [y.a y.b];
fprintf('N200 Coefficient 1: %.2f N200 Coefficent 2: %.2f \r\n',
N200calib1, N200calib2);

%Store the values into a and b
syms a b;

%Solve our two calibration points for the X^2
y = solve(x2data1*a+b==x2temp1,x2data2*a+b==x2temp2);

x2calib1 = double(y.a);
x2calib2 = double(y.b);

msgbox(sprintf('The calibrations points for the X^2 is: %f and %f
',x2calib1,x2calib2),CreateStruct);

x2calibration = [y.a y.b];
fprintf('X^2 Coefficient 1: %.2f X^2 Coefficent 2: %.2f \r\n',
x2calib1, x2calib2);
```

---

%

*%Read data files.*

*%GNURadio outputs a binary file and LabView outputs a TDMS file*

*%Ask for the filename that has the TPR data from GNURadio*

```
gnuradio_file = uigetfile('*.*','Select the GNURadio data file');
disp('Importing Radiometer data...')
```

*%Ask for the filename of the Square law detector. Comment out if  
not using*

```
square_law = uigetfile('.tdms','Select the Square_law data file'
);
disp('Importing Square Law data...')
```

*%Call the program that will convert the TDMS file format to a .  
mat file*

```
tdms = convertTDMS2(true,square_law);
```

*%The data created is nested in the array, we need to pull the  
data we want*

```
x2=tdms.Data.MeasuredData(1,4).Data;
```

*%Call the read\_float\_binary script. This scripts reads the  
GNURadio*

```
%binary protocol
gnuradio = read_float_binary(gnuradio_file);

%
-----



%Remove zeros which is common in files that use the value feature
to

%control flow
gnuradio = gnuradio(gnuradio^=0);

%Create a time index
timen200=(1:length(gnuradio))*5;
timex2=(1:length(x2))/100;

%
-----



%Calculate the calibrated noise temperature for the SDR
N200calib_data = ((gnuradio*N200calibration(1))+N200calibration
(2));

%Calculate the calibrated noise temperature for the X^2
x2calib_data = ((x2*x2calibration(1))+x2calibration(2));

%
-----
```

```

%The square-law data is fairly noise, so we will filter it to
smooth
%it out.

%First, convert from a sym matrix to a double
temp1=double(x2calib_data);
temp2=double(x2);

%Now filter it
avgx2_calib=filter(ones(1,windowSize)/windowSize,1,temp1);
avgx2=filter(ones(1,windowSize)/windowSize,1,temp2);

%
-----


%Convert voltage from square-law to dBm. 53 mV is 1 dBm
dbmx2=x2./.053;
avgdbmx2=avgx2./.053;

%Calculate N E Delta T (NEAT)

%First calculation is the NEAT expected based on BW and other
parameters
%NEAT = (Ta+Tsys)/SQRT(tau+beta)

NEAT = (Trec)./sqrt(tau+beta);

%Now we can calculate the actual NEAT
%Look at a sample that is stable, in the LN2 area

for n = 1:100;
rQ_stddev(n) = gnuradio(n+610);

```

```

end

estNEAT = std(rQ_stdev);

%Now print this information out

fprintf('Calculated NEAT: %.2f Actual NEAT: %.2f \r\n',NEAT,
estNEAT);

%
-----
%Plot the calibrated data

figure;
subplot(2,1,1);
plot(N200calib_data);
title('N200 TPR Calibrated Data');

% Create xlabel
xlabel('Time');

% Create ylabel
ylabel('Calibrated Noise Temperature in K');
subplot(2,1,2);
plot(avgx2_calib);
title('x^2 Calibrated Data');

figure
timeshift = timex2+75;
plot(timen200,N200calib_data,'r');
hold on;

```

```

plot(timeshift,avgx2_calib,'g');

title('X^2 and N200 calibrated data');

ylabel('Noise Temp K');

xlabel('Time sec');

legend('N200','X^2');

%
-----
```

```

%Plot the raw data

figure;

subplot(2,1,1);

plot(timen200,gnuradio);

title('N200 TPR Raw Data');

xlabel('Time Sec');

ylabel('rQ Value');

subplot(2,1,2);

plot(timex2,avgx2);

title('x^2 Raw Data');

ylabel('Raw Voltage');

xlabel('Time Sec');

axis([-inf inf 2.1 2.4]);
```

```
%
```

```

-----
```

```

%Plot the calibration line

figure;

x=linspace(str2double(N200data2),str2double(N200data1),200);
```

```
y=linspace(str2double(x2data2),str2double(x2data1),200);  
subplot(2,1,1);  
plot(x, N200calib1*x+N200calib2,'-r');  
title('Calibration line for N200 SDR');  
xlabel('raw value');  
ylabel('Noise Temperature K');  
subplot(2,1,2);  
plot(y,x2calib1*y+x2calib2,'-b');  
title('Calibration line for X^2 detector');  
xlabel('raw value');  
ylabel('Noise Temperature K');  
%
```

---

```
%plot x2 with dBm  
figure  
plot(timex2,avgdbmx2);  
title('x^2 power readings');  
ylabel('dBm');  
xlabel('Time Sec');  
axis([-inf inf 37 40]);
```

## Python code for analyzing data

---

### Total Power Radiometer

```

#-*- coding: utf-8

#Radiometer Parsing Function

#This code shows an example of reading in and plotting data that
is outputted from a GNURadio GRC file.

#In this example a Total Power Radiometer is developed in
GNURadio GRC and uses the File Sink function to store the data
.

#The plot then shows the total power output from the radiometer
as a matched load is submerged in Liquid Nitrogen,
#then Ice Water and then left to dry.

# - - -
#
#### Read the data

# Import Needed functions

# Import needed libraries
from pylab import *
import pylab
import scipy
import numpy
import scipy.io as sio
import csv

```

```
# Use this to set the filename for the data file and CSV
# Calibration file.

tpr = 'tpr_2014.06.12.Lab0.dat'
calib = 'tpr_calib_2014.06.12.Lab0.csv'
x2_data = 'tpr_x2_2014.06.12.Lab0.csv'

# Uses SciPy to open the binary file from GNURadio

f = scipy.fromfile(open(tpr), dtype=scipy.float32)

# Because of the value function in GNURadio, there are zeros that
# get added to the file. We want to trim out those zeros.

# In [5]:

f = numpy.trim_zeros(f)

# Create an index array for plotting. Also, since we know the
# interval the data is taken, we can convert this to an actual
# time.
```

```
# In [6]:
```

```
y = numpy.linspace(0,(len(f)*.5),numpy.size(f))
```

```
### Plot the data
```

```
# In [7]:
```

```
plot(y,f)
```

```
xlabel('Time (sec)')
```

```
ylabel('rQ Values')
```

```
title('rQ vs Time')
```

```
grid(True)
```

```
pylab.show()
```

```
## Calibration
```

# The rQ values are the raw values from the total power radiometer and are uncalibrated. While the graph shows the change in the total power recorded and shows that the radiometer can detect changes in noise temperature, it has no other meaning than that. What we want is to show what the total power is in relation to a noise temperature. Since we have recorded the values of the rQ at fixed and known teperatures, we can create a calibration line and calibrate

*the radiometer. For this experiment, we found that the following values matched our two known temperatures.*

```
#  
# /rQ Value/X^2 Voltage/Temperature  
# /-----/-----  
# .0977    / 1.9617      /77 K  
# .1507    / 2.085       /273.15 K  
  
#  
# We can now solve for  $y = mx + b$  since we have two equations and  
two unknowns.  
  
#  
# To work with this, a calibration file is created. This is a  
very simple CSV file that contains 3 values: The raw rQ value,  
the raw voltage from the square-law detector (discussed later  
) and the observed temperature. The table above would then  
look like the following in the file.  
#   ''''  
# .0977,1.9617,77  
# .1507,2.085,273.15  
#   ''''  
# - - -  
  
# We need to read in the values from our CSV file that contains  
the values  
  
# In [67]:  
  
read_csv = open(calib, 'rb')
```

```

csvread = csv.reader(read_csv)

rQ_values = []
temp_values = []
voltage = []

for row in csvread:
    rQ, volt, temp = row
    rQ_values.append(float(rQ))
    voltage.append(float(volt))
    temp_values.append(float(temp))
read_csv.close()

a = numpy.array([[rQ_values[0], 1.0], [rQ_values[1], 1.0]], numpy.
    float32)
b = numpy.array([temp_values[0], temp_values[1]])

z = numpy.linalg.solve(a, b)
print z

# Now we apply these values to the array that holds our raw rQ
# values

g = f*z[0]+z[1]

# Now we can re-plot the graph but this time with the calibrated
# noise temperatures

```

```

plt.figure()
plot(y,g)
xlabel('Time')
ylabel('Noise Temperature (K)')
title('Temp vs Time')
grid(True)

pylab.show()

# This is looking better, but the time at the bottom doesn't have
much meaning. Since we know the sample rate of the Software
Defined Radio, we can calculate the time interval between each
sample.

# - - -
# # Square-law data
#
# We now want to look at the data from the Square-Law detector to
verify the operation of the SDR. In the experiment that was
conducted above, a power splitter was used to split the RF
signal so that one went to the SDR and the other to a square-
law detector (with a 3.1 dB loss though). Therefore both data
should be the same. Let's read and then plot this data.

read_csv = open(x2_data, 'rb')
csvread = csv.reader(read_csv)
dummy = []

```

```

x2_voltage = []

for row in csvread:
    dummy, x2voltage = row
    x2_voltage.append(float(x2voltage))
read_csv.close()

# Like the SDR data, we want to have a time reference at the bottom.

w = numpy.linspace(0,(len(x2_voltage)*.01),numpy.size(x2_voltage))
)

plt.figure()
plot(w,x2_voltage)
xlabel('Time (sec)')
ylabel('Voltage (V)')
title('X^2 Voltage vs Time (Noisy)')
grid(True)

pylab.show()

# The Square-law detector doesn't have a filter on it unlike the data we get from the SDR. The GNURadio program takes the data and applies a Low Pass Filter to "clean up" the information. We need to do the same with our Square-law data.

```

```

from scipy import signal

N=100
Fc=2000
Fs=1600

h=scipy.signal.firwin(numtaps=N, cutoff=40, nyq=Fs/2)
x2_filt=scipy.signal.lfilter(h,1.0,x2_voltage)

plt.figure()
plot(w,x2_filt)
xlabel('Time (sec)')
ylabel('Voltage (V)')
title('X^2 Voltage vs Time')
axis([0, 610, 1.94, 2.12])
grid(True)

pylab.show()

# Now we wish to calibrate this data as well. We will use the same file and use the calibration points in that file.

a = numpy.array([[voltage[0],1.0],[voltage[1],1.0]],numpy.float32)
b = numpy.array([temp_values[0],temp_values[1]])

z = numpy.linalg.solve(a,b)
print z

```

```
x2_calib = x2_filt*z[0]+z[1]
```

```
plt.figure()
plot(w,x2_calib)
xlabel('Time (sec)')
ylabel('Voltage (V)')
title('X^2 Noise Temp vs Time')
axis([0, 610, 70, 300])
grid(True)
```

```
pylab.show()
```

*# This looks to be the same as our SDR graph, but let's overlay them to make sure*

```
plt.figure()
plot(w,x2_calib,'r',label='X^2')
plot(y,g,'b',label='SDR')
xlabel('Time (sec)')
ylabel('Voltage (V)')
title('Noise Temperature vs Time')
axis([0, 610, 70, 300])
grid(True)
legend(loc='lower right')
```

*# We have some timeshift due to two reasons. One, the timing isn't always perfect when starting the collection of the two data*

*sets. And two, we get a timeshift from filtering the square-law data*

```
pylab.show()
```

## APPENDIX B. EE 518 Test Results

### E E 518 Lab Tests

Further testing of the square-law detector was performed by using the radiometer in a real world event. This test was exercised in conjunction with the Microwave Remote Sensing class (E E 518) under Dr. Brian Hornbuckle. In the Spring of 2012 the radiometer was moved to the roof of agronomy and the EE 518 students conducted a number of tests using the N200 software defined radio to collect the data.

The E E 518 test however showed that there were additional problems with the radiometer. While the test showed that the SDR could in fact read data, the data was skewed. It was later found out that the radiometer was generating an interfering signal that caused the power readings to be elevated. It was also found that the interfering signal was also fluctuating and seemed to correspond somewhat to the physical position of the radiometer. This was found as a result of having the SDR record the raw I/Q values and then was analyzed later. Through this analysis, we found that a strong harmonic was developed and caused a spike in signal being recorded. Although the exact reason for this has not been found, the problem has been isolated to something in the RF Front End of the ISU radiometer.

In the Spring of 2014 the E E 518 class ran another experiment, but this time a different one. This experiment mimicked the experiments that the author ran to calibrate and test the radiometer. This allowed an outside source to validate the results that I was getting with running the radiometer. Like my tests, the students submerged a matched load into liquid nitrogen and then in boiling water. The liquid nitrogen was assumed to be at 77 K and the boiling water was measured to be at 99 C or 372 K. The students were then given a mystery sample in which they had to determine the temperature of a water sample. Since the students had to points,

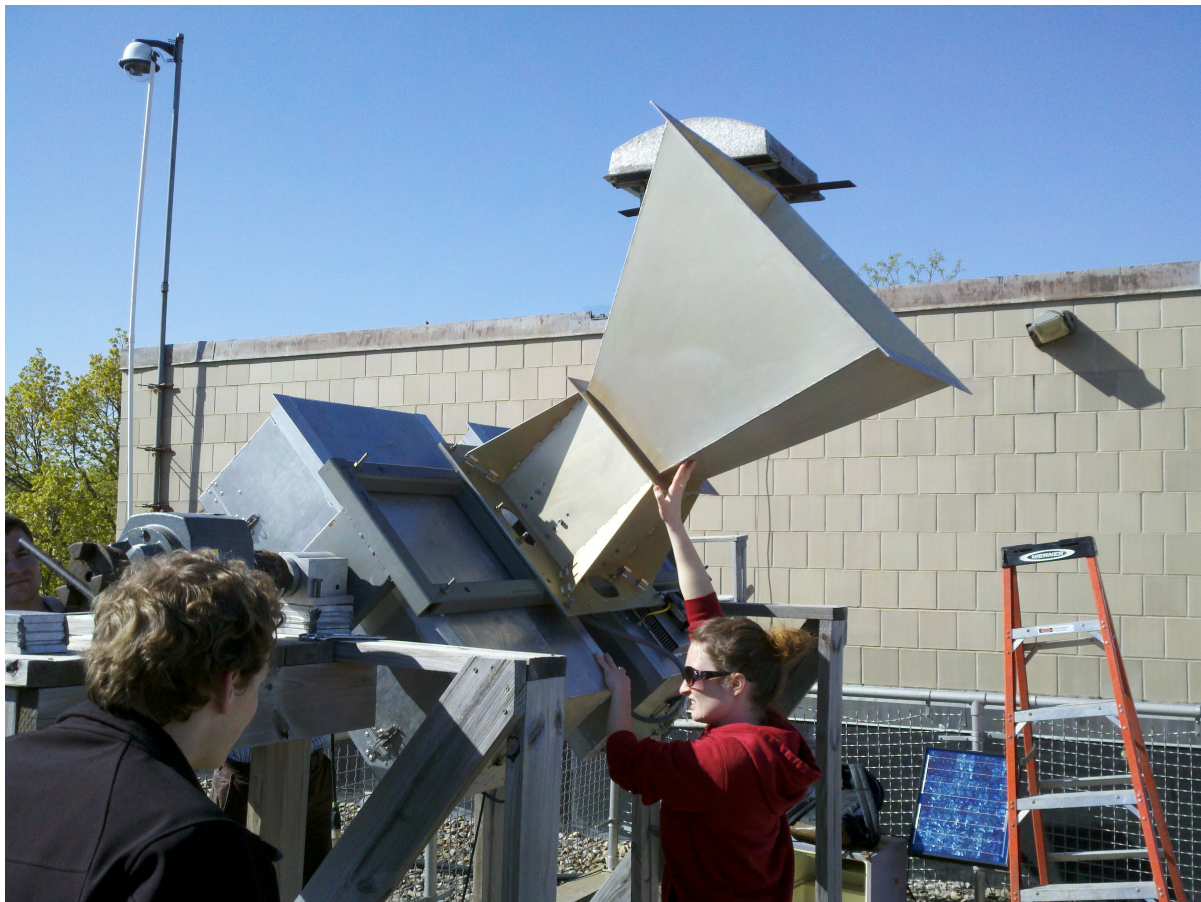


Figure B.1 Students rotating the radiometer for an experiment on Agronomy Hall

they could find the calibration line and determine the temperature. The experiment was run twice as we expected the radiometer may have drifted between measurements.

#### B.0.5 Test setup

For the E E 518 class, the setup was similar to experiments that was run to test the results in this thesis. For the E E 518 however the students only used the N200 SDR for recording the total power readings. The ISU RF front end was used only to provide the RF front end as in other tests and the output from that RF front end was feed into the N200. A matched load was attached to the input of the RF front end. This matched load was then submersed into either the liquid nitrogen or water baths.

### B.0.6 Lab Experiment

Students conducted the experiment by submerging the matched load into Liquid Nitrogen, then boiling water, then an unknown sample. The LN2 was believed to be at 77 K. The boiling water was measured by the students and was recorded to be 99 C. The mystery water was then measured by myself and recorded both before the students placed the match load in there and after to see if it changed temperature between the experiments. During this time the GNURadio program that I wrote recorded the total power information to the hard drive. This file was then given to the tests and an example Matlab script was also provided for them to use to read the data file.

### B.0.7 Lab Results

Two labs were conducted, however the data from the first lab was more stable and had better results than the second lab. Therefore the students only used the data set from the first lab experiment. Students were then asked to write a lab report that calculated the temperature of the mystery water, write up what each component in the radiometer does, plot the raw  $rQ$  values, calculate and plot the calibration lines and finally calculate the  $NE\delta T$  for the system by doing a standard deviation on a section of the data that was at a stable temperature.

The results of the lab experiments were mixed in the students reports. Almost all of the students reported a temperature cooler than the actual recorded temperature. After looking at the data and the student reports, there is a couple of reasons this may have happened. First, it would appear that there may not have been enough time to allow the matched load to equalize. The graph of the  $rQ$  values does not show a stable line as expected with the LN2 and hot water baths. It appears that there was a dip in the  $rQ$  values and that the students picked that lowest point as the mystery water temperature. It is uncertain what caused the dip. Second, it is safe to say that the temperature of the mystery water changed due to the matched load being inserted in it. There was nothing to keep the mystery water at a fixed temperature as it was simply water at room temperature. These may have caused some of the odd readings and made it difficult for the sample to stabilize unless it was allowed to sit longer.

### B.0.8 Conclusion

While the students were not able to get an accurate reading of the mystery water, the calibration points, and  $NE\delta T$  values were within what was expected of the system and matched fairly close to those calculated by the author. Overall, this experiment proved to be a good exercise for the students as it allowed them to have a hands on exercise and see and operate a radiometer for themselves.

## APPENDIX C. Direct-Sampling Digital Correlation Radiometer

### Theory of Operation

The original ISU Radiometer was constructed by the University of Michigan and was based on Dr. Mark Fischman's dissertation on a Direct-Sampling Digital Correlation Radiometer [Fischman (2001)]. This type of radiometer amplifies the signal but then immediately digitizes the signal to be processed. In many ways, this is how a software defined radio works, however in this case the ISU radiometer is under-sampled. However, as explained by Dr. Fischman this is acceptable for a total power radiometer since the only information we need is power information. The radiometer that Dr. Fischman proposes also correlates the signals, one from the vertical polarization and the other from the horizontal polarization from the antenna.

#### C.0.9 Implantation in the ISU Radiometer

The original ISU radiometer worked by under-sampling the RF signal coming into the analog to digital converters. This under-sampled signal lacks enough sample to recreate the full signal, however the power information can be extracted. The original ISU radiometer also used both the vertical and the horizontal polarization coming from the antenna. This allowed the radiometer to correlate between the vertical and horizontal polarization.

## BIBLIOGRAPHY

- Aitken, G. J. M. (1968). A new correlation radiometer. *Antennas and Propagation, IEEE Transactions on*, 16(2):224–228.
- Behnke, P., Soberal, D., Bredeweg, S., Dunne, B., Sterian, A., and Furton, D. (2013). Senior capstone: A software defined radio design for amateur astronomy. In *Interdisciplinary Engineering Design Education Conference (IEDEC), 2013 3rd*, pages 104–111.
- Bremer, J. C. (1979). Improvement of scanning radiometer performance by digital reference averaging. *Instrumentation and Measurement, IEEE Transactions on*, 28(1):46–54.
- Clapp, R. and Maxwell, J. (1967). Complex-correlation radiometer. *Antennas and Propagation, IEEE Transactions on*, 15(2):286–290.
- Cross, D. (1998). Time domain filtering techniques for digital audio. Website. <http://groovit.disjunkt.com/analog/time-domain/timfilt.html>.
- De Roo, R., Ruf, C., and Sabet, K. (2007). An l-band radio frequency interference (rfi) detection and mitigation testbed for microwave radiometry. In *Geoscience and Remote Sensing Symposium, 2007. IGARSS 2007. IEEE International*, pages 2718–2721.
- Dicke, R. H. (1946). The measurement of thermal radiation at microwave frequencies. *Review of Scientific Instruments*, 17(7):268–275.
- Ellingson, S., Hampson, G., and Johnson, J. (2003). Design of an l-band microwave radiometer with active mitigation of interference. In *Geoscience and Remote Sensing Symposium, 2003. IGARSS '03. Proceedings. 2003 IEEE International*, volume 3, pages 1751–1753.

- Erbas, C., Hornbuckle, B., and De Roo, R. (2006). Iowa state university/the university of michigan direct sampling digital radiometer. In *Geoscience and Remote Sensing Symposium, 2006. IGARSS 2006. IEEE International Conference on*, pages 3074–3077.
- Evans, G. and McLeish, C. W. (1977). *RF Radiometer Handbook*. Artech House, Dedham, MA.
- Fischman, M. A. (2001). *Development of a direct-sampling digital correlation radiometer for earth remote sensing applications*. PhD thesis, University of Michigan.
- Forte, G., Tarongi Bauza, J., dePau, V., Vall llossera, M., and Camps, A. (2013). Experimental study on the performance of rfi detection algorithms in microwave radiometry: Toward an optimum combined test. *Geoscience and Remote Sensing, IEEE Transactions on*, 51(10):4936–4944.
- Fujimoto, K. (1964). On the correlation radiometer technique. *Microwave Theory and Techniques, IEEE Transactions on*, 12(2):203–212.
- Goggins, W. B. (1967). A microwave feedback radiometer. *Aerospace and Electronic Systems, IEEE Transactions on*, AES-3(1):83–90.
- Hach, J. P. (1968). A very sensitive airborne microwave radiometer using two reference temperatures. *Microwave Theory and Techniques, IEEE Transactions on*, 16(9):629–636.
- Hardy, W. N., Gray, K., and Love, A. (1974). An s-band radiometer design with high absolute precision. *Microwave Theory and Techniques, IEEE Transactions on*, 22(4):382–390.
- Jonard, F., Weihermuller, L., Jadoon, K., Schwank, M., Vereecken, H., and Lambot, S. (2011). Mapping field-scale soil moisture with l-band radiometer and ground-penetrating radar over bare soil. *Geoscience and Remote Sensing, IEEE Transactions on*, 49(8):2863–2875.
- Jondral, F. K. (2005). Software-defined radio: basics and evolution to cognitive radio. *EURASIP journal on wireless communications and networking*, 2005(3):275–283.
- Kerr, Y. (2012). Smos rfi detection: Today's maps. Website. [http://www.cesbio.ups-tlse.fr/SMOS\\_blog/?p=2963](http://www.cesbio.ups-tlse.fr/SMOS_blog/?p=2963).

- Leech, M. (2006). Gnuradio and usrp: Solderless breadboarding for the 21st century. In *25th Anniversary Conference of the Society of Amateur Radio Astronomers*.
- Leech, M. and Ocame, D. (2007). A year of gnu radio and sdr astronomy: experience, practice and observations. Website. [http://www.sbrac.org/documents/gnuradio\\_at\\_one\\_year\\_20070401.doc](http://www.sbrac.org/documents/gnuradio_at_one_year_20070401.doc).
- Leinweber, G. (2001). Square law diode detectors in 50 ohm systems.
- Liu, P.-W., Judge, J., DeRoo, R., England, A., and Luke, A. (2013). Utilizing complementarity of active/passive microwave observations at l-band for soil moisture studies in sandy soils. In *Geoscience and Remote Sensing Symposium (IGARSS), 2013 IEEE International*, pages 743–746.
- McIntyre, E. and Gasiewski, A. (2012). A new technique for detecting the presence of weak interfering digital signals in radiometric noise. In *Geoscience and Remote Sensing Symposium (IGARSS), 2012 IEEE International*, pages 1517–1520.
- McIntyre, E. and Gasiewski, A. (2007). An ultra-lightweight l-band digital lobe-differencing correlation radiometer (ldcr) for airborne uav sss mapping. In *Geoscience and Remote Sensing Symposium, 2007. IGARSS 2007. IEEE International*, pages 1095–1097.
- McMullan, K. D., Brown, M., Martin-Neira, M., Rits, W., Ekholm, S., Marti, J., and Lemanczyk, J. (2008). Smos: The payload. *Geoscience and Remote Sensing, IEEE Transactions on*, 46(3):594–605.
- Misra, S., De Roo, R., and Ruf, C. (2012). An improved radio frequency interference model: Reevaluation of the kurtosis detection algorithm performance under central-limit conditions. *Geoscience and Remote Sensing, IEEE Transactions on*, 50(11):4565–4574.
- Mitola, J. (1995). The software radio architecture. *Communications Magazine, IEEE*, 33(5):26–38.
- Nyquist, H. (1928). Thermal agitation of electric charge in conductors. *Physical review*, 32(1):110–113.

- Ohm, E. and Snell, W. (1963). A radiometer for a space communications receiver. In *Antennas and Propagation Society International Symposium, 1963*, volume 1, pages 16–20.
- Rashid, R. A., Sarijari, M. A., Fisal, N., Yusof, S. K. S., and Mahalin, N. H. (2011). Spectrum sensing measurement using gnu radio and usrp software radio platform. In *ICWMC 2011: The Seventh International Conference on Wireless and Mobile Communications*, pages 237–242.
- Richaume, P. (2012). Outburst of anger. Website. [http://www.cesbio.ups-tlse.fr/SMOS\\_blog/?p=3381](http://www.cesbio.ups-tlse.fr/SMOS_blog/?p=3381).
- Ruf, C. and Gross, S. (2010). Digital radiometers for earth science. In *Microwave Symposium Digest (MTT), 2010 IEEE MTT-S International*, pages 828–831.
- Sarijari, M., Marwanto, A., Fisal, N., Yusof, S. K. S., Rashid, R., and Satria, M. (2009). Energy detection sensing based on gnu radio and usrp: An analysis study. In *Communications (MICC), 2009 IEEE 9th Malaysia International Conference on*, pages 338–342.
- Shi, J., Njoku, E., Chen, K., Jackson, T., and O’niell, P. (2003). Estimation of soil moisture with repeat-pass l-band radiometer measurements. In *Geoscience and Remote Sensing Symposium, 2003. IGARSS ’03. Proceedings. 2003 IEEE International*, volume 1, pages 413–415 vol.1.
- Skou, N. and Vine, D. L. (2006). *Microwave Radiometer Systems Design and Analysis*. Artech House, Norwood, MA.
- Terlep, D. (2002). How quantization and thermal noise determine an adc’s effective noise figure. Website. <http://www.maximintegrated.com/app-notes/index.mvp/id/1197>.
- Tiuri, M. (1964). Radio astronomy receivers. *Antennas and Propagation, IEEE Transactions on*, 12(7):930–938.
- Uengtrakul, B. and Bunnjaweht, D. (2014). A cost efficient software defined radio receiver for demonstrating concepts in communication and signal processing using python and rtl-sdr. In *Digital Information and Communication Technology and it’s Applications (DICTAP), 2014 Fourth International Conference on*, pages 394–399.

Ulaby, F. T. and Long, D. G. (2014). *Microwave Radar and Radiometric Remote Sensing*. The University of Michigan Press, Ann Arbor, MI.

Ulaby, F. T., Moore, R. K., and Fung, A. K. (1981). *Microwave Remote Sensing*. Artech House, Dedham, MA.

Villarino, R., Enrique, L., Camps, A., Corbella, I., and Blanch, S. (2002). Design, implementation and test of the upc l-band automatic radiometer. In *Proc. URSI Commission-F 2002 Open Symp.*

Wang, Z., Liu, J., Lu, H., Zheng, W., Wang, X., and Li, B. (2012). A digital correlation full-polarimetric microwave radiometer design and calibration. In *Geoscience and Remote Sensing Symposium (IGARSS), 2012 IEEE International*, pages 4688–4690.

Weng, Q. (2012). *An Introduction to Contemporary Remote Sensing*. McGraw-Hill's AccessEngineering. McGraw-hill.